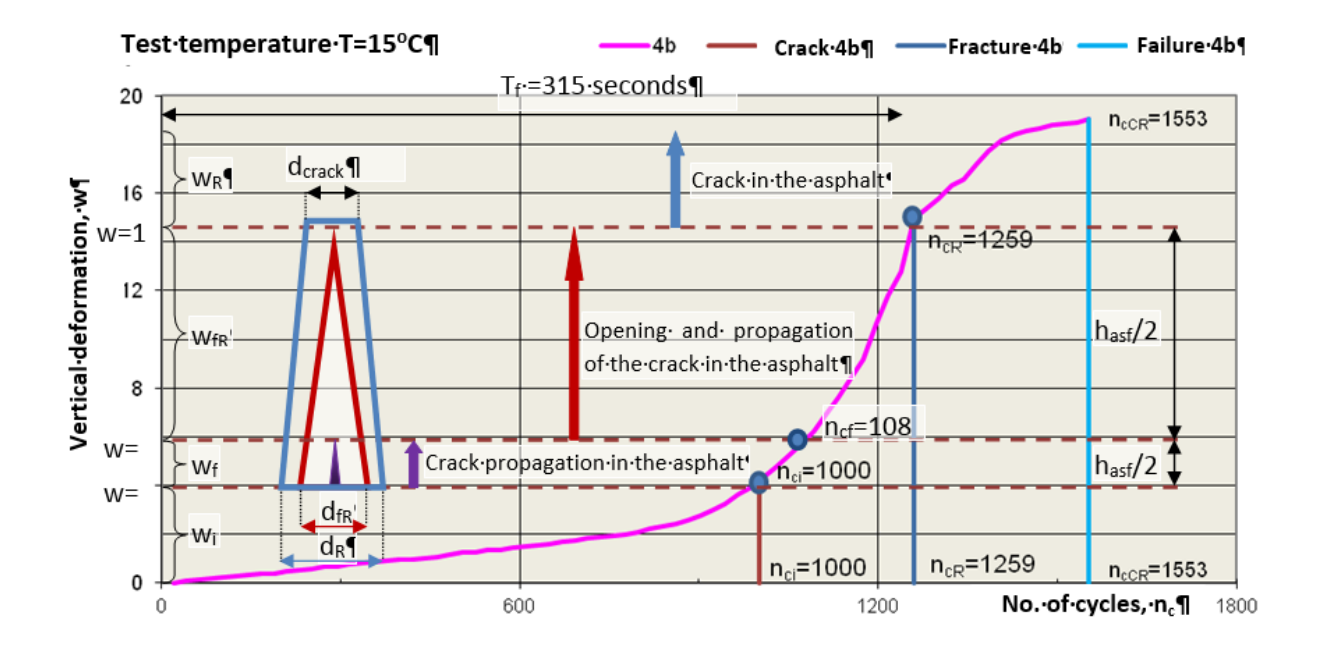
RESEARCH REPORT NUMBER 3

IDENTIFICATION OF THE PARAMETERS OF INFLUENCE OF CRACK PROPAGATION THROUGH PROTECTIVE ASPHALT LAYERS FOR DEGRADED PAVEMENTS



Scientific Coordinator: Prof. Dr. Ing. Mihai Dicu

PhD Student: ing. Mihai Gabriel LOBAZĂ

Cuprins

1	INT	ROD	DUCTION	4		
	1.1	, , ,				
	traffic	on	rehabilitated road structures	5		
	1.2 accele		search report no. 2. Analysis by statistical interpretation of the solutions obtained regime in the laboratory at loads equivalent to road traffic			
	1.3 throu		search Report no. 3. Identification of the parameters of influence of crack propagrotective asphalt layers for degraded pavements	_		
2	FRA	ACTU	JRE MECHANICS	11		
	2.1	The	e energy criterion	11		
	2.2	Str	ess intensity factor K	12		
	2.3	Cra	ack propagation over time (material fatigue)	13		
	2.4	Cra	acking of materials with linear elastic behavior	13		
	2.5	Cra	acking of materials with elasto-plastic behavior	16		
	2.5	.1	CTOD	17		
	2.5	.2	J-contour path integral	19		
3	THE	CO	NCEPT OF REFLECTIVE CRACKING PUBLISHED IN THE SPECIALTY LITERATURE	21		
	3.1 Paulo		ediction of existing reflective cracking potential of flexible pavements", Jorge C Pereira [13]	-		
	3.2	"La	b asphalt testing evaluation of reflective cracking", Fujie Zhou, Lijun Sun[14]	23		
	3.3 failure		ew procedures and criteria for asphalt mixes and pavements design regarding f d thermal stresses", F. Perez Jimenez, R. Miro, A. Martinez, R. Botella, G. Valdes[1	_		
	3.4 H. Di		vestigation of cracking in bituminous mixtures with a 4PBT", M.L. Nguyen, C. Sa edetto, L. Wendling[16]			
	3.5	The	e conclusions extracted from the specialized literature	29		
4	COI	NTRI	BUTIONS AND INTERPRETATIONS OF REFLECTIVE CRACKING PARAMETERS THR	OUGH		
0	BSERV	'ATIC	ONS AND PROCESSING OF EXPERIMENTAL RESULTS	31		
	4.1	4b	specimen	31		
	4.2	5a :	şi 5b specimens	40		
	4.3	6a :	specimenspecimen	47		
	44	7a -	si 7h snecimens	53		

	4.5	8a şi 8b specimens	61
	4.6	9a şi 9b specimens	68
5	CRA	ACKING PARAMETERS	74
6	MU	LTICRITERIAL INTERPRETATION OF THE REFLECTIVE CRACKING PROCESS	75
7	CON	NCLUSIONS	80
	7.1	Reflective cracking parameters	80
	7.2	Asphalt mixture	81
	7.3	Cracking Device with Temperature Control	81
8	BIBI	LIOGRAPHY	82

1 INTRODUCTION

The development of efficient design / research methods, which guarantee a long service life of the road structure, without unnecessary consumption of resources or aggression of the environment, is a mandatory condition in our times.

Cracking is one of the main causes of damage to road structures, which involves the allocation of large financial resources to repair and maintain them in optimal operating parameters.

Through the approached topic, the doctoral thesis entitled Contributions on Analysis by Modeling Road Structures Rehabilitated to Assimilations of Assimilated Road Traffic, studies by experimental modeling of road structure, requirements equivalent to an assimilated road traffic at the scale of the model. Through these atypical tests of regulated laboratory tests, it is desired to obtain new information on the behavior of asphalt wear layers, used for the protection of old cracked pavements. They are assimilated in the laboratory research process as pre-cracked mixed road structures, in various application cases, under the conditions of its use as a protective layer of asphalt laid over a cement concrete road pavement, cracked during standard operation.

The main objective of the thesis is to reduce the research costs intended to anticipate the behavior of asphalt road materials, used as protective layers in the rehabilitation activity of cracked road structures. Thus, through accelerated tests in the laboratory, to simulate road traffic that requires the experimental model of small-scale road structure, the aim is to obtain the performance of optimal recipe solutions designed in the laboratory through traditional tests.

The results of the work can be achieved by obtaining a new way to anticipate the propagation of the crack by reflection on asphalt layers that will be used as protective road cover, other than the classic attempts, faster and cheaper, to anticipate the life cycle of the layer. protective asphalt, placed over an old road pavement, to anticipate the appearance and spread of the crack to the surface.

The three research reports related to the doctoral thesis have as final goal the establishment of a test methodology for the test specimens with the help of the Thermostatic Physurometer, by simulating the effects of traffic on them. Processing the results by identifying the parameters that influence the cracking of asphalt layers placed over a pre-cracked cement concrete is another necessary step of the doctoral thesis, as well as establishing calculation relationships between these parameters, taking into account the applicability of previous research in the literature.

1.1 Research Raport no. 1. Research by structural modeling in the laboratory of the effects of traffic on rehabilitated road structures

Thus, in the first research report, *Research by structural modeling in the laboratory of the effects of traffic on rehabilitated road structures*, highlighted how the asphalt pavement improves the transfer of traffic loads from the foundation, reducing the level of stress in the concrete layer.[1]

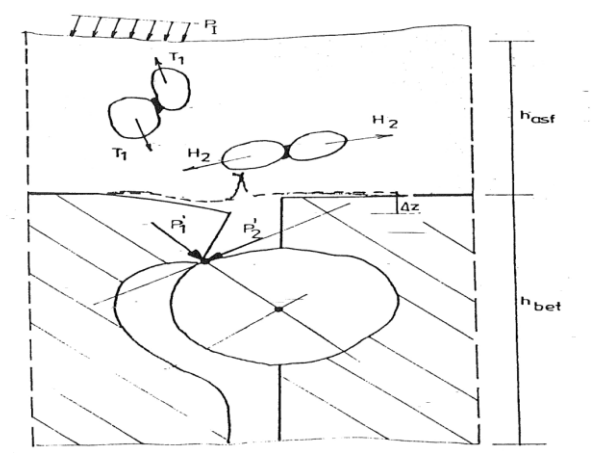


Figure 1.1 Transfer of the load to the crack in the presence of the protective asphalt layer.[2]

The effects of traffic on the road structure (mixed, in the case of the present thesis) were analyzed in AASHTO studies, introducing the notion of load equivalency factor (LEF), but the applicability of AASHTO equations is limited nowadays due to changes in vehicle configuration and loads. [3]

$$LEF = \frac{The number of loads of the standard axle that causes a certain loss of service level}{The number of loads of an X-axis that causes a certain loss of service level}$$
(1)

A similar approach is to express these effects by a notion called Aggressivity, **A**. This allows the comparison of road damage when passing a heavy vehicle, to the damage suffered by the road when passing a heavy reference vehicle. [4]

$$A = \sum (n_i \cdot y_i)$$
 Where: A- aggressivity
$$n_i \text{- number of axles } i \text{ (symple, tandem, tridem) recorded}$$

$$y_i \text{- aggressivity of the different types of axles, } i.$$
 (2)

These ways of assessing the effects of traffic require knowledge of how a type of axle vehicle influences the road structure, taking into account, among others, the type of structure, the environment. The equations **LEF**, respectively **A**, must be applied in the areas where they are the same conditions in which they were determined. Their extrapolation implies a certain degree of distrust.

Therefore, the theoretical and experimental study of the development mode, the appearance of the crack until the whole structure yields, is extremely necessary for researchers in the field of road transport infrastructure, but also for specialists who approve protection solutions through asphalt layers for cracked road pavements during its exploitation.

Among those who initially dealt with the mechanical explanation of cracking at load cycles (temperature and traffic) were Griffith, Irwin, Kies. Irwin introduced the stress intensity factor, noted by K. [5]

$$K^2 = \frac{G \cdot E}{1 - \mu^2} \tag{3)[5]}$$

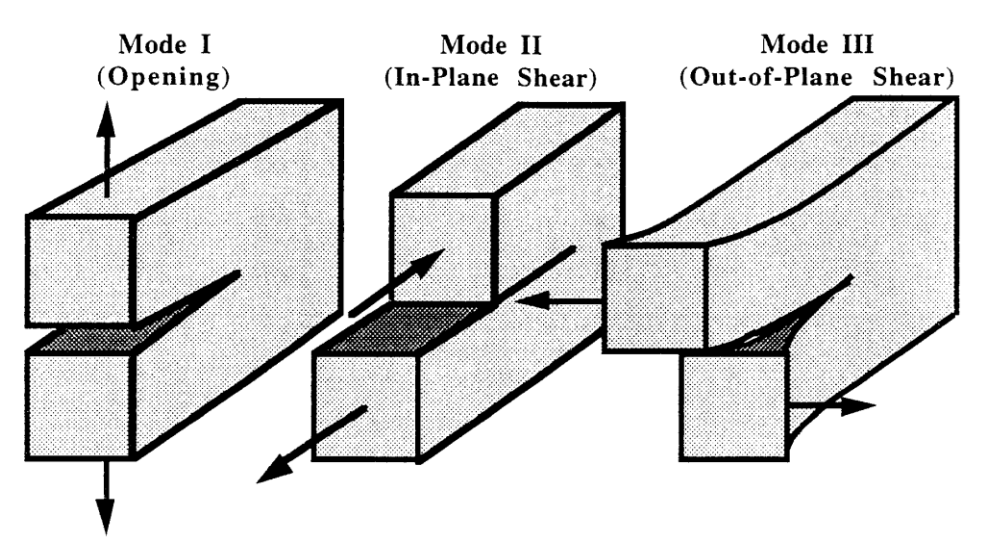
where: K = stress intensity factor, by Irwin

G = energy release rate, by Griffith

E = the modulus of the material in the road layer

 μ = Poisson coefficient for the same material.

Irwin observed that three stages of the tensile stress can be distinguished in the crack initiation as a measure of the propagation of this phenomenon.



Mode I (Normal stress)

Mode II (Shearing stress)

Mode III (Tearing stress)

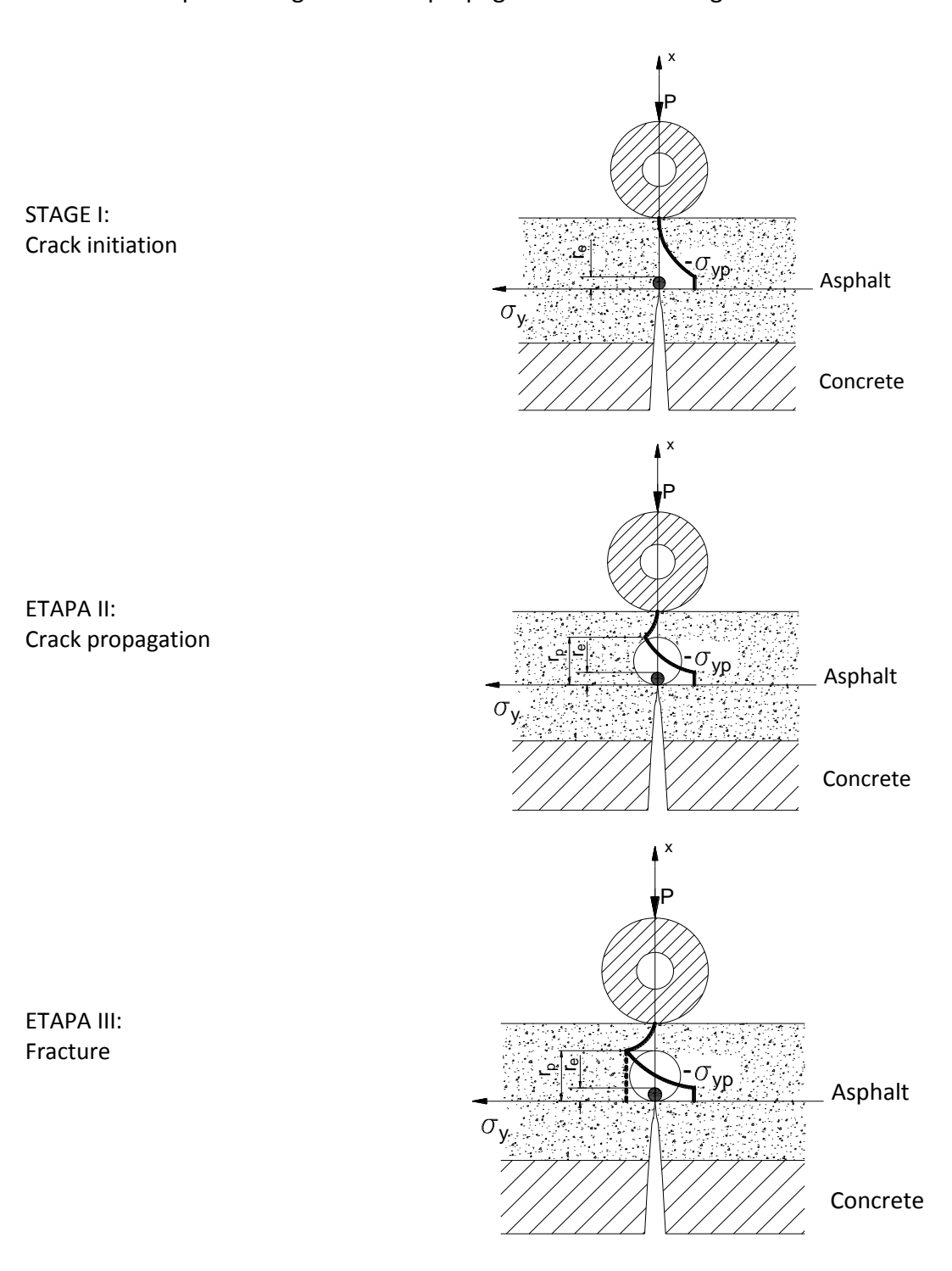
Figure 1.2 Modes of development of the stress state [6]

Stress intensity factor \mathbf{K} can be determined in all three ways of applying the stress (KI, KII, KIII).

The phenomenon of fatigue, due to traffic loads, can be associated with mode I of demand, so with \mathbf{K}_{I} . Structural fatigue occurs as a result of the appearance of microcracking which, by accumulating loading cycles, develops in the form of open cracks in the road layer. The

development of the crack on the thickness of the asphalt protection layer of the concrete is due to the exceeding of the plasticization limit of the material in the crack head.

There are accepted 3 stages of crack propagation in the existing theories:



Irwin calculated the size of the crack tip plastic zone in mode I of stress, rp:

$$r_{y} = \frac{1}{2\pi} \cdot \left(\frac{K_{I}}{\sigma_{YS}}\right)^{2} \tag{4)[6]}$$

Where:

 K_I –stress intensity factor in mode I σ_{YS} –Elasticity limit (the stress in the direction of crack propagation) r_Y –the size of the plastic zone

Fatigue crack growth was studied by Paris, who found an equation describing this parameter (the Paris-Erdogan law). The law can be used to quantify the residual life (cyclic loading) of a specimen.

$$\frac{\mathrm{d}f}{\mathrm{d}N} = A \cdot \Delta K^m \tag{5}$$

Where:

 $\frac{\mathrm{d}f}{\mathrm{d}N}$ -fatigue crack growth,

df -crack length growth,

dN -number of cycles growth N,

A, m -constants of the material,

 ΔK --stress intensity factor amplitude.

If we integrate the law of Paris (relation 5), by introducing in the formula the factor KI according to Irwin's relation (relation 4), both for traffic and temperature loads, we obtain a graph in the form of the one in Figure 1.3. Taking into account separately the number of stress cycles compared to the total number of cycles, when the crack propagated to the road surface, the following observations could be made:

- The crack propagation speed is slower at the traffic load, compared to the temperature initial load
- In the final stage, this behavior is revearsed.

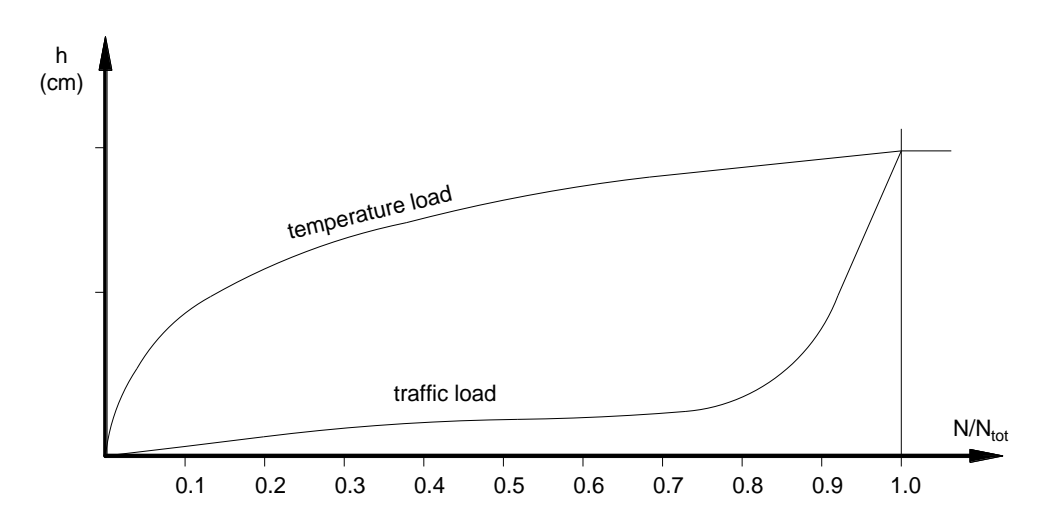


Figure 1.3 Crack propagation speed.[4]

In Figure 1.3 the following notations appear:

N = number of load cycles (temperature or traffic);

N_{tot} = total number of load cycles when the crack appears on the road surface.

h = the protective asphaltic layer thickness.

These analytical relations are used to analyze the parameters of crack propagation in composite road structures (asphalt on precast cement concrete), structures that are the object of study of this doctoral thesis.

The theory behind the phenomenon of cracking in road layers can be subjected to simplifying hypotheses by accepting some experimental observations obtained by testing on different laboratory devices.

1.2 Research report no. 2. Analysis by statistical interpretation of the solutions obtained in accelerated regime in the laboratory at loads equivalent to road traffic

In the second research report, Analysis by statistical interpretation of the solutions obtained in accelerated regime in the laboratory at loads equivalent to road traffic, is presented the preparation of specimens in the laboratory, the results of experimental tests, using the The Cracking Device with Temperature Control prototype, and mathematical processing. The conclusions of this report are as follows:

• There is an initial settlement period for the specimen between the supports of about 500-600 cycles (Figure 1.4)

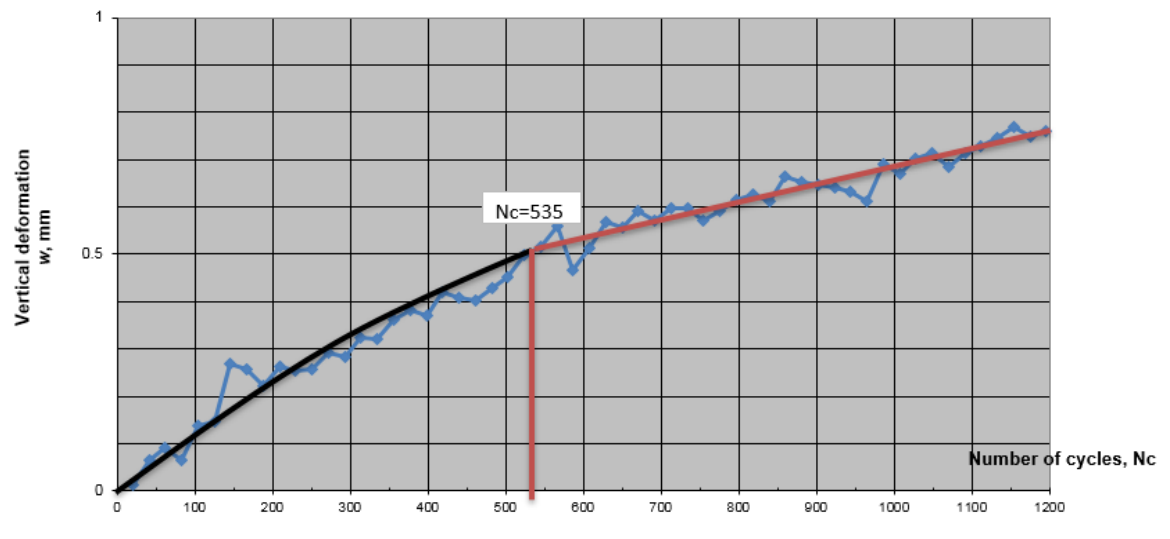


Figure 1.4 The initial settlement period

• The exponential function, $y = a \cdot e^{b \cdot x}$, describes best the evolution of the vertical deformation, w, in relation to the number of cycles, N_c (Table 1.1).

Table 1.1 Exponential functions corresponding to the studied specimens						
Specimen	Exponential function $y = a \cdot e^{b \cdot x}$	Coefficient of determination r^2	The number of cycles in which the crack appears in the asphaltic mixture, N_f			
2a	$y = 0.647 \cdot e^{0.000177 \cdot x}$	0.9661	9281			
3a	$y = 0.519 \cdot e^{0.00017 \cdot x}$	0.9643	11675			
3b	$y = 1.113 \cdot e^{0.000507 \cdot x}$	0.9957	3002			
6a	$y = 0.403 \cdot e^{0.000223 \cdot x}$	0.9389	10037			
7a	$v = 0.613 \cdot e^{0.00025 \cdot x}$	0.9901	7450			

0.9815

7b

Table 1.1 Exponential functions corresponding to the studied specimens

the cement concrete support layer influences the behavior of the specimen at loads equivalent to road traffic P (Figure 1.5), by the sizes of the aggregates in the cracked area (their friction), but also by the initial opening of the concrete crack, db (table 2, figure 6).

4178

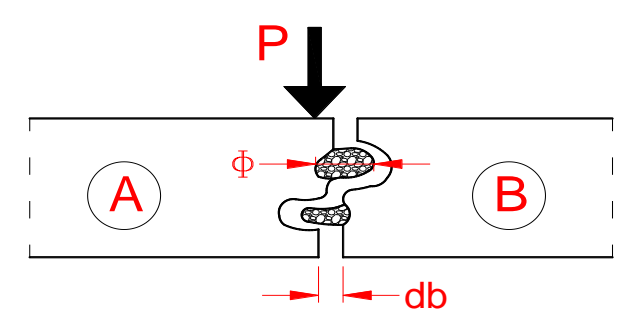


Figure 1.5 The influence of the size of the aggregates Φ , and of the initial opening of the crack, db, on the load transfer

Table 1.2 The initial crack opening of the concrete, db.

Specimen	The initial crack opening of the concrete, db	db/db _{4b}	The number of cycles a which fracture occurs, n _{cR}	
6a	5.492	0.3815	10520	
7a	5.974	0.4150	7790	
7b	8.445	0.5867	4283	
4b	14.39	1	1553	

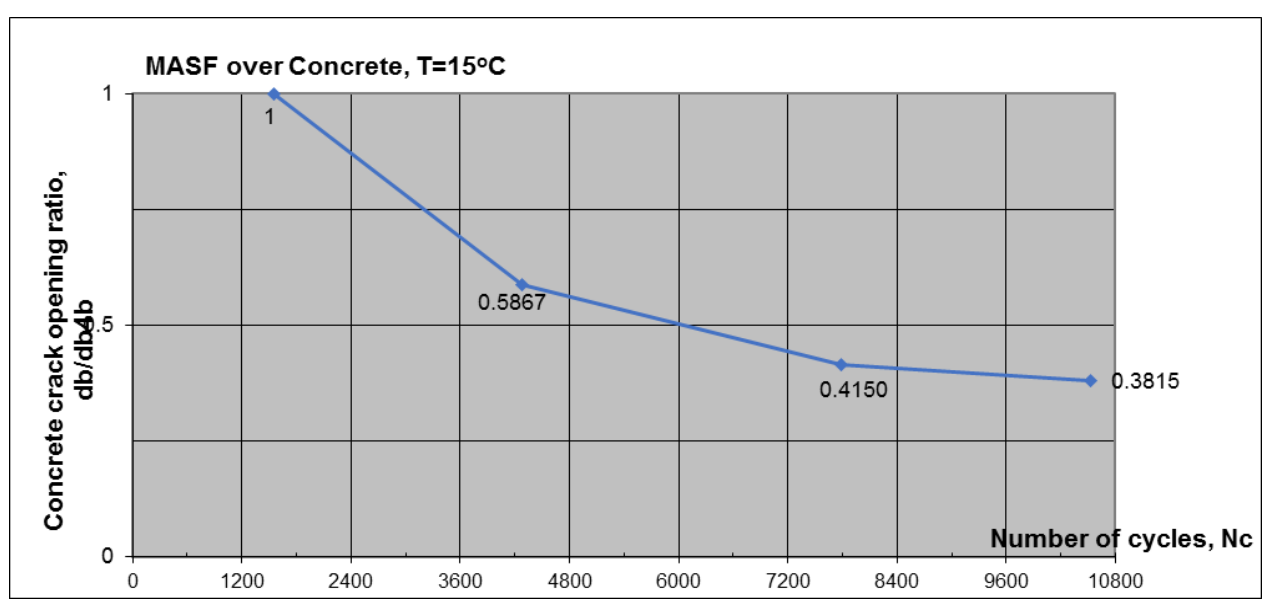


Figure 1.6 The initial crack opening of the concrete depending on the number of cycles

1.3 Research Report no. 3. Identification of the parameters of influence of crack propagation through protective asphalt layers for degraded pavements

The present research report contains interpretations of how the parameters influence the propagation of cracking. It tries to use and adapt some functions known in the literature (exp. Paris Law) to the results obtained, as well as find a way to assess the the behavior of an asphalt protection layer of a degraded road pavement, from the point of view of reflective cracking (transmission of cracks from the old degraded pavement in the asphalt protection layer).

2 FRACTURE MECHANICS

In order to better understand the results of researchers in the issue of cracking of asphalt protection layers, I will review the approaches to cracking in general: the energy criterion (G) and the stress intensity factor (K).

2.1 The energy criterion

It was Griffith who initiated this theory, Irwin further developing it. This approach assumes that the crack propagates when the energy accumulated in its area is greater than the strength of the material. [6]

The variation of the energy G is defined as the variation of the potential energy with the cracked surface of an elastic linear material.

$$G = \frac{\pi \cdot \sigma^2 \cdot a}{E} \tag{6}$$

Relation 6 is valid in the case of a plate of infinite dimensions (the width of plate B is much larger than 2a) subjected to a stretching force, having a crack length equal to 2a (Figure 2.1).

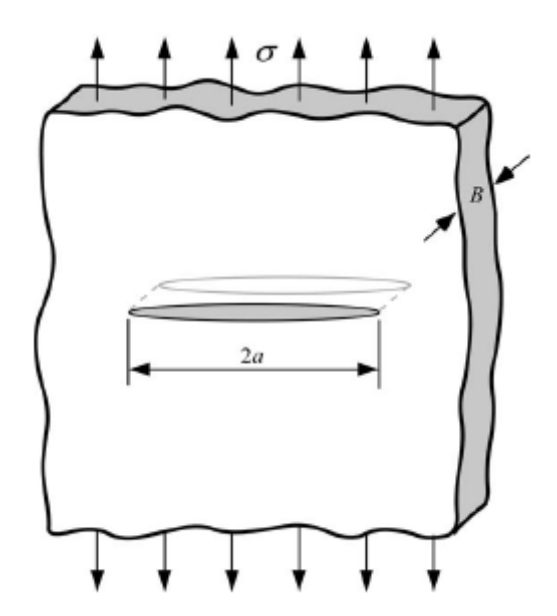


Figure 2.1 Crack in a plate of infinite size [6]

2.2 Stress intensity factor K

The stress intensity factor characterizes the state of stresses and deformations at the top of the crack (Figure 2.2) and has as [6]:



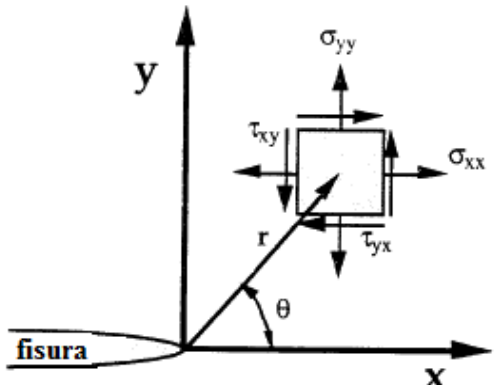


Figure 2.2 The stresses present near the tip of the crack [6]

The relationship between energy variation and stress intensity factor is obtained from the equations 6 şi 7:

$$G = \frac{K_I^2}{E} \tag{8)[6]}$$

2.3 Crack propagation over time (material fatigue)

To determine how a crack propagates through the material, Paris's law can be used (equation 5) which expresses the speed of crack propagation $\left(\frac{da}{dN}\right)$, the stress intensity factor K. We can thus find out at any time what is the length of the crack, so in the case of asphalt protection layers, what is the optimal time to be intervened by the responsible authorities, with minimal costs.

The materials to which this approach can be applied can be divided into linear-elastic and elasto-plastic (these are not influenced by the loading time), but also visco-elastic and visco-plastic materials, which depend on the loading time.

Research in the field of cracking has used existing theories and adapted them to the observed material, the calculation of K becoming more complicated as its behavior changes from linear to nonlinear (including variation over time). If in the case of linearly elastic materials, it was possible to find empirical relations that would determine its value as correctly as possible, in the case of elasto-plastic, but also in those with a viscous component, it was necessary to use the finite element.

2.4 Cracking of materials with linear elastic behavior

A material has an elastic linear behavior when the relationship between stress and strain is linear, and the strain returns to 0 when the applied load is removed. (Figure 2.3). The law that governs these materials is Hooke's law.

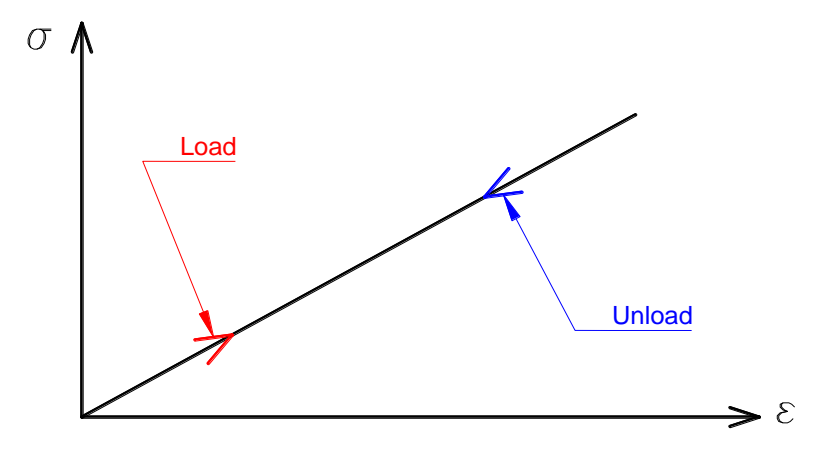


Figure 2.3 Liniar elastic behavior

In the case of these materials, the stress intensity factor was determined taking into account the size of the plasticized area r, which appears at the top of the crack.

In the case of the Irwin model, this area has the shape of a circle of radius r.

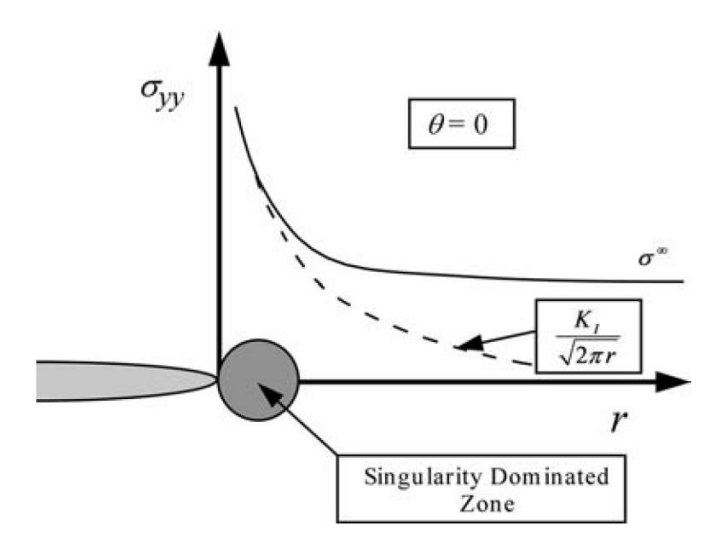


Figure 2.4 Plasticised zone, Irwin model.

The stresses in the cracking plane (r axis, Figure 2.4) from the immediate vicinity of the crack tip, in the mode I of stress, are obtained considering $\theta = 0$ (Figure 2.2):

$$\sigma_{xx} = \sigma_{yy} = \frac{K_I}{\sqrt{2 \cdot \pi \cdot r}} \tag{9}[6]$$

Starting from equation 7, valid in the case of an element with infinite dimensions, the relation (10) was determined also in the case of an element with finite dimensions, introducing a dimensionless constant Y, which depends on the geometry of the sample and the stress mode.

$$K_I = Y \cdot \sigma \cdot \sqrt{\pi \cdot a} \tag{10}$$

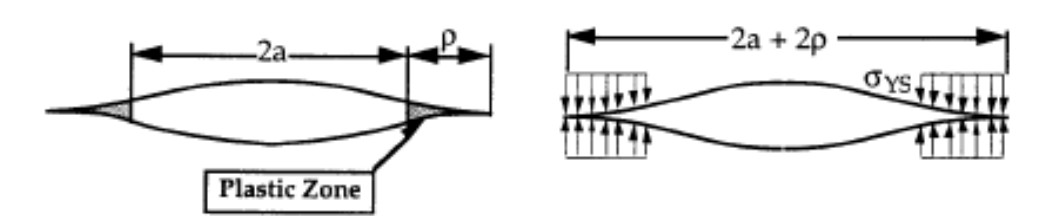
The relation for which the values of K_I were found in the Table 2.1 is given by the equation 11:

$$K_{I} = \frac{P}{B \cdot \sqrt{W}} \cdot f\left(\frac{a}{W}\right) \tag{11)[6]}$$

GEOMETRY f(a/w)*Single Edge Notched Tension (SENT) 11-Single Edge Notched Bend (SENB) ₽₽ $1-0.025\left(\frac{a}{w}\right)$ Center Cracked Tension (CCT) Double Edge Notched Tension (DENT) Compact Specimen

Table 2.1 Calculation relations for K_I, linear elastic materials [6]

The Dugdale-Barenblatt model is another approach to finding the plasticized area, which is no longer in the shape of a circle, but has the shape from Figure 2.5.



a. The shape of the plasticized area

b. compressive stress

Figure 2.5 The Dugdale-Barenblatt model

It was possible to determine the size of the plasticized area, ρ , depending on the stress intensity factor K and the compressive stress, an effort that has values σ_{YS} around the flow resistance of the material.

$$\rho = \frac{\pi}{8} \cdot \left(\frac{K_I}{\sigma_{VS}}\right)^2 \tag{12)[6]}$$

The 2 models, Irwin şi Dugdale, give approximately the same values for the plasticized area.

The stress intensity factor, using the Dugdale-Barenblatt model, was determined by Burdekin and Stone, with values much closer to the truth than that obtained by Dugdale and Barenblatt.

$$K_{eff} = \sigma_{YS} \cdot \sqrt{\pi \cdot a} \cdot \left[\frac{8}{\pi^2} \cdot lnsec\left(\frac{\pi \cdot \sigma}{2 \cdot \sigma_{YS}} \right) \right]^{\frac{1}{2}}$$
 (13)[6]

Throughout this study, it was considered that the actual length of the crack is equal to the visible length of the crack plus the size of the plasticized area. These plasticity corrections can extend the conclusions from the elastic linear domain and beyond, but when the behavior of the material becomes nonlinear, as in the case of asphalt mixture, the stress intensity factor no longer characterizes the crack (calculated with the relationships in crack mechanics at the stage linear elastic). That is why two other ways of calculating its behavior at the top of the crack were introduced, CTOD (crack type opening displacement) - the displacement of the opening from the top of the crack and the integral on the contour *J*.[6]

2.5 Cracking of materials with elasto-plastic behavior

In a material with elasto-plastic behavior, the relationship between stresses and deformations is more linear, and the deformation returns to 0 when the applied load is removed. (Figure 2.6). At the beginning of the load the material behaves elastically, the relationship between stress and deformations being linear, and after the stress exceeds a certain value, the material becomes plastic, the relationship becoming nonlinear, the discharge being linear with a slope equal to the modulus of elasticity elastic zone).

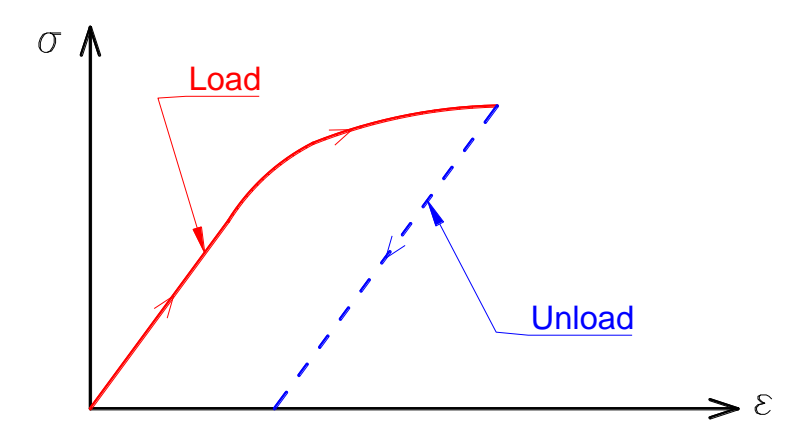


Figure 2.6 Elasto-plastic behavior

As mentioned above, in order to be able to model the crack in the case of materials with nonlinear behavior, the two parameters CTOD and J-integral were introduced.

2.5.1 CTOD

The need for the CTOD parameter arose when Wells noticed that before the crack propagated (the stresses in the plasticized area reach and exceed the crack resistance of the material), the tip of the crack no longer has a sharp shape, but has a bluntness. It can be said that the tip of the crack has a certain opening noted with δ (Figure 2.7, [6]).

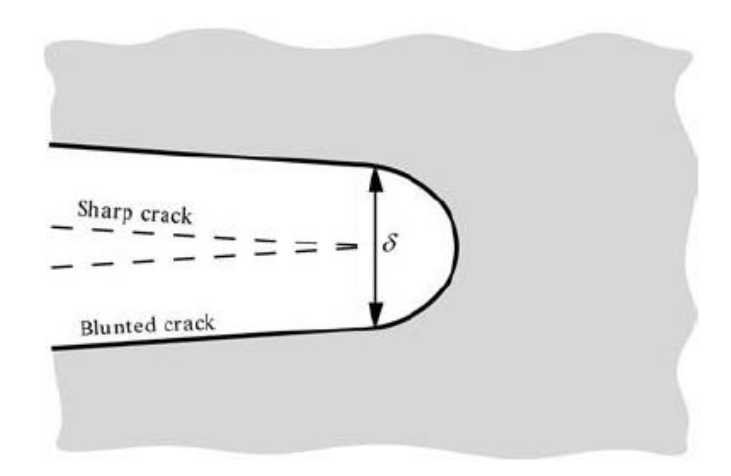


Figure 2.7 The opening at the top of the crack, δ

The CTOD parameter was determined (Figure 2.8, [6]), starting from the Irwin model, with the plasticized radius area r_y (relation 4), considering the opening $\delta = 2 \cdot u_y$. u_y is the displacement in the y direction of the crack determined in the hypothesis of linear elastic behavior. Relation 14 is valid when the flow area of the material is very small.

$$\delta = \frac{4}{\pi} \cdot \frac{K_I^2}{\sigma_{YS} \cdot E} = \frac{4}{\pi} \cdot \frac{G}{\sigma_{YS}} \tag{14}$$

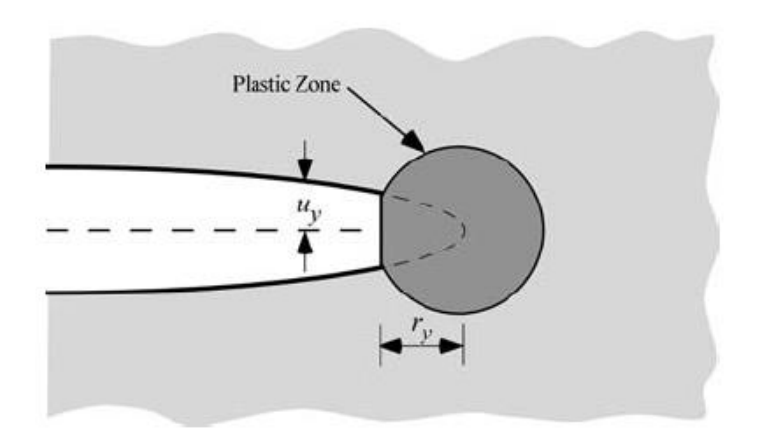


Figure 2.8 CTOD calculated according to the Irwin model

Another method of calculation is based on the Dugdale-Barenblatt model (Figure 2.9, [6]). The hypotheses of this model are a plane stress state and material that retains its elasticity (does not stiffen).

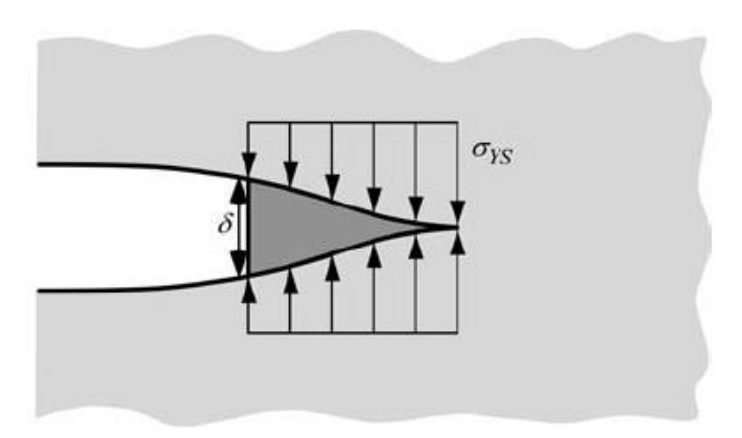


Figure 2.9 CTOD calculated according to the Dugdale-Barenblatt model

$$\delta = \frac{\kappa_I^2}{\sigma_{YS} \cdot E} = \frac{G}{\sigma_{YS}} \tag{15}$$

Regarding the 3-point test (Figure 2.10), the CTOD is determined by measuring the crack opening at the top (V), assuming that the two halves are rigid and rotate around a point (joint) at the intersection of the 2 faces of the crack.

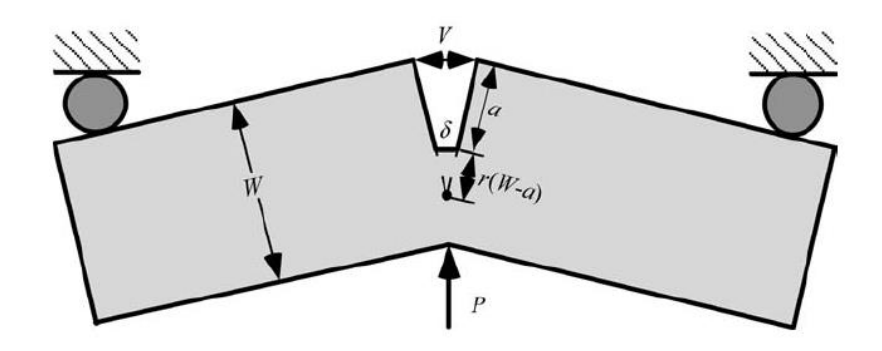


Figure 2.10 Experimentally determined CTOD, 3-point bending test

Research Report no. 3. Identification of the parameters of influence of crack propagation through protective asphalt layers for degraded pavements

$$\delta = \frac{r(W-a) \cdot V}{r(W-a) + a} \tag{16}[6]$$

r (rotation factor) is a adimensional constant with values between 0 and 1.

This "articulated" model is not very correct when we have mainly elastic deformations. That is why both the elastic component through the stress intensity factor and the plastic component in the shape of the equation 16 are introduced in the CTOD calculation.

$$\delta = \delta_{el} + \delta_{pl} = \frac{K_l^2}{m \cdot \sigma_{YS} \cdot E'} + \frac{r_p \cdot (W - a) \cdot V_p}{r_p \cdot (W - a) + a}$$

$$\tag{17)[6]}$$

m is a adimensional constant

m = 1 for constant stress

m=2 for constant deformation

2.5.2 J-contour path integral

J-integral was introduced by Rice [8] in 1968 and represents the energy available per unit area of the crack (taking into account the plasticized area) [9]. Its applicability to nonlinear-elastic and elasto-plastic materials has several restrictions, the most important being that the unloading must not take place. In other words, it is not valid for cyclic uploads (these involve load-unload).

The J-integral was expressed in several forms, this characterizing the crack both in terms of energy and stresses at its peak for a non-linear elastic material (which can be similar to an elastic-plastic material).

 Variation of energy released during loading (ratio between the variation of potential energy and the area considered)

$$J = -\frac{dE_p}{dA}$$

Or for constant stress load (as it is the case of the test made with the Cracking Device with Temperature Control for this thesis), the relation becomes:

$$J = \left(\frac{dU^*}{da}\right)_p \text{ sau } J = \left(\frac{\partial}{\partial a}\int_0^p \Delta dP\right)_p$$

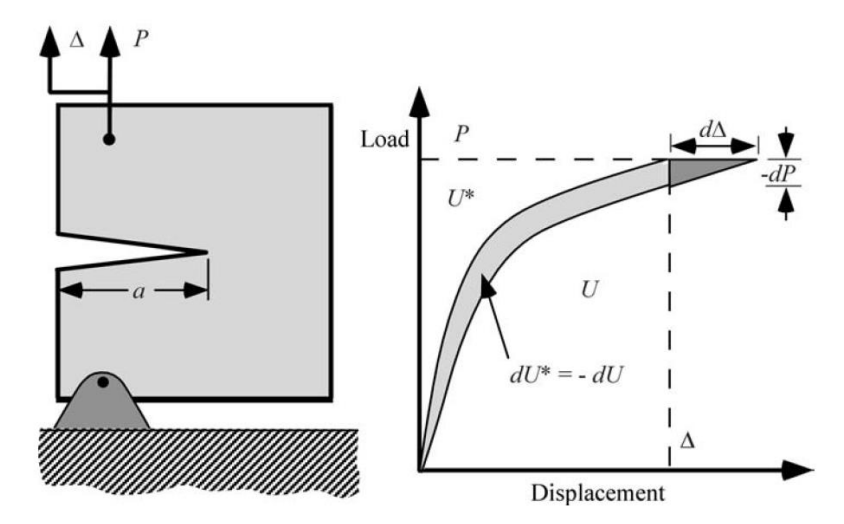


Figure 2.11. J-integral expressed as the variation of the released energy [6]

• J-integral as a independent contour line (Figure 2.12). This contour should be chosen as far as possible from the plasticized area at the top of the crack.

$$J = \int_{\Gamma} \left(w \cdot dy - T_i \cdot \frac{\partial u_i}{\partial x} ds \right)$$

w -the specific deformation energy

 T_i –Traction vector in a point of the contour

u_i –Displacement vector

ds -Length growth on the considered contour

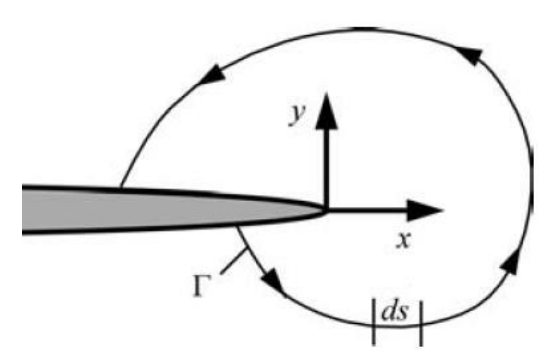


Figure 2.12 Arbitrarily chosen contour around the crack [6]

• J as a parameter for the stress intensity factor

$$\sigma_{ij} = k_1 \cdot \left(\frac{J}{r}\right)^{\frac{1}{n+1}}$$

 k_1 –constant of proportionality

It should be noted that for n = 1, the relationship is similar to that of the stress intensity factor K in linear elastic mechanics

3 THE CONCEPT OF REFLECTIVE CRACKING PUBLISHED IN THE SPECIALTY LITERATURE

Reflective cracking is the process of transmitting to the surface of the roadway the cracks of hydraulic or thermal contraction in the layers composed of natural aggregates stabilized with hydraulic or puzzolanic binders, or from the dynamic stresses generated by an intense and heavy road traffic. In the case of reinforcing existing roads, this process may refer to the transmission to the surface of the new bituminous pavement of cracks and/or cracks existing in the old road pavement [10]. So, the reflective cracking occurs due to the traffic loads, but also to the temperature variations that induce in the structure contraction and stretching efforts.

We can consider that there are 2 stages of the cracking process [11], without taking into account the last stage of failure, in which the crack propagation speed increases rapidly:

- **Crack initiation** characterized by microcracks that transform into macrocracks and can be defined as the number of cycles in which the stress to which the crack is visible in the protective layer is applied.
- The propagation of the crack represents the stage in which the crack propagates to the surface of the layer, on its entire thickness. The propagation of the crack in the case of flexible layer can be expressed by the law of Paris and Erdogan (relation 5).

The following empirical relations can be used to determine the parameters A and n (material constants) [12]:

$$n = c_1 \cdot \frac{2}{m}$$
-for controlled displacement (18)

$$n = c_1 \cdot 2 \cdot \left(1 + \frac{1}{m}\right)$$
 -for controlled stress (19)

Where m – the slope of the compliance curve for a given loading time (t)

$$m = a_2 + 2 \cdot a_3 \cdot \log t \tag{20}$$

 c_1 şi c_2 – coefficients that depend on the rigidity of the mixture, respectively on the air voids in the mixture

Material constant A is determined by several factors, such as the complex modulus (E*), the tensile strength of the mixture (σ_t), the fracture energy of the mixture (Γ), but also the slope of the compliance curve (m).[12]

Another relation used by Mostafa M. Elseifi şi Imad L. Al-Qadi [11], has the following expression:

$$logA = -2.605104 + 0.184408 \cdot AV - 4.704209 \cdot logAC - 0.00000066 \cdot E \tag{21}$$

where AV -air voids%

AC -bitumen content %

E - the resilient modulus of the mixture. (also called dynamic modulus of elasticity if the determination is made in the elastic domain).

However, in order to find out these constants as accurately as possible, it is necessary to carry out tests on beams made of the respective mixture, beams subjected to repeated loads.

In the experiments performed by Mostafa M. Elseifi and Imad L. Al-Qadi, a finite element program was used that determines the indirect K factor using the independent contour integral J.

3.1 Prediction of existing reflective cracking potential of flexible pavements", Jorge C. Pais și Paulo A.A. Pereira [13]

In this material the authors reach the following conclusions:

- The potential of reflective cracking is generated by a characteristic function of the properties of the materials, mainly the thickness of the protective layer and its rigidity.
- Reflective cracking is the result of vertical and horizontal differential movements above the
 crack in the existing structure. These movements, also called crack activity, are caused by
 temperature stress, traffic loads, or a combination of the two.
- Crack activity in existing cracked structures was measured by Rust, 1987, using a device called CAM (Figure 3.1) that measures the relative movement of the crack edges.

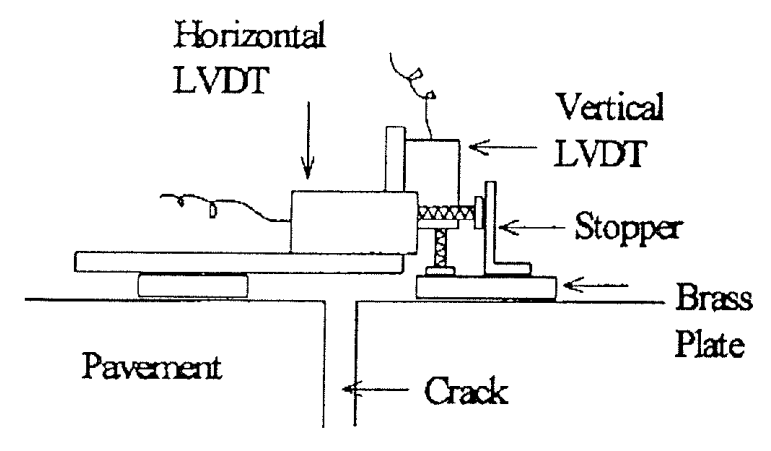


Figure 3.1 CAM Device (Crack Activity Meter)

The test was based on finding a function that predicts the evolution of the crack after laying the protective layer, using the evolution of the crack before laying, the existing structure, taking into account the characteristics of the component materials of the protection.

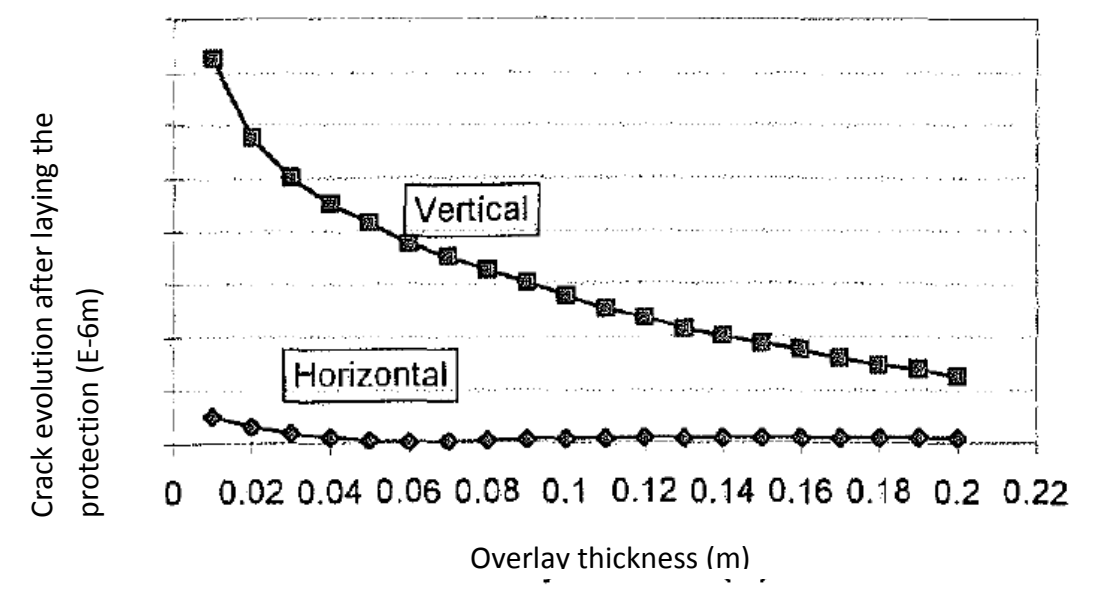


Figure 3.2 Crack evolution measured with CAM, depending on the thickness of the protective layer

Using the finite element method, they reached to 2 conclusions:

- After laying, the horizontal component of the crack is of little importance compared to the vertical one. In all simulations performed, the horizontal component may not reach a level higher than 50% of the vertical
- After laying, the vertical component is much smaller and follows a logarithmic function that depends on the thickness of the layer

To take into account the effects of temperature that affect the horizontal component, it must reach at least 50% of the vertical component after laying. Since the maximum horizontal value is 50% of the vertical value, the effects of temperature are negligible in reflective cracking.

3.2 "Lab asphalt testing evaluation of reflective cracking", Fujie Zhou, Lijun Sun[14]

In this paper it is concluded that reflective cracking occurs in 3 stages, namely:

- Detachment of the asphalt layer from the existing structure occurs due to the high tangential force present at the interface between the 2, given by traffic loads.
- As the number of loading cycles increases, this detachment area increases. Studies show that part of this detachment is beneficial for preventing the process of reflective cracking, but up to a width of 10cm. In other words, there is an optimal dimension of this detachment. The effort σ_1 is found at 5-10cm from the joint (crack) for a detachment of 5-32cm. This is the 2nd stage, when the crack occurs at 4-6cm from the joint, and not near the joint.

• σ_y predominates in σ_1 , especially after the width of the detachment is greater than 5cm. So, the propagation of the crack is mainly due to σ_y . The third stage is the vertical development of the crack towards the upper face of the protective layer.

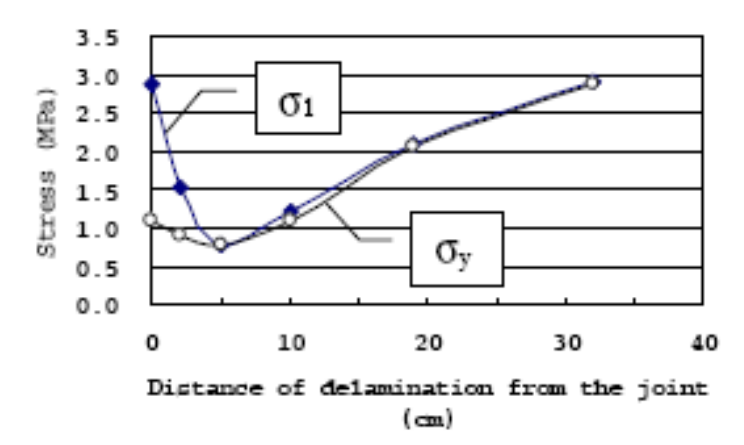


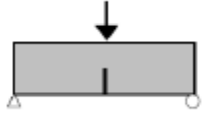
Figure 3.3 The effect of detachment of asphalt from cement concrete on σ_1 and σ_v efforts

3.3 "New procedures and criteria for asphalt mixes and pavements design regarding fatigue failure and thermal stresses", F. Perez Jimenez, R. Miro, A. Martinez, R. Botella, G. Valdes[15]

Although it is not a study of reflective cracking, these 2 new test methods must be mentioned. The methods were developed in the Road Research Laboratory of the Technical University of Catalonia for the design of asphalt mixtures but also for the evaluation of fatigue cracking: Fenix and EBADE

Existing experimental methods that simulate crack initiation and propagation:

• 3- or 4-point bending tests for a rectangular edge notched beam, SENB type (single edge notched beam specimen)



• 3-point bending tests for a semicircular beam with marginal notch type SCB (semicircular bending test)



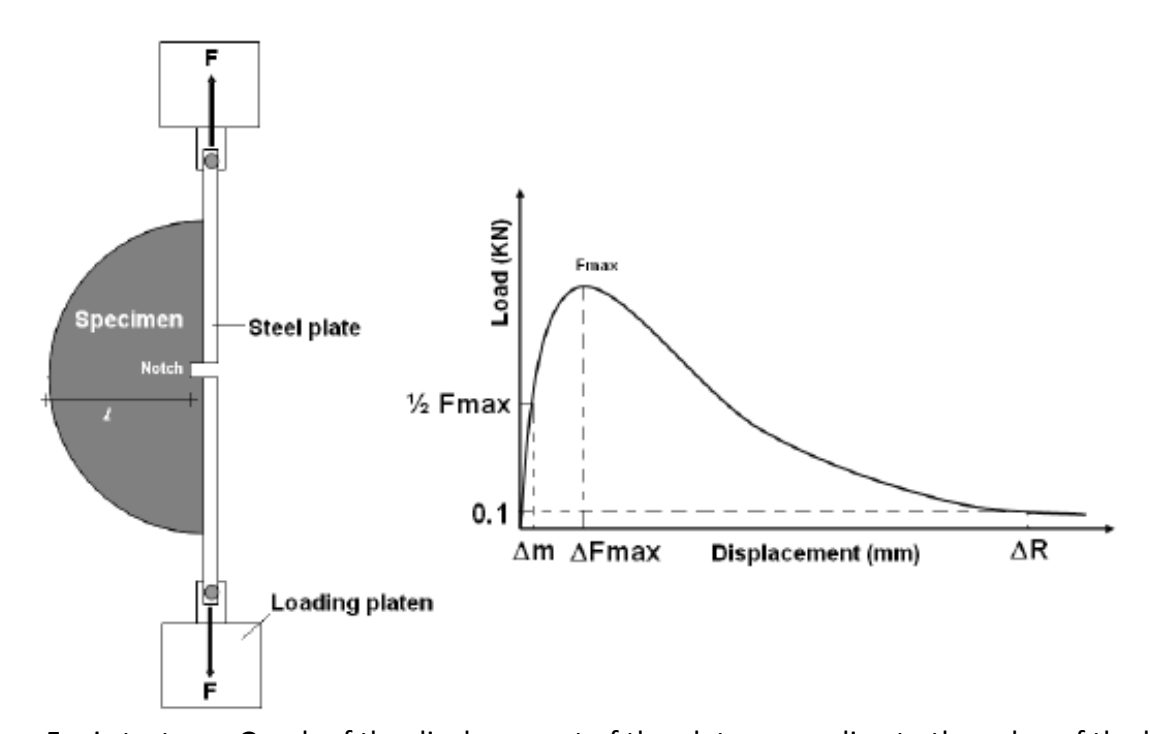
 compact tensile test on a disked-shaped compact tension test DC(T) (disked-shaped compact tension test)



Fenix method

The method combines bending tests on the SCB semicircular beam and the traction beam. The test piece is a semicircular notched beam (6mm deep) located in the middle of the flat face, tested for traction, a load made by applying a displacement (speed of 1mm/min) on the metal plates glued to one side and the other of the notch.

The purpose of this laboratory test is to evaluate the crack strength of bituminous mixtures by determining the energy dissipated during the test (a combination of creep dissipated energy and crack energy).



Fenix test Graph of the displacement of the plates according to the value of the load Figure 3.4 Experimental data: strength and displacement

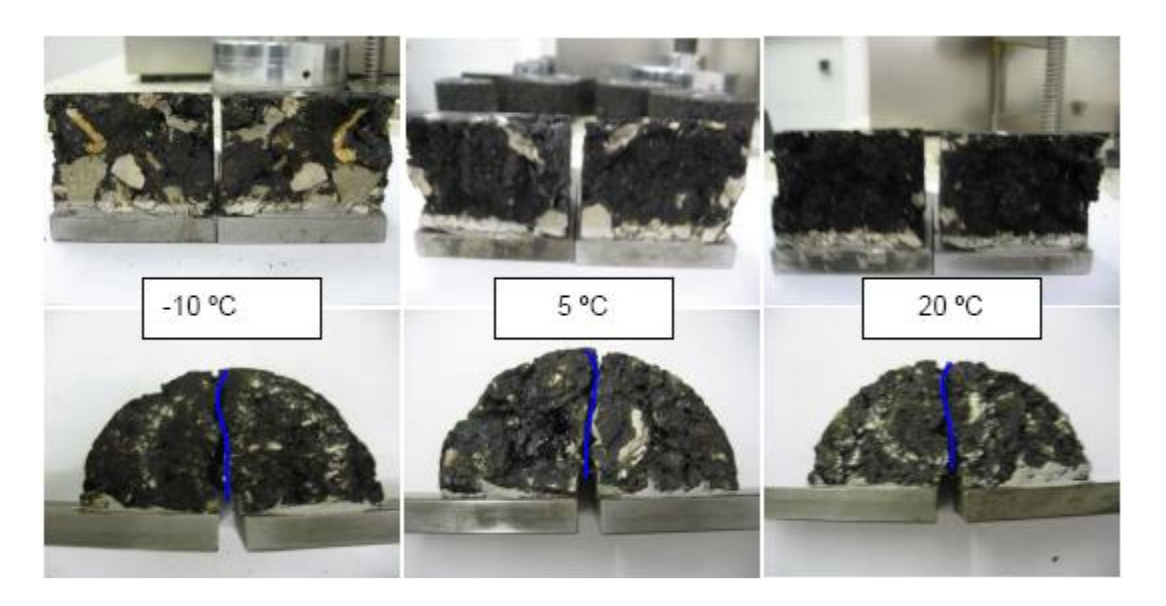


Figure 3.5 Views of the cracked surface (top) and crack propagation (bottom), respectively

$$G_{D} = \frac{W_{D}}{h \cdot l}$$

Dissipated energy:

G_D –dissipated energy (J/m2)

 W_D –dissipated mechanical work =the area made by the strength-displacement curve (kN.mm)

h -specimen thickness (m)

I –circular beam radius minus the notch

$$I_{RT} = \frac{\frac{1}{2} \cdot F_{\text{max}}}{\Delta_{\infty}}$$

Tensile stifness index IRT.

Conclusion: Fatigue cracking resistance can be expressed as a function of the dissipated energy G_D and I_{RT} by defining an area with mixtures that have a better fatigue behavior. At the same I_{RT} , mixtures with a higher value of dissipated energy G_D perform better.

EBADE method (Strain Sweep Fatigue Test)

Unlike the Fenix method, this involves the application of displacement steps (a certain number of cycles is kept constant, after which it is gradually increased). It is a fatigue test that involves a shorter and less expensive time than the classic ones (fatigue test on trapezoidal samples, 4-point test on prismatic specimens).

The method involves applying a constant displacement (positive and negative) through a piston, on one end of the prismatic specimen, the other being fixed. This simulates compressive and tensile loads (sinusoidal load).

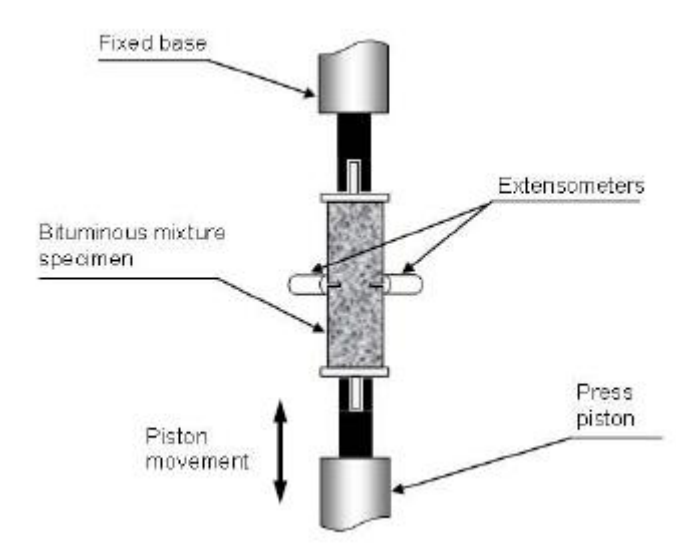


Figure 3.6 Testing stand of the EBADE method

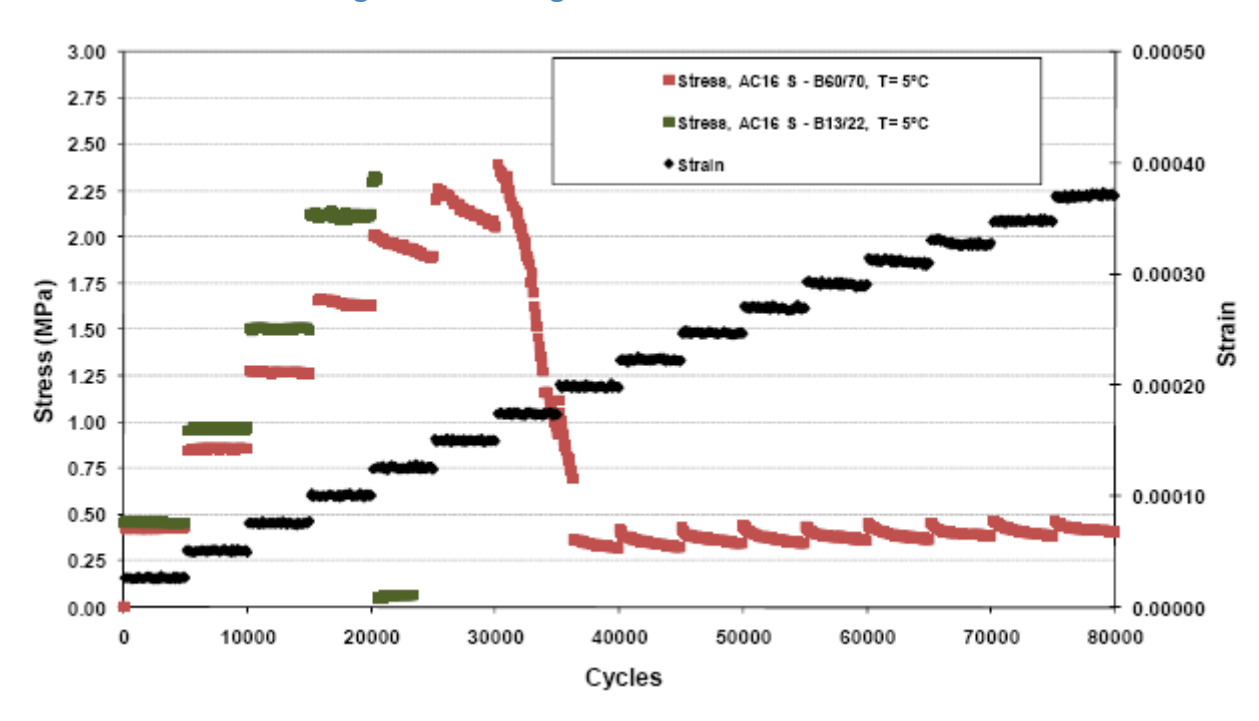


Figure 3.7 Graph of stresses and strains depending on the number of cycles, EBADE method.

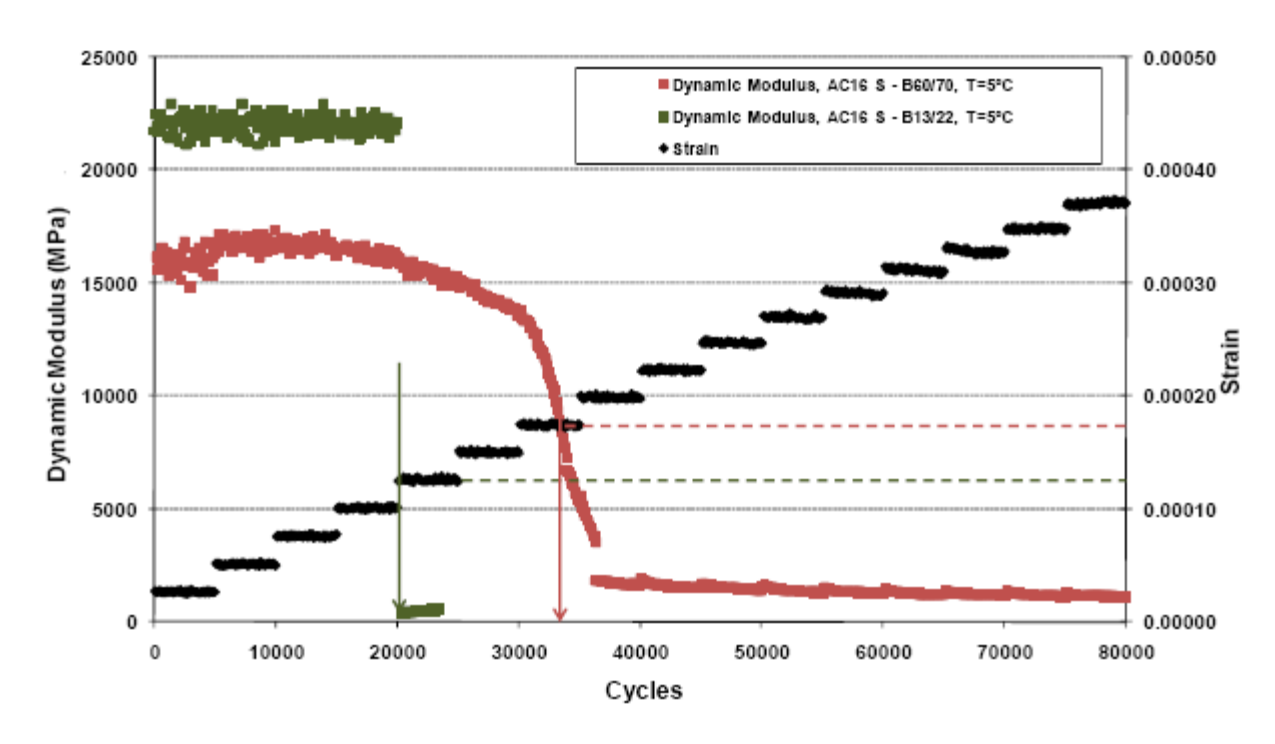


Figure 3.8 Stiffness modulus depending on the number of cycles.

3.4 "Investigation of cracking in bituminous mixtures with a 4PBT", M.L. Nguyen, C. Sauzeat, H. Di Benedetto, L. Wendling[16]

The authors performed tests using the 4-point test, in which the load is applied to the top, and the sample has a cut of 2 cm in the middle, across the entire width (simulating the presence of a crack).

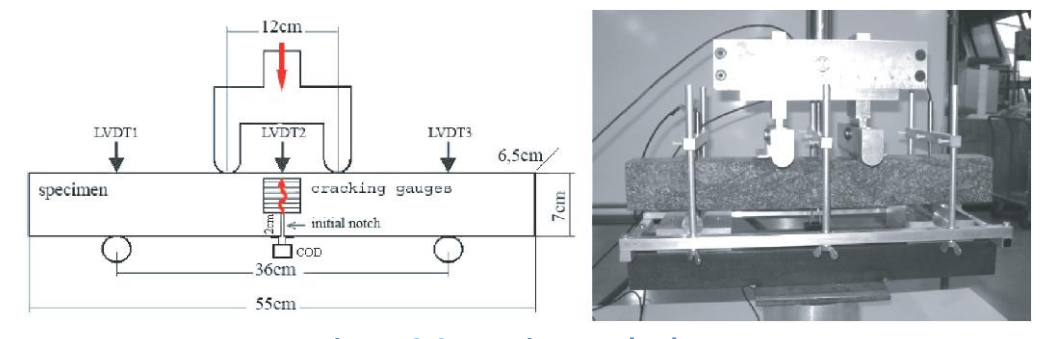


Figure 3.9. 4-point notched test

The arrow (deformation) of the specimen is measured by means of sensors (LVDT) which record their movement during the test. They noted it with f.

$$f = LVDT2 - \frac{LVDT1 + LVDT3}{2}$$

The crack length was measured experimentally with 2 devices glued to one side and the other of the sample. The device consists of 21 parallel wires at a distance of 2.5mm (they have a length of 8cm). A disadvantage of this method is that crack detection can be delayed by wire resistance.

As we saw in the previous chapter, one of the methods for evaluating crack propagation is CTOD. In this article we use something similar, namely COD (crack opening displacement), measured with an extensiometer.

The method used below is called DRCL (displacement ratio method for predicting crack length).

$$r_{\rm dm \check{a}s} = \frac{{\it COD}}{f}$$

Using the finite element, this ratio was calculated for different values of the crack length (a), following that in the last part of the method the measured values will be compared with the calculated ones. Finite element modeling calibration is considered good when the experimental results are close to the experimental ones.

$$f(a)_{EF} = r_{dm\bar{a}s}$$

For the calculation, the known formula of the $\mathbf{K}_{\mathbf{I}}$ stress intensity factor was used, which includes the form factor \mathbf{Y} .

$$K_{I} = \frac{3}{2} \cdot \frac{P \cdot (L - l)}{B \cdot w^{2}} \cdot Y(x) \cdot \sqrt{a}$$

where:

P -the load at which the fracture occurs

I – the upper opening of the supports

L – the lower opening of the supports

B -specimen width

w -specimen height

a -crack length

x=a/w – the relative depth of the cut

$$Y(x) = \left[\frac{w}{3 \cdot (L-l)}\right] \cdot \sqrt{\frac{3 \cdot E \cdot B}{x} \cdot \frac{dC}{dx}}$$
 -form factor

C -compliance

3.5 The conclusions extracted from the specialized literature

From the processing of the extracted information, the following defining conclusions can be drawn for the reflective cracking and the characterization of the parameters for its generation, as follows:

- The potential of reflective cracking is generated by a characteristic function of the properties of the materials, mainly the thickness of the overlay and its rigidity
- Reflective cracking is the result of vertical and horizontal differential movements above the crack in the existing structure. These movements, also called crack activity, are caused by temperature stress, traffic load, or a combination of the two.
- To consider the effects of temperature that affect the horizontal component, it must reach at least 50% of the vertical component after laying. Since the maximum horizontal value is 50% of the vertical value, the effects of temperature are negligible in reflective cracking.
- In this overlapping effect of road traffic demands with seasonal temperature variations in the composite road structure (asphalt on cement concrete), there are requests to shear the asphalt layer over the existing crack / crack in the cement concrete support layer, which by developing the phenomenon of local fatigue, leads to the initiation and development during the exploitation of the road of the cracking and its transmission through the asphalt layer
- The notion of equivalent shear appears in the area of the existing crack / crack in the asphalt support layer, which can be defined by the fatigue life.
- Reflective cracking occurs in 3 stages:
 - Detachment of the asphalt layer from the existing structure occurs due to the high tangential force present at the interface between the 2, given by traffic loads.
 - O As the number of load cycles increases, this detachment area increases. Studies show that part of this detachment is beneficial for preventing the process of reflective cracking, but up to a width of 10cm. In other words, there is an optimal dimension of this detachment. The effort s1 is found at 5-10cm from the joint (crack) for a detachment of 5-32cm. This is the 2nd stage, when the crack occurs at 4-6cm from the joint, and not near the joint.
 - \circ σ y predominates in σ 1, especially after the width of the detachment is greater than 5cm. So, the propagation of the crack is mainly due to σ y. The third stage is the vertical development of the crack towards the upper face of the protection layer.
- In the experiments performed by Mostafa M. Elseifi and Imad L. Al-Qadi, a program
 was used that determines indirect the K factor using the integral independent of
 contour J. This is defined as the change of mechanical energy in the unit area of the
 new cracked surface.
- The FPBNF test has an approach similar to that performed in this doctoral thesis and may be a different approach to that presented in this research report.

4 CONTRIBUTIONS AND INTERPRETATIONS OF REFLECTIVE CRACKING PARAMETERS THROUGH OBSERVATIONS AND PROCESSING OF EXPERIMENTAL RESULTS

Below are some observations on the experiments performed on 10 specimens (4b, 5a, 5b, 6a, 7a, 7b, 8a, 8b, 9a, 9b).

I mention that they had the same pre-cracked cement concrete slab, but also the same asphalt mixture as MASF16 protection layer, as presented in research report number 2, Analysis by statistical interpretation of the solutions obtained in accelerated regime in the laboratory at loads equivalent to road traffic.

The notation of the specimens with **a** and **b** were made for mixture plates (15x30cm) cut from the same plate 30x30cm. Example: a plate called 5 was made measuring 30cm wide, 30cm long; from this, by cutting in half, resulted 2 plates 5a and 5b corresponding to a small-scale slab model, according to which the level of stress assimilated to a road traffic was established. These asphalt slabs, which retain the thickness of an asphalt layer, were glued to the pre-cracked concrete support with a bitumen primer and then tested in turn. The request for cyclic loads assimilated to a road traffic, is applied to the Cracking Device with Temperature Control in ascending loading steps (the force is variable depending on the rigidity of the asphalt mixture), in order to test the specimen in accelerated regime. The application of the accelerated regime is done for the protection of the prototype device used. The reflective crack test is evaluated by performance indices. These are dimensionless coefficients, which represent behavioral reports of tests performed in the same stress regime on road layers made in similar conditions (results on average of at least two attempts resulting from identical making of the 30x30cm plate, divided into 15x30cm specimens) and in controlled temperature conditions.

The experimental observations are related to the different conditions for priming the asphalt slab on the pre-cracked cement concrete support, to the initial opening of the existing crack in the cement concrete slab and, of course, to the structural conditions obtained when making the asphalt slabs.

Interpretations of experimental observations on each test specimen are presented below.

4.1 4b specimen

The force at which the crack of the precast concrete was transmitted in the protection layer and the specimen yielding occurred is 80daN, the number of cycles at which the cracking occurred is $n_{\text{ci4b}} = 1000$ (crack initiation in the asphalt layer), respectively $n_{\text{cCR4b}} = 1553$ yield (crack propagation over the entire thickness of the asphalt layer). The total test time is 388 seconds (provided that the frequency of requests to the Cracking Device with Temperature Control is constant.

Figure 4.1 shows the evolution of the vertical deformation (determined by imaging and recorded by the equipment software) depending on the number of cycles. The number of cycles at which the experiment was stopped was noted with Failure 4b, and with Fracture 4b the moment when the crack propagated through the entire thickness of the protective asphalt mixture. Thus, we can consider the reflective crack resistance capacity for 4b a number of cycles of 1259 and as the lifetime (315 seconds). The calibration of these data obtained by experimental modeling can be achieved by comparative analysis with an experimental sector, when the situation of defects by cracking a rigid road pavement is known, before the application of a protective asphalt layer. The analysis would be lengthy, as the sector will have to be observed during operation and to determine the actual traffic, transformed into computational traffic when the reflective cracks appear on the surface of the protective asphalt layer. This research variant, which requires an adequate financing, constitutes a future direction of analysis of the experimental program proposed by the research project related to the doctoral thesis.

For now, the analysis by experimental modeling in the laboratory will be done only up to the breaking point, respectively until the crack appears on the surface of the asphalt layer and is "visible" over 80% of the thickness of this layer.

In order to have a sufficient period for the capability of the device to record the progressive reflection of the reflective crack through the asphalt layer of the specimen, the test temperature is set at 15 °C, corresponding to a controlled rigidity of the asphalt layer.

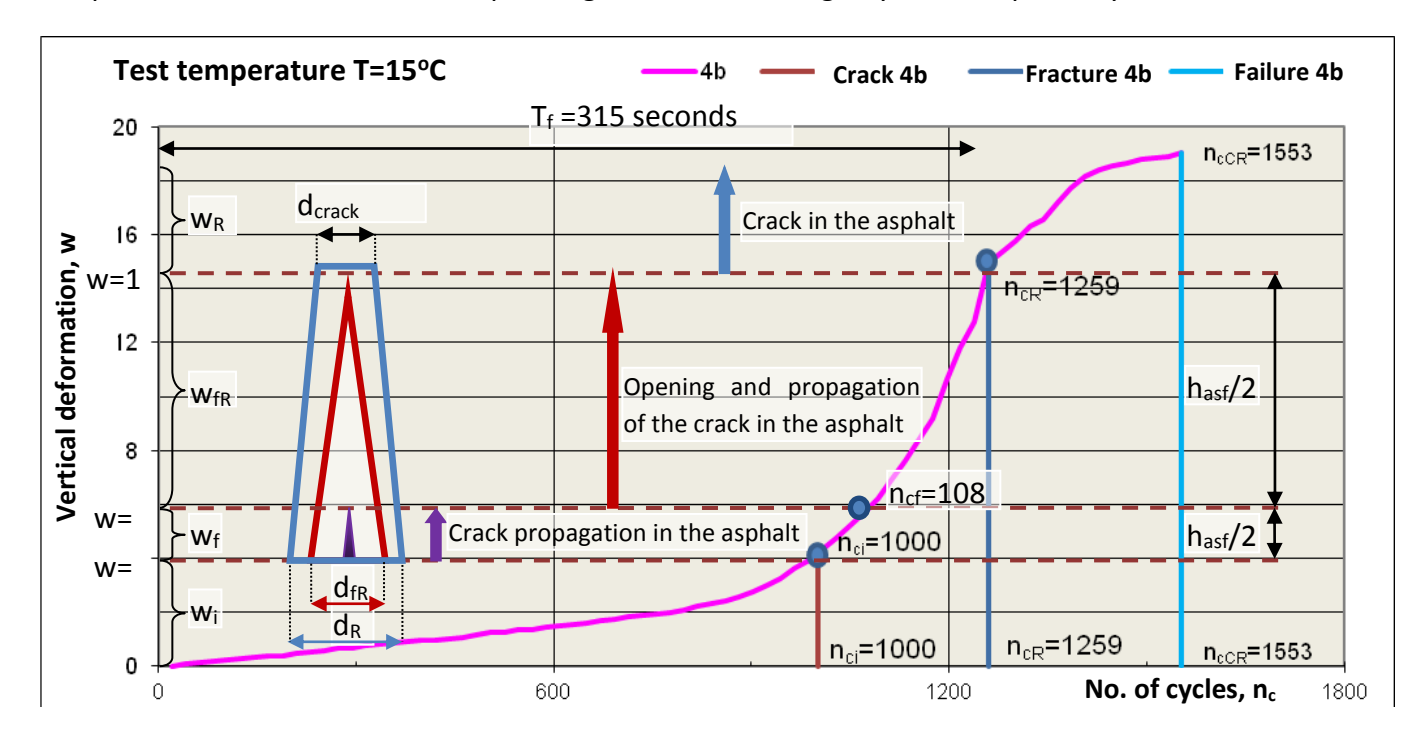


Figure 4.1. Increase of the vertical deformation according to the number of cycles for 4b

Test specimen 4b was used to calibrate the experimental program, in order to identify the parameters of the reflective crack test for the simulation of the asphalt protection layer for cracked concrete pavements degraded by cracking.

Thus, Figure 4.1 highlights the main terms of cracking in the accelerated test by experimental modeling in the laboratory. Considering the variation of the vertical deformation according to the increase of the number of cycles from repeated tensile bending of the precast concrete specimen over which a protective asphalt (4 cm MASF16) was laid, in case of application of the maintenance-repair solution to the rigid road structure, the following analysis parameters can be identified:

- Accelerated cracking service life (T_f)
- Crack opening in the asphalt layer (d)
- Detachment of the asphalt from concrete in the crack area (e)
- Number of cycles at the initiation and propagation of the crack n_{ci}, at the opening and propagation of the crack on the thickness of the asphalt layer n_{cf} and at the yield by fracture n_{cR}=n_{ctot}.
- Vertical deformation (deflection) at the initiation and propagation of the crack $\mathbf{w_i}$, at the opening and propagation of the crack on the thickness of the asphalt layer $\mathbf{w_f}$, at the yield by rupture $\mathbf{w_{fR}}$ and at the appearance of the crack in the asphalt layer $\mathbf{w_{R}}$.

One parameter that should not be neglected, although it does not appear in Figure 4.1, is the opening of the crack in the concrete support layer, db.

The vertical deformation (deflection) at the initiation of the crack $\mathbf{w_i}$ can highlight the maximum deflection in the ground (δ_{adm}), and when the crack appears on the surface of the asphalt protection layer in the ground ($\delta > \delta_{adm}$).

On the experimental sector, by means of deflectometric measurements, Nci corresponding to reaching the admissible deflection (δ_{adm}) and N_{cf} corresponding to the compaction related to the appearance of the crack at the surface of the asphalt layer can be determined.

For the asphalt material used, n_{ci} and n_{cf} are determined experimentally, thus, for other works with the same recipe, times related to the life cycle can be anticipated.

Table 4.1 shows the number of cycles and the vertical deformation at which the cracking, fracture, respectively failure of the test piece 4b occurred.

Table 4.1 The number of cycles and the vertical deformation at cracking, fracture, failure of 4b

Cracking	4b	Failure	4b	
Number of cycles, n _{ci}	Vertical deformation,	Number of cycles, n c	Vertical deformation,	
Number of cycles, ng	w	Number of cycles, ne	w	
n _{ci} =1000	4.3086	n _{cCR} =1553	19.0684	
		Fracture	4b	
		n _{cR} =1259	12.768	

A simple calculation indicates that approximately 80% of the life cycle of the mixture is consumed until the crack appears and 20% of the time is the propagation of the crack through the asphalt layer (Table 4.2). The number of cycles corresponding to crack propagation is 259.

Specimen	Reflective cracking index. If	Number of cyclesat reflective crack propagation				
4b	$I_f = \frac{n_{ci}}{n_{cR}} = \frac{1000}{1259} = 79.43\%$					

Two of the parameters measured in the experiment, which indirectly influence the propagation of the crack through the asphalt protection layer, are: the initial opening of the cement concrete crack (d_{bi} , friction cooperation between aggregates and / or between the cement stone), and the initial detachment of the layer of asphalt from the concrete slab (e_i , the bitumen bonding between the concrete and the mixture). These are shown in Figure 4.2, and the values for sample 4b, used in the experimental program calibration study, are given in Table 4.3.

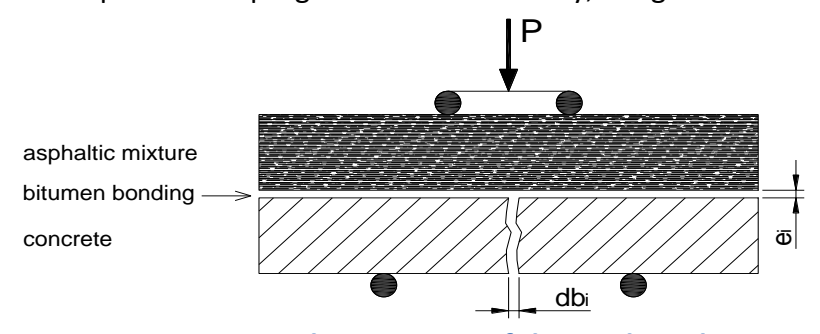


Figure 4.2 Initial parameters of the crack study

Table 4.3 Initial opening values dbi and the initial detachment (bitumen bonding) ei

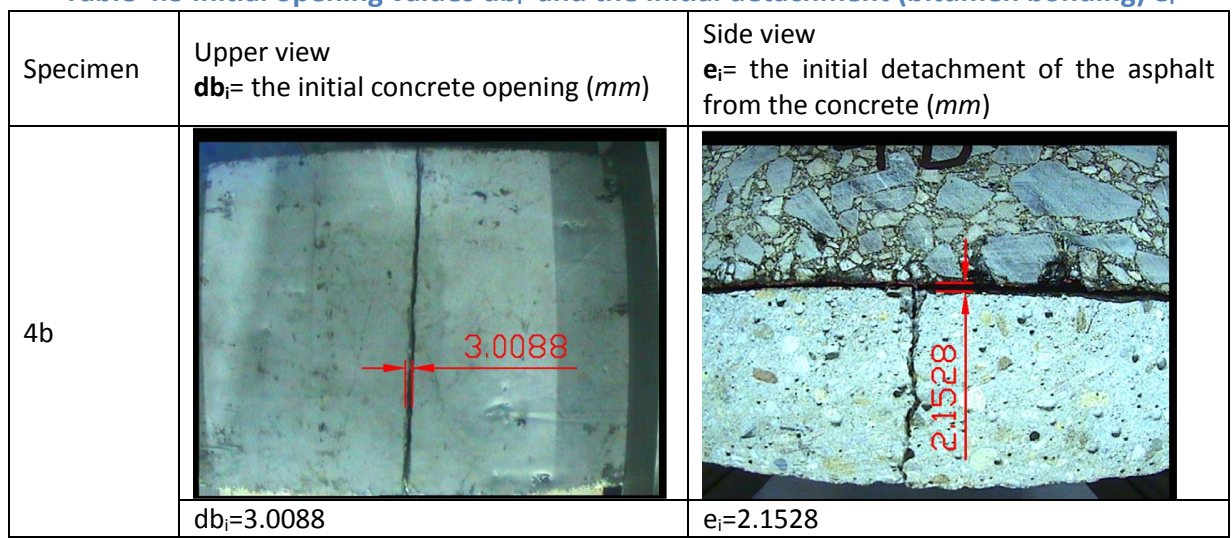
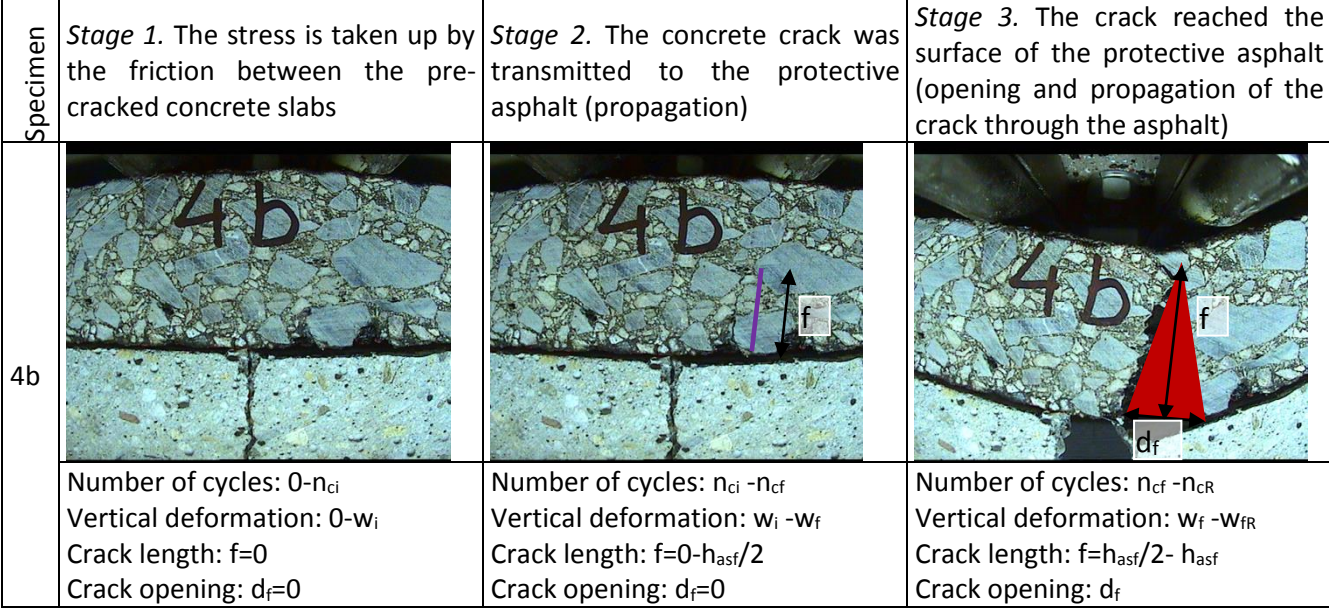


Table 4.4 Stages of reflective cracking in the case of laying the protective asphalt layer over a concrete pavement



In the second part of the test, when the crack was transmitted to the asphalt slab, other parameters were measured such as the opening \mathbf{d} and the length \mathbf{f} of the crack in the asphalt (Figure 4.3).

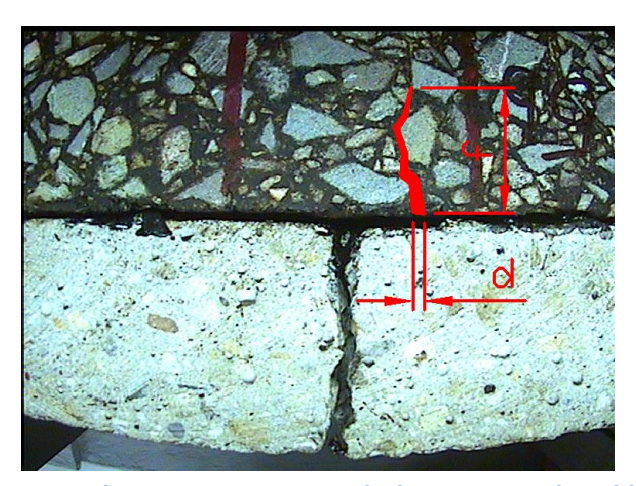


Figure 4.3 Crack parameters in asphalt, opening d and length f

The following notations will be used below:

- $n=rac{n_c-n_{ci}}{n_{cR}-n_{ci}}$ -pentru $n_c\geq n_{ci}$
- **d exp** asphalt crack opening measured on an experimental model
- d calc asphalt crack opening measured on an mathematical model
- **f exp** asphalt crack length measured on an experimental model
- f calc asphalt crack length measured on an mathematical model
- **db exp** concrete crack opening measured on an experimental model
- **db calc** concrete crack opening measured on an mathematical model

The measurements and processing of these parameters (Table 4.5), crack length and opening, for 4b specimen indicate:

• The variation of the crack opening **d**, but also of the length **f** in relation to **n**, is nonlinear (Figure 4.4). The regression model that best describes this relationship is:

$$y = \frac{a_0 \cdot n}{1 + a_1 \cdot n + a_2 \cdot n^2} \tag{22}$$

When
$$y = d$$

$$a_0 = 6.43, a_1 = -0.6115, a_2 = 0.01166,$$

Standard deviation S=0.4708, and the correlation coefficient r=0.998.

When
$$y = f$$

 $a_0 = 0.01013, a_1 = 0.4565, a_2 = 0.5776,$

Standard deviation S=0.7936, and the correlation coefficient r=0.9993.

We can thus determine how many cycles the crack propagation reaches half the thickness of the protective asphalt plate (h=50mm): $n_{cf} = 1080$ cycles (n = 0.3, or we can say that the crack length has reached h/2, 30% of the total duration of its propagation.

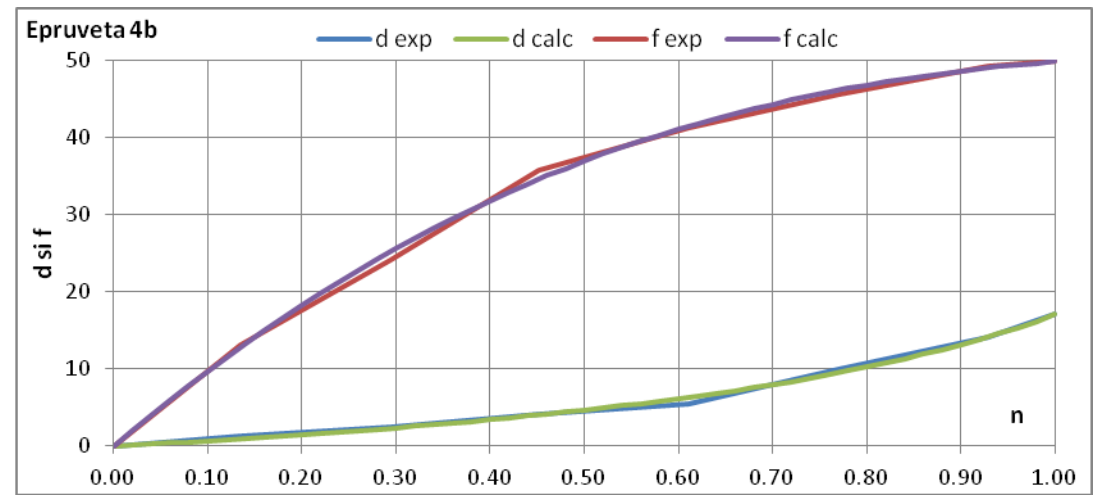


Figure 4.4 Variation of opening d and crack length f as a function of n, specimen 4b

• The regression model found for the evolution of the concrete opening db in relation to n is the MMF model (Morgan-Morgan-Finney), Figure 4.5:

$$db = \frac{a_0 \cdot a_1 + a_2 \cdot n^{a_3}}{a_1 + n^{a_3}}$$

$$a_0 = 4.144, a_1 = 1.936 \cdot 10^{-1}, a_2 = 4.58 \cdot 10, a_3 = 3.75$$
(23)

Standard deviation S=0.961, and the correlation coefficient r=0.9988.

To find out the actual opening of the concrete at a point, the value of the initial opening will be added to the value resulting from the MMF model. db_i (Table 4.3)

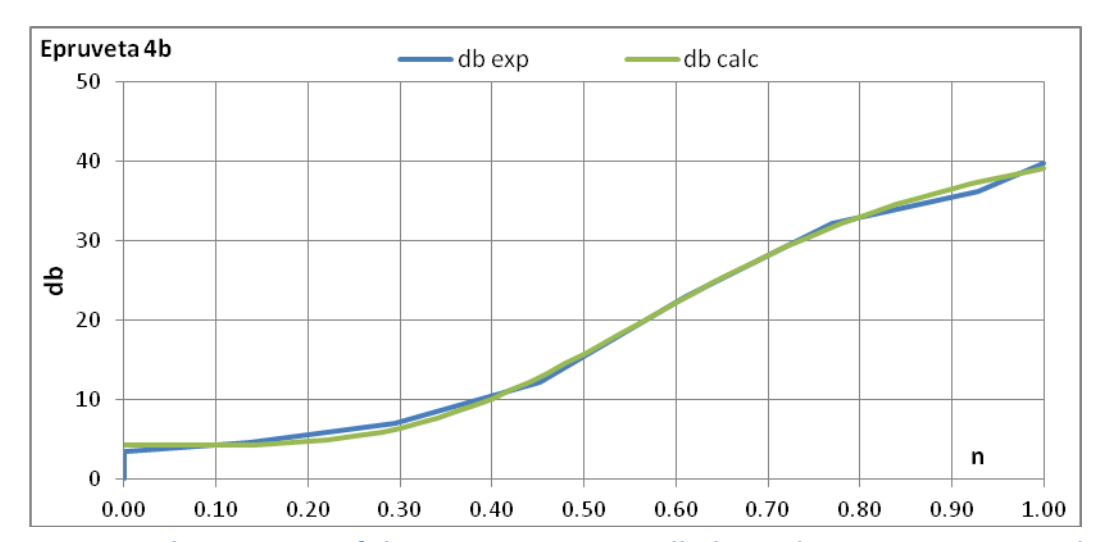


Figure 4.5 The variation of the concrete opening db depending on n, specimen 4b

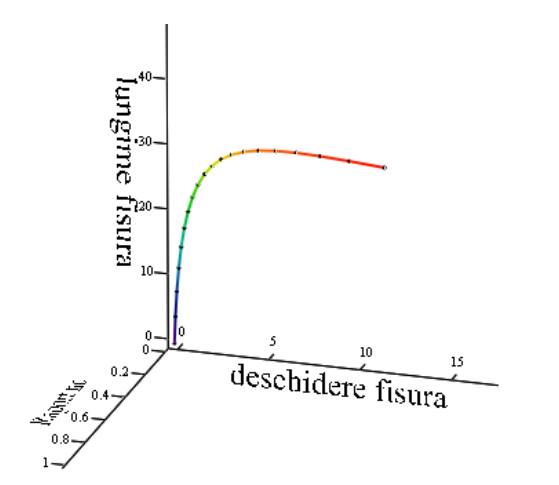
Specimen	ncf	n	d	f	db
	0				3.0088
	385				3.0088
	600				3.0088
	865				3.3028
	1007	0.00	0	0	6.4758
4 b	1041	0.13	1.2226	13.1845	7.5449
4b	1081	0.29	2.4000	24.0375	9.9082
	1121	0.45	4.2037	35.7716	15.0728
	1161	0.61	5.4849	41.2156	25.9983
	1201	0.77	10.0141	45.5222	35.1315
	1241	0.93	14.1314	49.2098	39.2394
	1259	1.00	17.0370	49.8227	42.8079

Table 4.5 Experimental results, specimen 4b

Considering the regression models found between these 4 parameters (2 by 2), we can observe their evolution in a representation:

tridimensional

- o opening **d**, length **f** and number of cycles **n**, in the asphalt layer (Figure 4.6),
- o opening **d**, length **f** of the crack in the asphalt and concrete opening **db** (Figure 4.7)



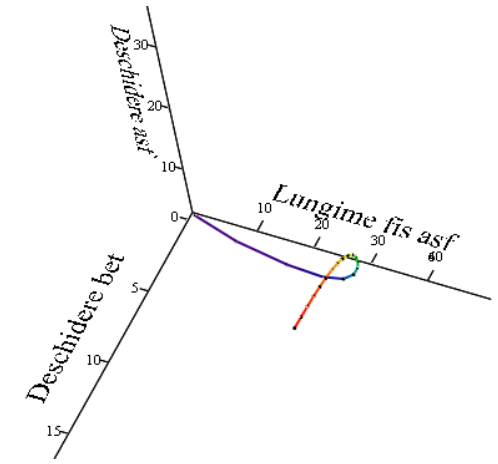


Figure 4.6 Tridimensional representation d, f, n, specimen 4b.

Figure 4.7 Tridimensional representation d, f, db, specimen 4b.

• in the same plan for all the 4 parameters (Figure 4.8). To make the drawing more suggestive, the value of the parameter was reported at one point to the total value (example: f/f_{tot} , where f –the length of the crack at the point considered, f_{tot} -

the length from the moment the crack propagates over the entire thickness of the asphalt layer)

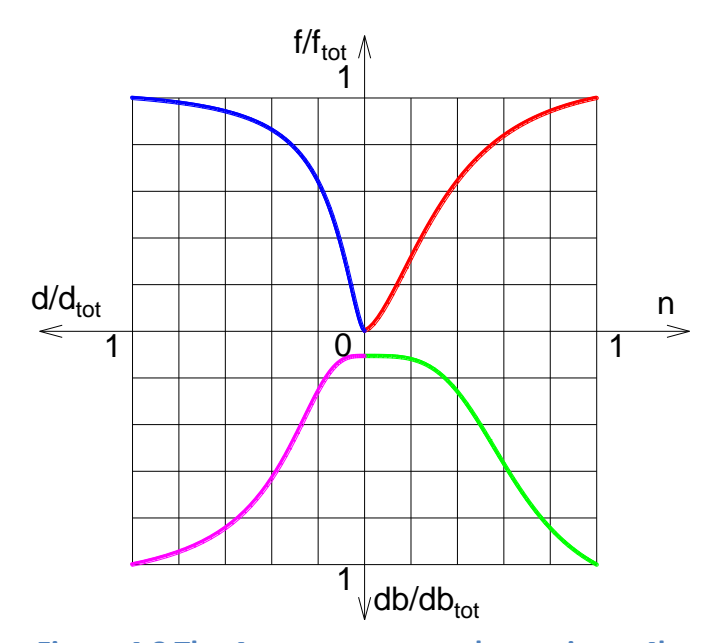
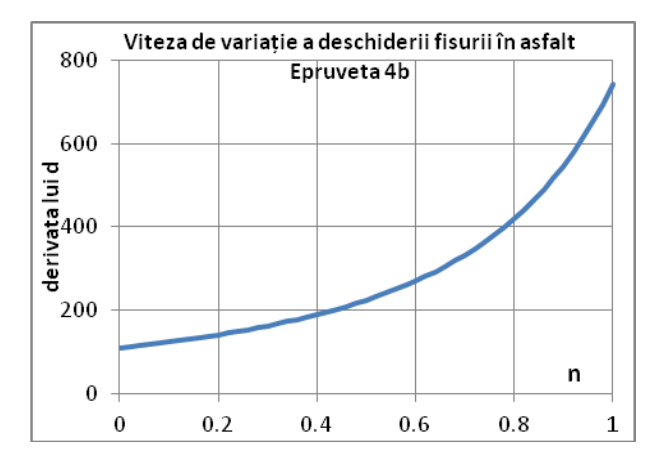


Figure 4.8 The 4 parameters graph, specimen 4b.

This multicriteria analysis diagram allows the identification of the less visible parameter in the imaging processing of the data obtained with the software related to the Cracking Device with Temperature Control.

• Variation rates of crack opening (Figure 4.9), of the propagation (length) of the crack (Figure 4.10) through asphalt, respectively of the opening of the concrete (Figure 4.11), is calculated by deriving the function $(\frac{d}{dn}d, \frac{d}{dn}f, \frac{d}{dn}db)$.



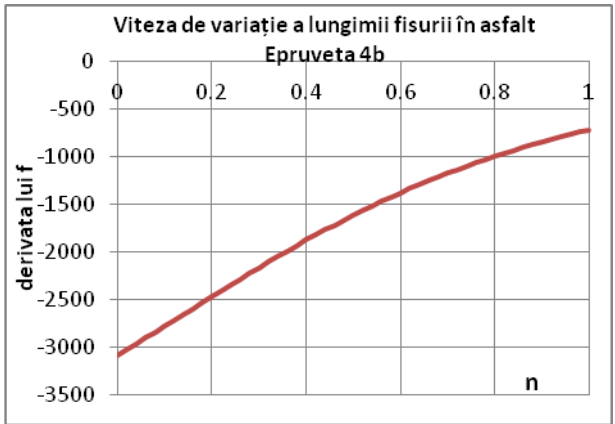


Figure 4.9 Variation rate of crack opening d, specimen 4b

Figure 4.10 Variation rate of crack length f, specimen 4b

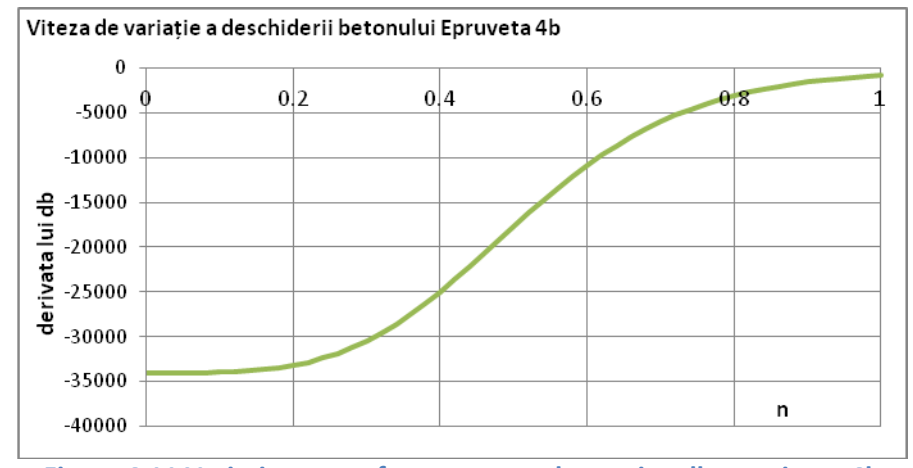


Figure 4.11 Variation rate of concrete crack opening db, specimen 4b

Depending on the curvature of the diagrams, the connection between the parameters of the reflective crack can be seen. Thus, if the variation speed at the opening of the crack in the asphalt is lower, following that at the end of the reflective propagation test it will increase sharply, the variation speed of the crack length is more accentuated at the beginning of the test, fading towards the end of the test. This different behavior between the crack opening speed and its length by propagation on the thickness of the asphalt layer, is explained by the rheological component of this road material and by the transition from elastic to plastic behavior during the development of local deformation at the crack tip, according Irwin's theory.

Figure 4.11, which shows the speed of variation of the crack opening in the concrete sublayer, highlights the phenomenon created by the effect of transfer to the crack by initial friction of the walls of this sublayer, attenuated by the damping of the transfer process by the presence of the asphalt layer at the upper fiber of the concrete layer, which works together with it

by applying the technological bonding operation between the layer. Thus, initially, when working the transfer from the crack of the concrete layer together with the damping of the asphalt layer present at its surface, the capacity to take over the vertical deformation (deflection under load) is higher and therefore the opening speed of the existing crack in concrete is small.

In the intermediate stage, when the transfer to the crack of the concrete support layer is consumed and the capacity to take over the transmission of the crack through the asphalt layer is mobilized, the curvature of the diagram changes, so that in the final phase of reflective propagation, the crack opening speed from the concrete layer to grow at a lower deflection.

4.2 **5a și 5b specimens**

The force at which the crack of the precast concrete was transmitted in the protection layer and the specimen yielding occurred is 440daN, the number of cycles being approximately equal: cracking at n_{ci5a} =12.200 compared to n_{ci5b} =12.116, and fracture at n_{cR5a} =12.556 compared to n_{cR5b} =12.429 (Table 4.6). The total test time is approximately 3140 seconds at 5a and 3108 seconds at 5b, respectively.

From the point of view of the evolution of the vertical deformation according to the number of cycles (Figure 4.12), until the moment of the appearance of the crack in the asphalt mixture, it is found that sample 5a has a faster growth compared to 5b. Instead, the crack appears at a lower number by 84 cycles (21 seconds) and the rupture by 127 cycles (32 seconds) at 5b compared to 5a

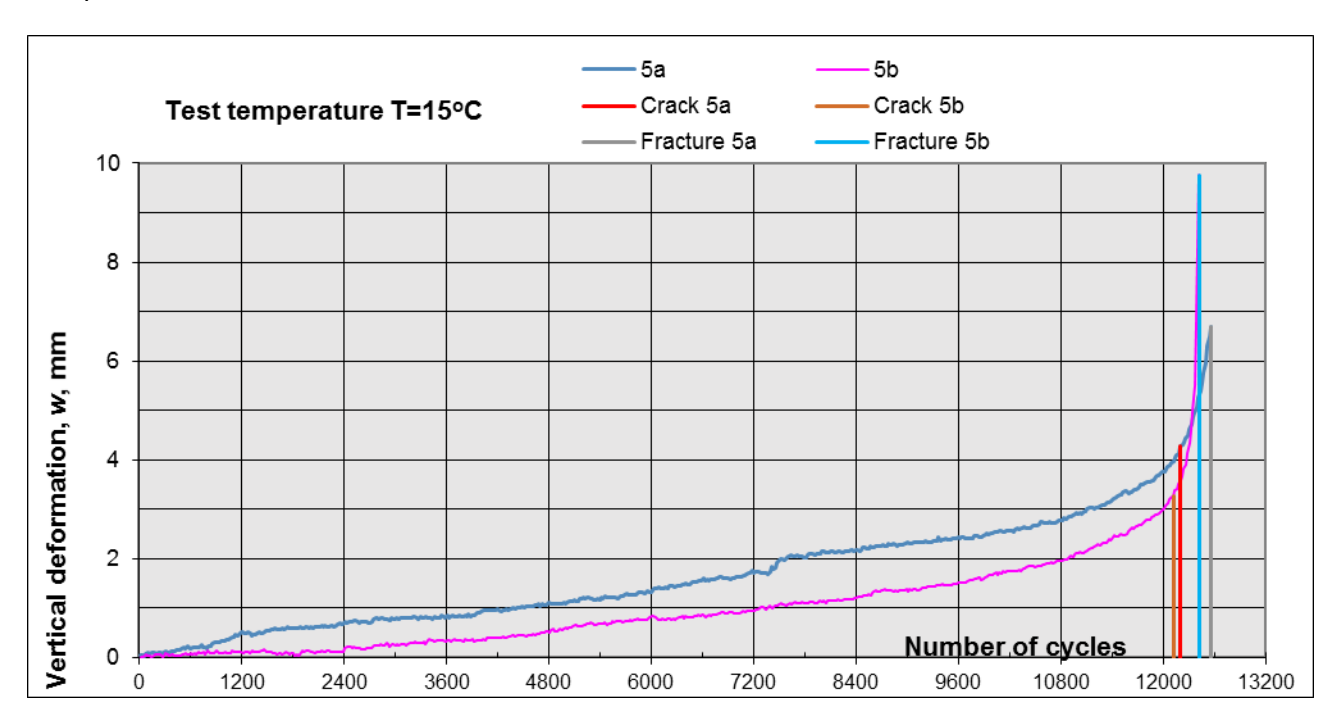


Figure 4.12 Increase of the vertical deformation according to the number of cycles for specimens 5a and 5b

Table 4.6 Number of cycles and vertical deformation at cracking / fracture, 5a și 5b

Cracking	5a	Cracking	5b
Number of cycles, n ci	Vertical deformation,	Number of cycles, n ci	Vertical deformation,
Number of cycles, no	w	Number of cycles, IIa	w
12200	4.2651	12116	3.2518
Fracture	5a	Fracture	5b
Number of cycles, n _{cR}	Vertical deformation,	Number of cycles, n _{cR}	Vertical deformation,
Number of Cycles, fice	w	indifficer of cycles, fice	w
12556	6.6868	12429	9.754

A simple calculation indicates that approximately 97% of the life cycle of the mixture is consumed until the crack appears and only 3% of the time is the propagation of the crack through the asphalt layer. (Table 4.7).

Table 4.7 Mixture crack index, specimens 5a și 5b

Specimen	Cracking index, $I_f = \frac{n_{ci}}{n_{cR}}$ (%)	Number of cycles
5a	97.16%	336
5b	97.48%	313

Analyzing from the point of view of the initial opening of the cement concrete crack (db_i), it is observed (Table 4.8) that db_{i5a} > db_{i5b} , which would indicate a better frictional cooperation between aggregates and / or between the cement stone (transfer to existing crack in the concrete layer). This would translate into a longer service life, as opposed to the experimental results.

Turning to the analysis of the other measured parameter, the initial detachment of the asphalt mixture from the concrete, it is found in Table 4.8 that e_{i5b} > e_{i5a} . This can be interpreted by a difference between the bitumen films with which the concrete asphalt slabs were glued (bonded at the interface) to the 2 specimens. We notice (Figure 4.13) that the bitumen is not present on the entire surface of the asphalt slab (implicitly on the pre-cracked concrete one, which can mean the non-uniformity of the working conditions).

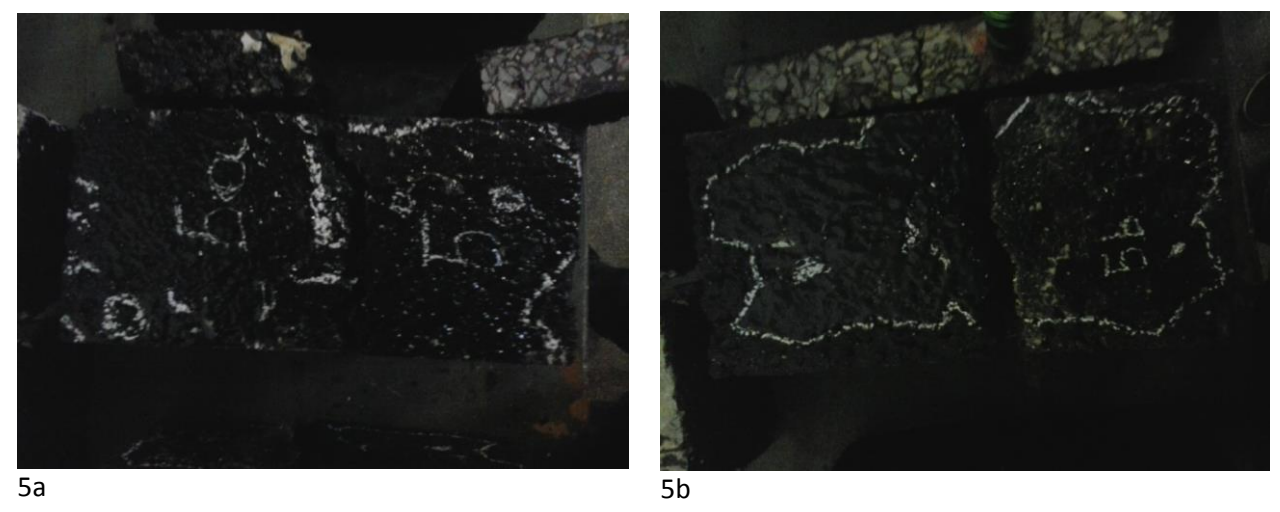
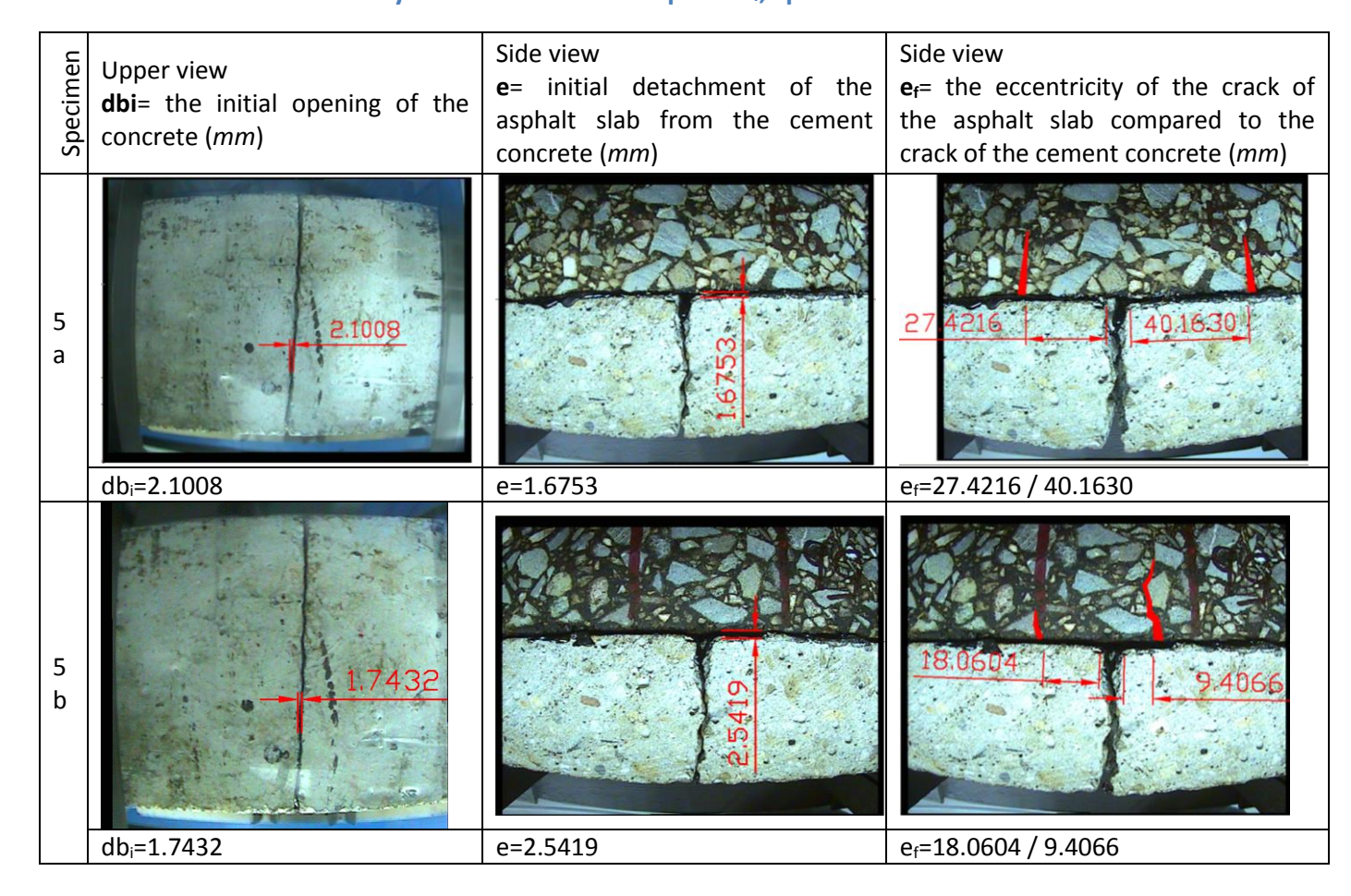


Figure 4.13 Suprafața de amorsare/lipire cu bitum, epruvetele 5a și 5b

In the case of specimen 5a, the bitumen covers about 95%, compared to 5b, where it is 80%. In both, the uncoated bitumen surface (where there is no collaboration between concrete and asphalt) is found at the ends of the slab.

Table 4.8 The values of the initial opening db_i, its initial detachment (bitumen bonding) and the eccentricity of the crack in the asphalt e_f, specimens 5a and 5b



In conclusion, it is necessary to consider not only the thickness of the applied bitumen layer, but also the way in which it is distributed on the surface of the asphalt slab and implicitly of the concrete. This is one of the explanations of the similar behavior in time of the 2 specimens, required at loads equivalent to road traffic, even if the initial opening of the concrete crack would have indicated a longer life cycle for 5a.

Another aspect is the position of the crack in the asphalt compared to the concrete. The eccentricity of the cracks, in relation to each other, may be due to the surface not covered by bitumen, after the asphalt plate has adhered to the concrete one. In Figure 4.13 there is a part where the bitumen is missing (marked in white), right next to the crack. In other words, when preparing the test pieces, the bitumen must be poured along the plate, linearly and evenly. The amount and type of bitumen used for bonding must also be checked in the future.

Measurements and processing of these parameters (Table 4.9), crack length and opening, for specimen 5b indicate:

• The variation of the crack opening **d**, but also of the length **f** in relation to **n**, is nonlinear (Figure 4.14). The regression model that best describes this relationship is:

$$y = \frac{a_0 \cdot n}{1 + a_1 \cdot n + a_2 \cdot n^2}$$

when
$$y = d$$

 $a_0 = 4.801$, $a_1 = 4.775$, $a_2 = -4.79$,

Standard deviation S=0.655, and the correlation coefficient r=0.9996.

when
$$y = f$$

 $a_0 = 62.13$, $a_1 = 4.984$, $a_2 = -4.734$,

Standard deviation S=1.636, and the correlation coefficient r=0.9973.

We can thus determine how many cycles the crack propagation reaches half the thickness of the protective asphalt plate (h=50mm): $n_{cf} = 12350$ cycles (n = 0.8, or we can say that the crack length has reached h/2, 80% of the total duration of its propagation).

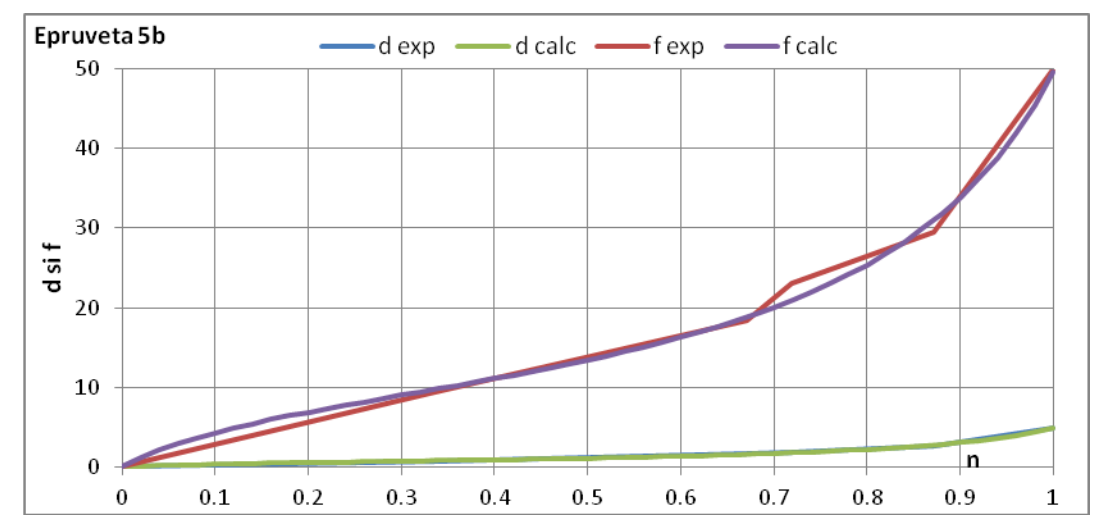


Figure 4.14 Variation of opening d and crack length f as a function of n, specimen 5b

• The regression model found for the evolution of the concrete opening db in relation to n is the Bleasdale model, Figure 4.15:

$$db = (a_0 + a_1 \cdot n)^{-\frac{1}{\alpha_2}}$$

$$a_0 = 2.965 \cdot 10^{-1}, a_1 = -2.694 \cdot 10^{-1}, a_2 = 1.386$$

Standard deviation S=0.3413, and the correlation coefficient r=0.998.

To find out the actual opening of the concrete at a point, the value of the initial opening will be added to the value resulting from the Bleasdale model db_i (Table 4.8)

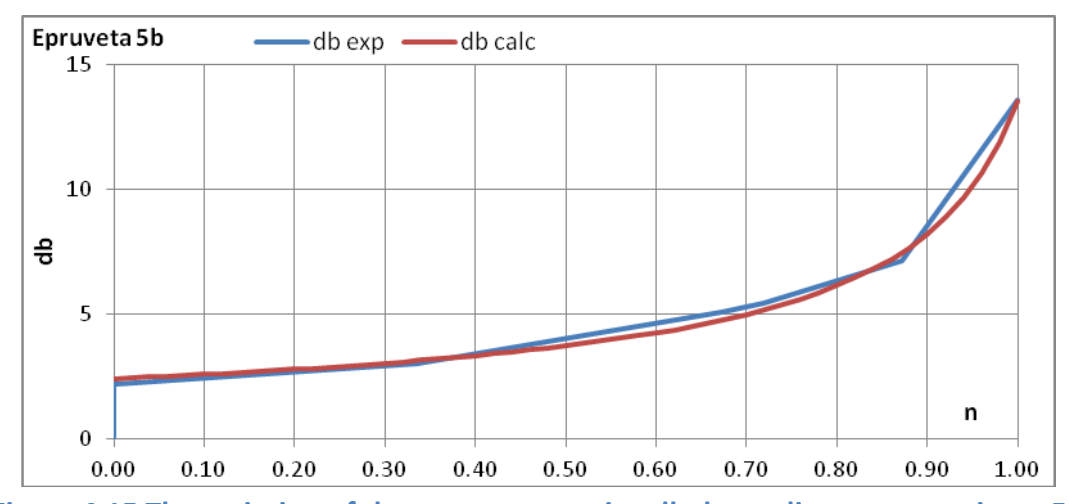


Figure 4.15 The variation of the concrete opening db depending on n, specimen 5b

	Table 4.5 Experimental results, specimen 35				
Specimen	nc	n	d	f	db
	0				1.7432
	5461				1.7432
	6661				1.8366
	7861				1.9549
	9061				2.173
	10261				2.3589
5b	11461				2.7259
	12116	0	0.0000	0	3.911
	12221	0.335463	0.7461	9.3256	4.7631
	12326	0.670927	1.6232	18.35478	6.8209
	12341	0.71885	1.8180	23.1514	7.1553
	12389	0.872204	2.6756	29.4654	8.9007
	12429	1	4.8850	50	15.3147

Table 4.9 Experimental results, specimen 5b

Considering the regression models found between these 4 parameters (2 by 2), we can observe their evolution in a representation:

- tridimensional
 - o opening **d**, length **f** și **n** (Figure 4.16),
 - o opening **d** and length **f** of the crack in the asphalt and concrete opening **db** (Figure 4.17)

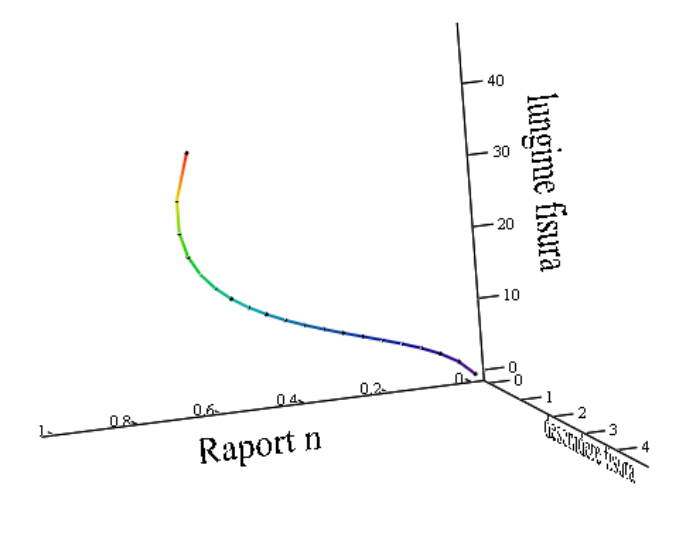


Figure 4.16 Tridimensional representation d, f, n, specimen 5b.

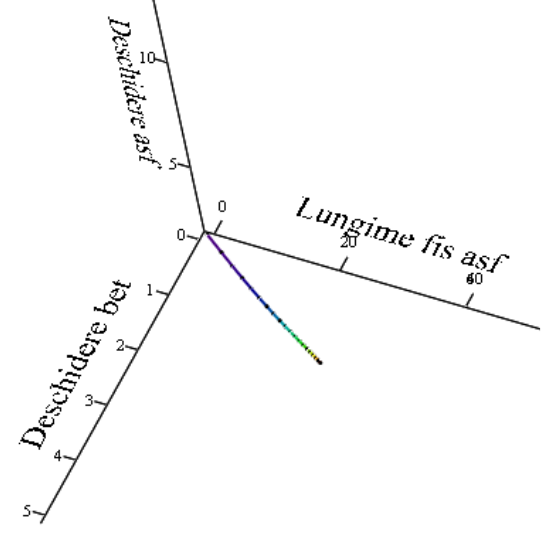
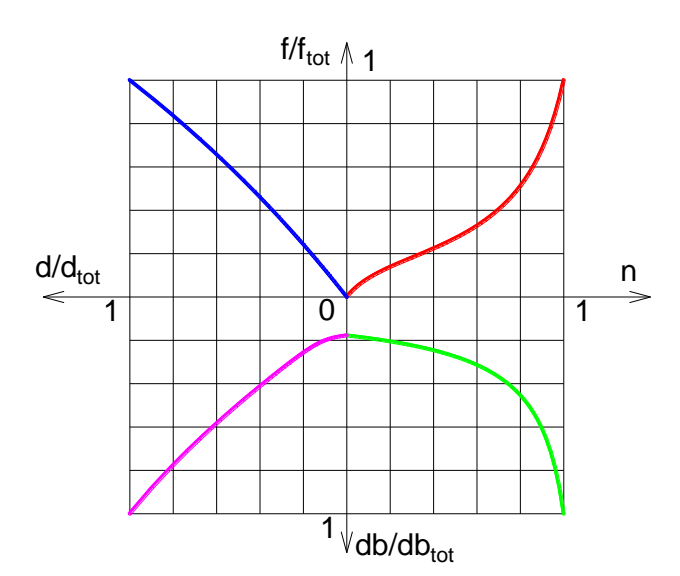


Figure 4.17 Tridimensional representation d, f, db, specimen 5b.



in the same plan for all the 4 parameters (Figure 4.18).

Figure 4.18 The 4 parameters graph, specimen 5b.

- The rates of variation of the crack opening (Figure 4.19), of the propagation (length) of the crack (Figure 4.20) through asphalt show a similar parabolic variation diagram, which is explained by the fact that at the initiation of the crack through asphalt, the section has the ability to withstand reflective propagation. This process corresponds to a lower rate of variation of the opening / length of the crack in the asphalt. A speed level follows during the plasticization period of the material at the top of the crack, according to the Irwin model, after which the speed increases significantly when the crack propagates over half the thickness of the layer.
- The variation speed of the cement concrete opening is shown in Figure 4.21. This
 has a variation corresponding to the transfer in the existing crack. When there is no
 more contact friction in the crack in the concrete layer (loss of transfer in the
 crack), the opening speed increases significantly.

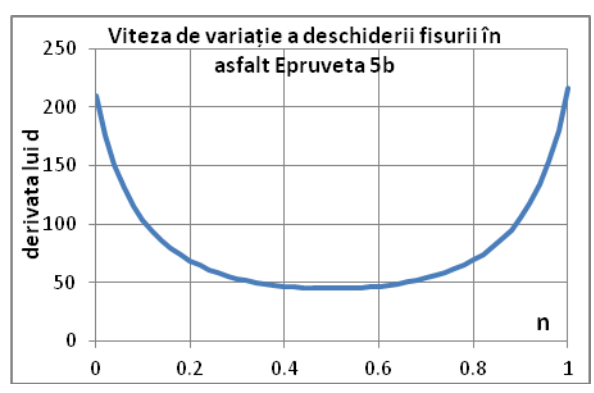


Figure 4.19 Variation rate of crack opening d, specimen 5b

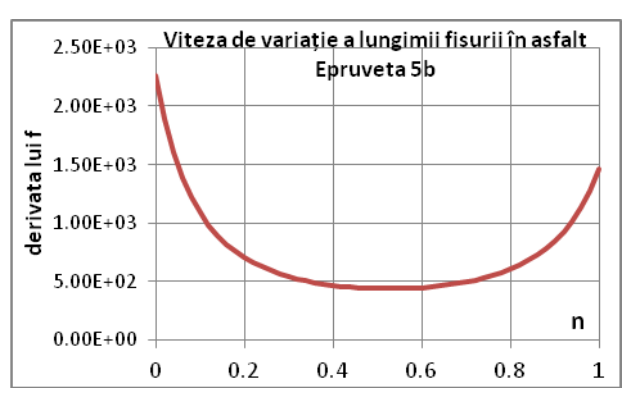


Figure 4.20 Variation rate of crack length f, specimen 5b

Research Report no. 3. Identification of the parameters of influence of crack propagation through protective asphalt layers for degraded pavements

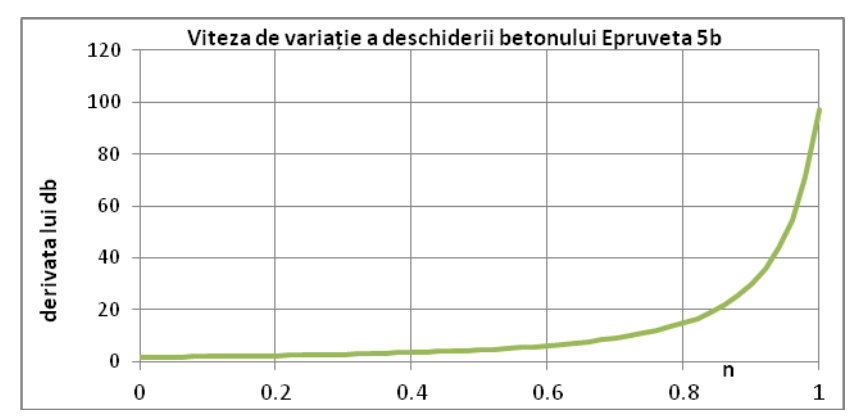


Figure 4.21 Variation rate of concrete crack opening betonului db, specimen 5b

4.3 6a specimen

The force at which the crack of the precast concrete was transmitted in the protection layer and the specimen yielding occurred is 360daN, and the number of cycles: n_{ci6a} =9974 (cracking), n_{cR6a} =10520 (fracture)(

Table 4.10). The total test time is 2630 seconds.

From the point of view of the evolution of the vertical deformation according to the number of cycles (Figure 4.22), , it is similar to the other specimens above.

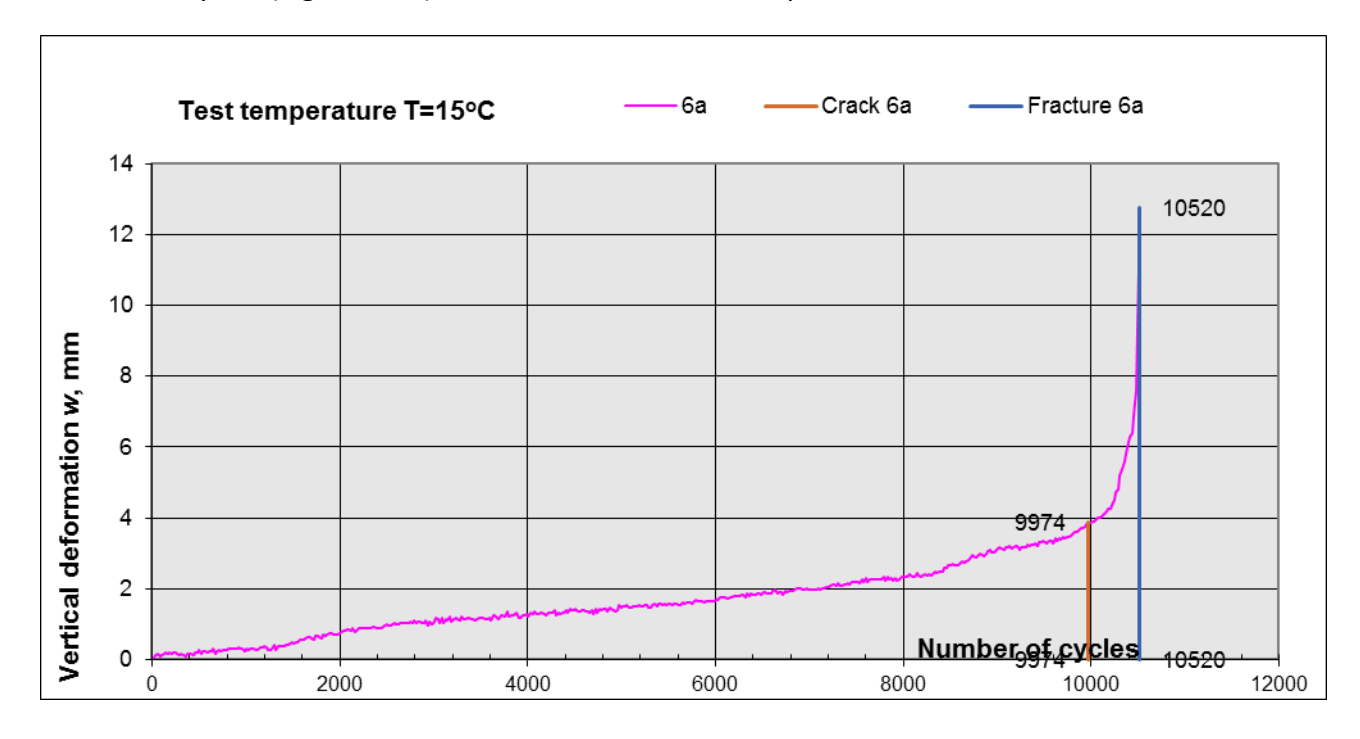


Figure 4.22 Increase of the vertical deformation according to the number of cycles for the specimen 6a

Table 4.10 Number of cycles and vertical deformation at cracking / fracture, specimen 6a

Cracking	6a
Number of cycles, n ci	Vertical deformation, w
9974	3.8933
Fracture	6a
Fracture Number of cycles, n _{cR}	6a Vertical deformation, w

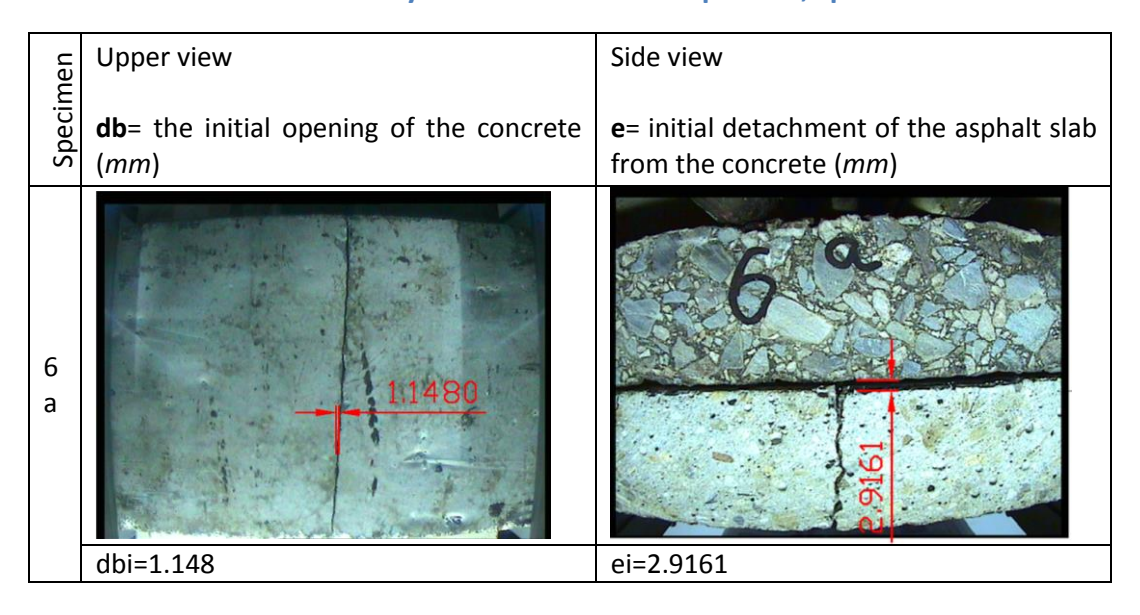
Approximately 95% of the life of the mixture is consumed until the crack appears and 5% of the time is the propagation of the crack through the asphalt layer (Table 4.11).

Table 4.11 Mixture crack index, specimen 6a

Specimen	Reflective crack index, $I_f = \frac{n_{ci}}{n_{cR}}$ (%)	Number of cycles
6a	94.81%	546

Table 4.12 Table 4.12 gives the two initial parameters of specimen 6a: the initial opening of the db_i concrete crack and the initial detachment of the asphalt layer from the concrete slab e_i .

Table 4.12 The values of the initial opening of the db_i, its initial detachment (bitumen bonding) and the eccentricity of the crack in the asphalt e_f, specimen 6a



Measurements and processing of crack parameters (Table 4.13), length and opening of the crack in asphalt, opening of concrete, for specimen 6a indicate:

• The variation of the crack opening **d**, but also of the length **f** in relation to **n**, is nonlinear (Figure 4.23). The regression model is the same as for the specimen 4b:

$$y = \frac{a_0 \cdot n}{1 + a_1 \cdot n + a_2 \cdot n^2}$$

when
$$y = d$$

$$a_0 = 4.545, a_1 = -1.018, a_2 = -0.189,$$

Standard deviation S=0.986, and the correlation coefficient r=0.9955.

Pentru
$$y = f$$

 $a_0 = 56.78, a_1 = 1.231, a_2 = -1.065,$

Standard deviation S=1.434, and the correlation coefficient r=0.997.

We can thus determine how many cycles the crack propagation reaches half the thickness of the protective asphalt plate (h=50mm): $n_{cf} = 10300$ cycles (n = 0.6, or we can say that the crack length has reached h/2, 60% of the total duration of its propagation).

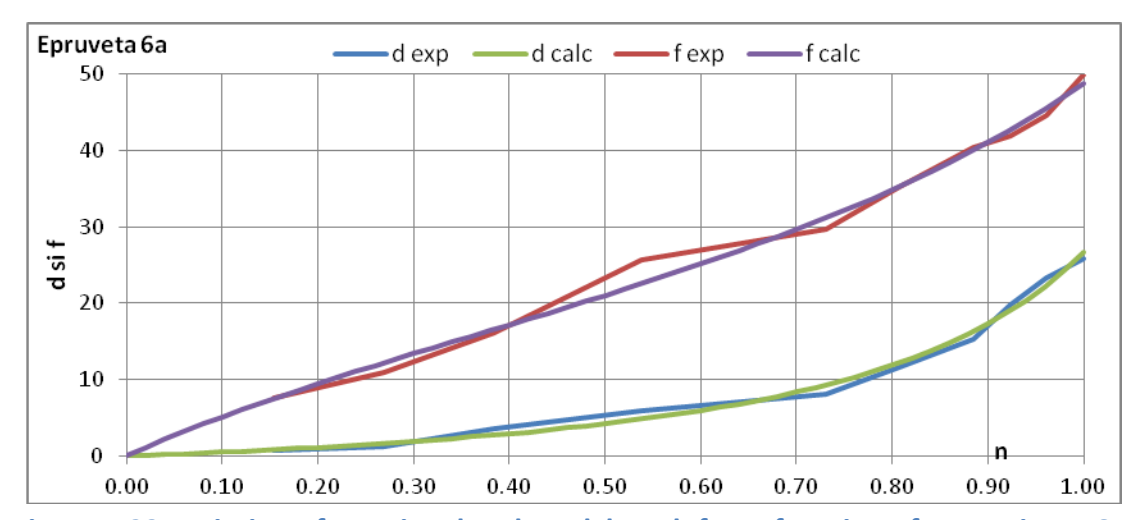


Figure 4.23 Variation of opening d and crack length f as a function of n, specimen 6a.

• The regression model found for the evolution of the concrete opening db in relation to n is the Bleasdale model, Figure 4.24:

$$db = (a_0 + a_1 \cdot n)^{-\frac{1}{a_2}}$$

$$a_0 = 4.49 \cdot 10^{-2}, a_1 = -4.168 \cdot 10^{-2}, a_2 = 2.746$$

Standard deviation S=0.228, and the correlation coefficient r=0.997.

To find out the actual opening of the concrete at a point, the value of the initial opening will be added to the value resulting from the Bleasdale model db_i (Table 4.12)

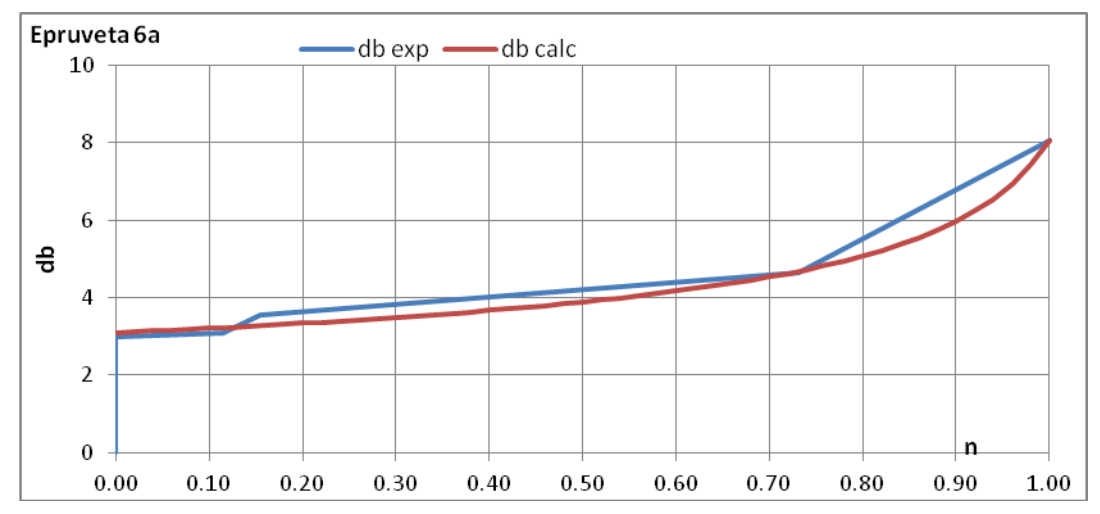


Figure 4.24 The variation of the concrete opening db depending on n, specimen 6a

Specimen	nc	n	d	f	db
-	0				1.1480
	6698				1.4525
	7286				1.8509
	8609				2.2960
	8987				3.0468
	9974	0.00	0.00	0.00	4.1328
	10037	0.12			4.2395
	10058	0.15	0.67	7.52	4.6858
6a	10121	0.27	1.26	10.97	4.6858
	10184	0.38	3.56	16.21	4.6858
	10268	0.54	5.99	25.61	4.6858
	10373	0.73	8.11	29.68	5.8034
	10415	0.81	11.56	35.29	5.8034
	10457	0.88	15.34	40.44	5.8034
	10478	0.92	19.79	41.82	5.8034
	10499	0.96	23.36	44.63	5.8034

Table 4.13 Experimental results, specimen 6ª

Considering the regression models found between these 4 parameters (2 by 2), we can observe their evolution in a representation:

1.00

- tridimensional
 - o opening **d**, length **f** and number of cycles **n** (Figure 4.25),

10520

opening **d** and the crack length of the asphalt **f** and the concrete opening **db** (Figura 4.26)

25.75

9.2098

50.00

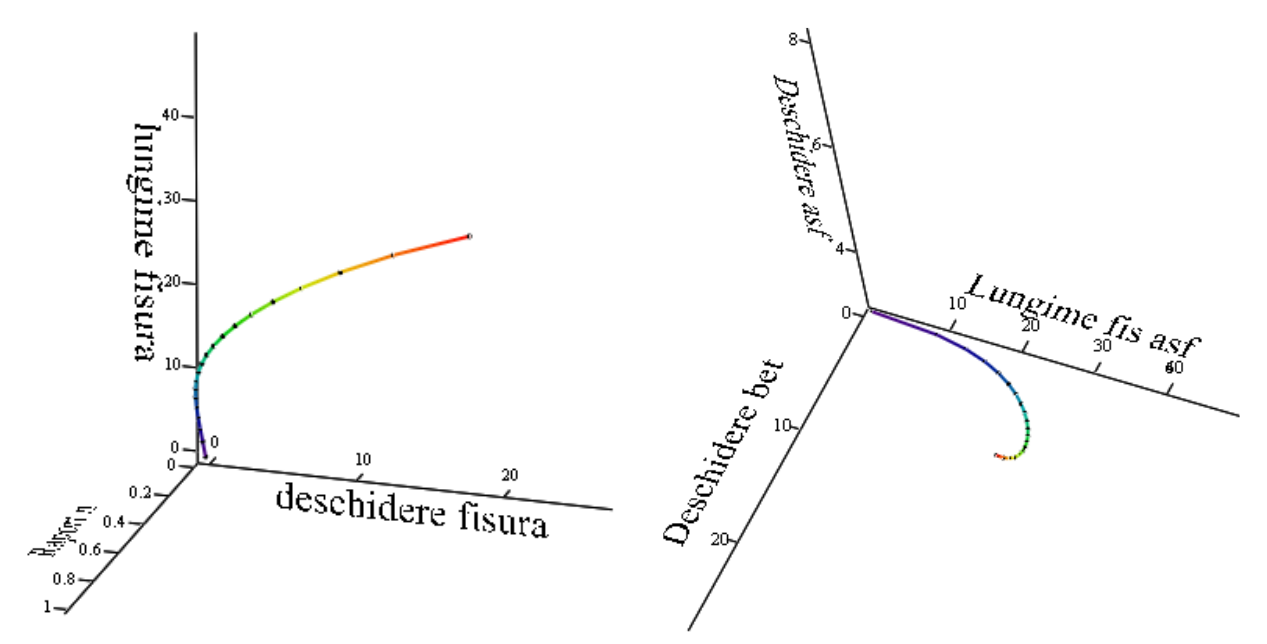


Figure 4.25 Tridimensional representation d, f, n, specimen 6a.

Figura 4.26 Tridimensional representation d, f, db, specimen 6a.

• in the same plan for all the 4 parameters (Figure 4.27).

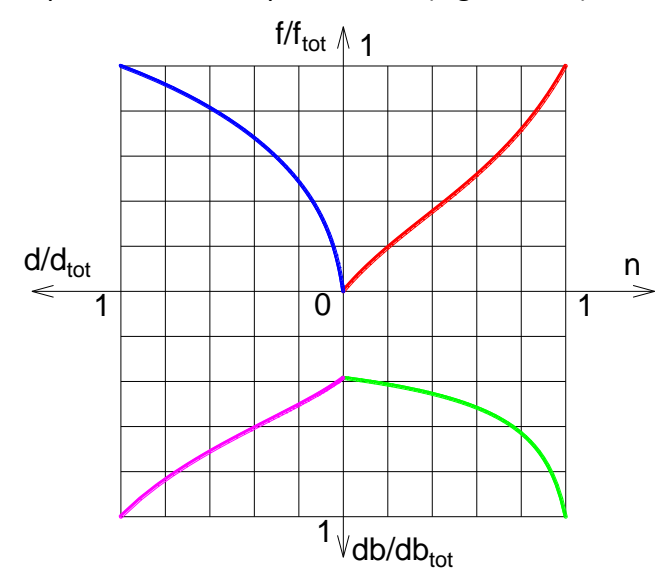
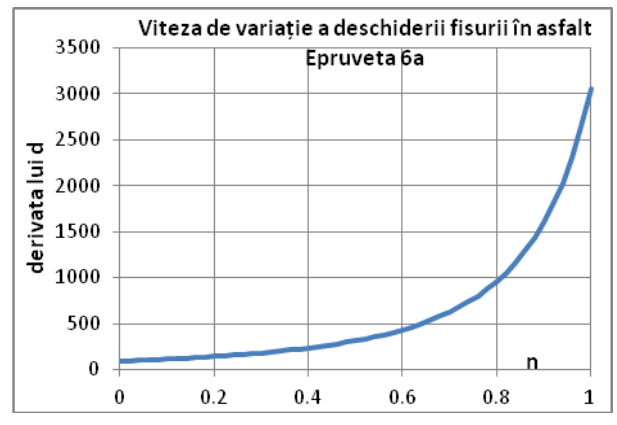


Figure 4.27 The 4 parameters graph, specimen 6a.

• Variation rates of crack opening (Figure 4.28), of the propagation (length) of the crack through asphalt (Figure 4.29), respectively of the opening of the concrete (Figure 4.30).



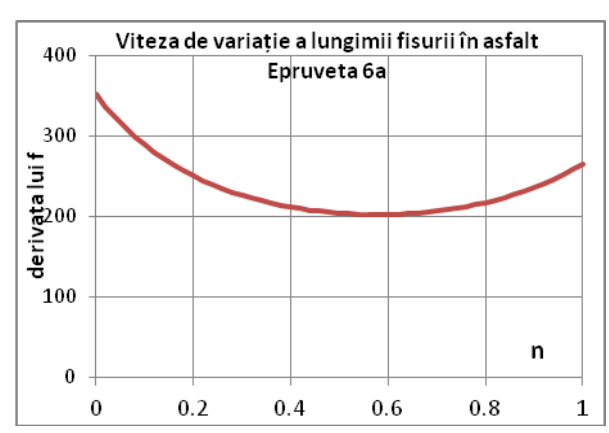


Figure 4.28 Variation rate of crack opening d, specimen 6a

Figure 4.29 Variation rate of crack length f, specimen 6a

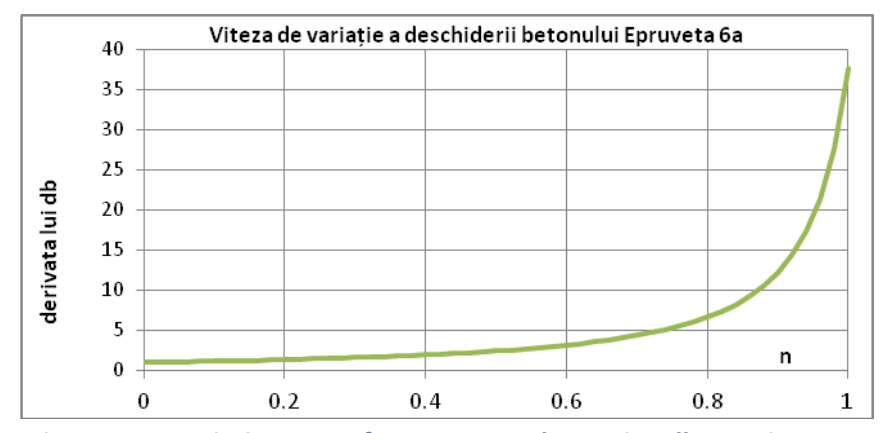


Figure 4.30 Variation rate of concrete crack opening db, specimen 6a

4.4 7a și 7b specimens

The force at which the crack of the precast concrete was transmitted in the protection layer and the specimen yielding occurred is 160daN for 7b and 280daN for 7a, the number of cycles at which the cracking occurred is n_{ci7a} =7.496 compared with n_{ci7b} =4178, respectively the fracture n_{cR7a} =7790, n_{cR7b} =4283 (Table 4.14). The total test time is 1948 seconds for 7a, respectively 1071 seconds for 7b.

From the point of view of the evolution of the vertical deformation according to the number of cycles (Figure 4.31), until the moment of the appearance of the crack in the asphalt mixture, it is found that sample 7b has a faster growth compared to 7a. The crack occurs at a lower number of cycles by 3318 (830 seconds), and the rupture by 3507 cycles (877 seconds) at 7b compared to 7a.

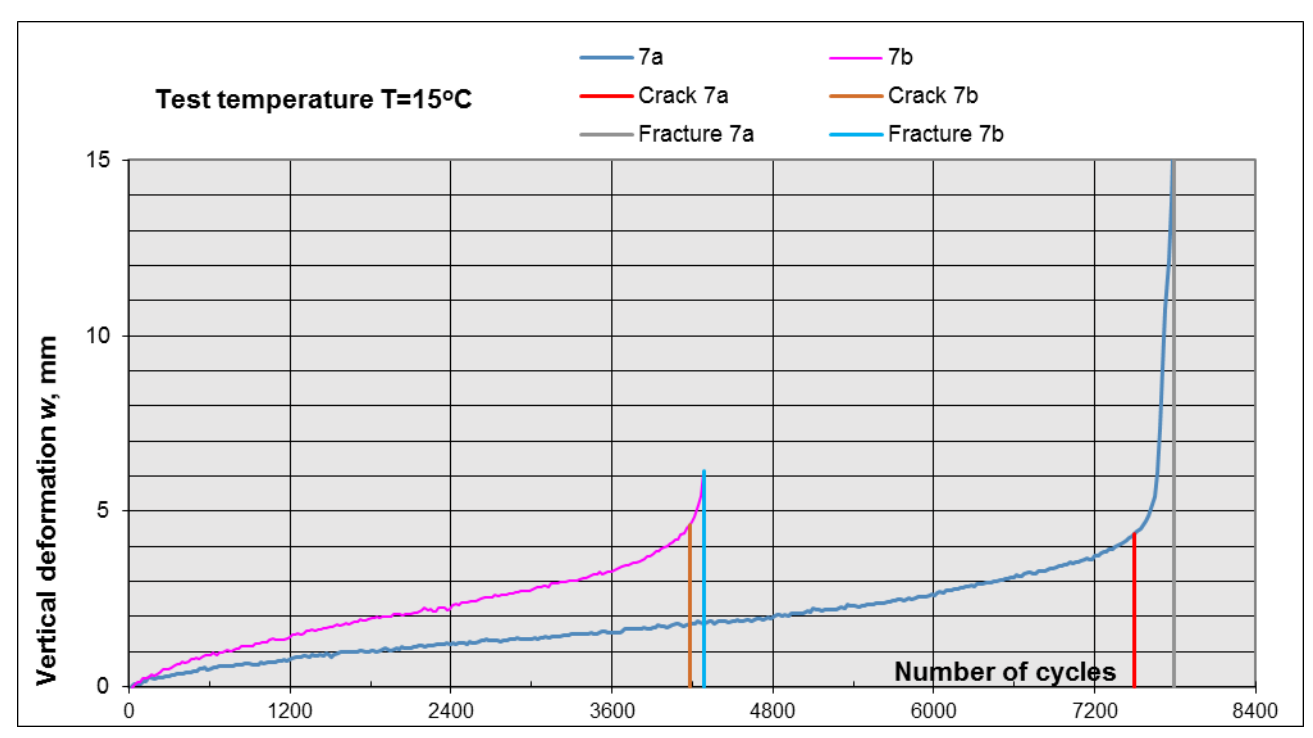


Figure 4.31 Increase of the vertical deformation according to the number of cycles for 7a and 7b

Table 4.14 The number of cycles and the vertical deformation at cracking/fracture failure, 7a and 7b

Cracking	7a	Cracking	7b
Number of cycles, n ci	Vertical deformation,	Number of cycles, n ci	Vertical deformation,
Nulliber of cycles, no	w	Number of cycles, no	w
7496	4.3402	4178	4.5984
Fracture	7a	Fracture	7b
Number of cycles, n cR	Vertical deformation,	Number of cycles, n cR	Vertical deformation,
Number of Cycles, HcR	w	Number of Cycles, HcR	w
7790	16.2704	4283	6.1332

A simple calculation indicates that approximately 96-97% of the life of the mixture is consumed until the crack appears and 3-4% of the time is represented by the propagation of the crack through the asphalt plate (Table 4.15).

Table 4.15 Mixture crack index, 7a și 7b

Specimen	Reflective cracking index, $I_f = \frac{n_{ci}}{n_{cR}}$ (%)	Number of cycles
7a	96.23%	294
7b	97.57%	105

Both the initial crack opening of the db_i cement concrete and the initial detachment of the asphalt layer from its concrete slab are smaller in the case of specimen 7a compared to specimen 7b (Table 4.16). The measurements of these 2 parameters represent a confirmation of the better behavior of the sample 7a.

Upper view Side view Side view Specimen **db**= the initial concrete opening e= the initial detachment of the **e**_f= the eccentricity of the crack of asphalt from the concrete (mm) the asphalt slab compared to the (mm)crack of the concrete (mm) 7 a $e_f=0$ dbi=1.2487 ei=2.5909 7 b dbi=1.7652 ei=3.7385 $e_f = 5.2845$

Table 4.16 Initial opening values db_i and the initial detachment (bitumen bonding) e_i and the eccentricity of the crack in the asphalt e_f, 7a and 7b

The measurements and processing of the cracking parameters (

Table 4.18), the length and opening of the crack in the asphalt, the opening of the concrete, for specimens 7a and 7b indicate:

• The variation of the crack opening **d**, but also of the length **f** in relation to **n**, is nonlinear (Figure 4.32, Figura 4.33). The regression model is the same as in specimen 4b:

$$y = \frac{a_0 \cdot n}{1 + a_1 \cdot n + a_2 \cdot n^2}$$

when
$$y = d$$

7a
$$a_0 = 3.584, a_1 = -0.9611, a_2 = 0.2085,$$

Standard deviation S=0.4336, and the correlation coefficient r=0.9965.

7b
$$a_0 = 1.199, a_1 = 1.527, a_2 = -2.169,$$

Standard deviation S=0, and the correlation coefficient r=1.

when
$$y = f$$

7a
$$a_0 = 25.54, a_1 = -0.7563, a_2 = 0.2773,$$

Standard deviation S=1.434, and the correlation coefficient r=0.997.

7b
$$a_0 = 23.66, a_1 = -0.2574, a_2 = -0.2694,$$

Standard deviation S=0, and the correlation coefficient r=1.

We can thus determine the number of cycles the crack propagation reaches half the thickness of the protective asphalt plate. (h=50mm):

- 7a $-n_{cf} = 7680$ cycles (n = 0.62, or we can say that the length of the crack reached h / 2, at 62% of the total duration of its propagation).
- 7b $-n_{cf} = 4250$ cycles (n = 0.69, or we can say that the length of the crack reached h / 2, at 69% of the total duration of its propagation).

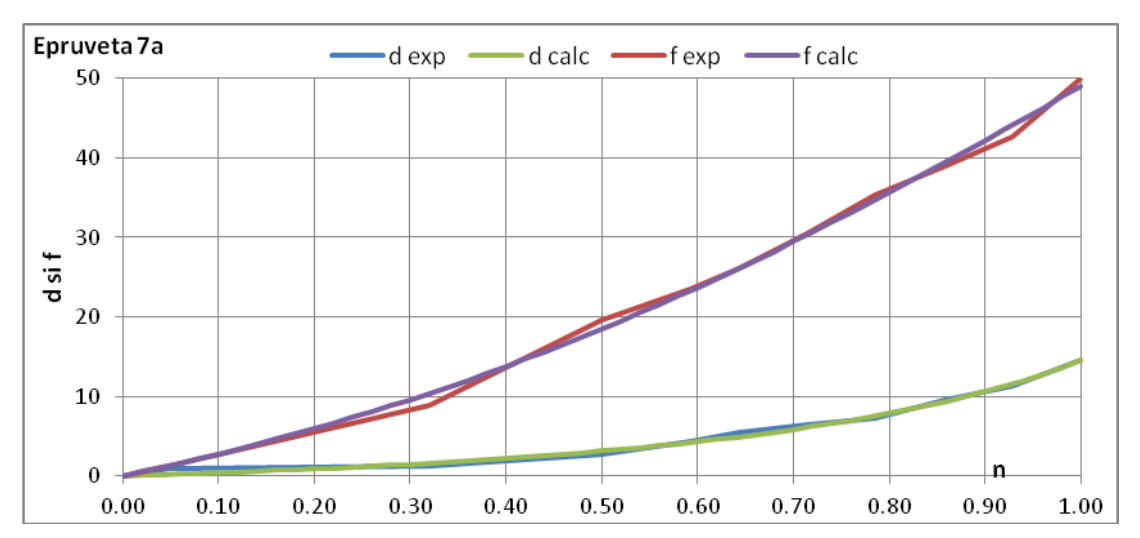


Figure 4.32 Variation of opening d and crack length f as a function of n, specimen 7a.

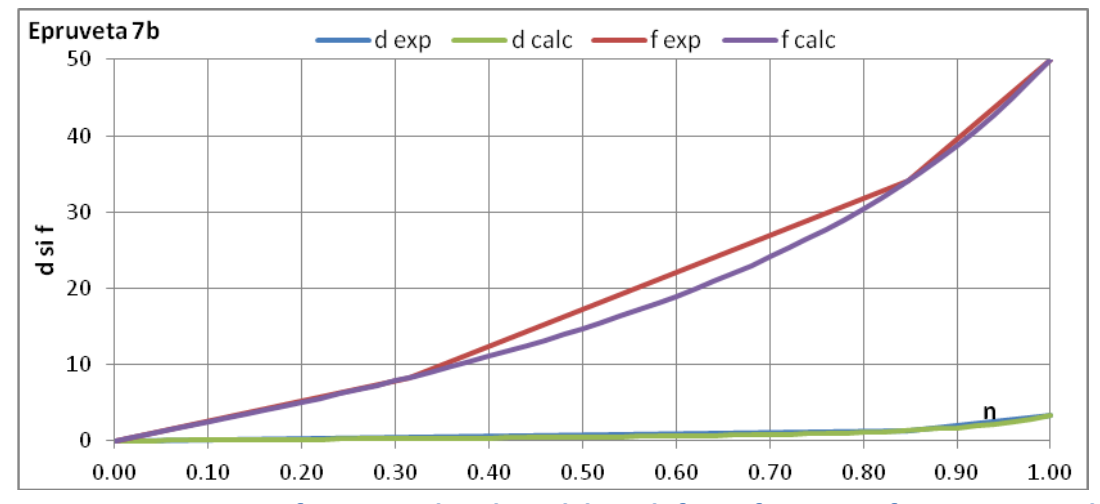


Figura 4.33 Variation of opening d and crack length f as a function of n, specimen 7b.

• The regression model found for the evolution of the concrete opening db in relation to n is the MMF for 7a and Bleasdale for 7b, Figure 4.34 and Figure 4.35:

$$7a - db = \frac{a_0 \cdot a_1 + a_2 \cdot n^{a_3}}{a_1 + n^{a_3}}$$

$$7b \cdot db = (a_0 + a_1 \cdot n)^{-\frac{1}{a_2}}$$

7a
$$a_0 = 6.323, a_1 = 2.367 \cdot 10, a_2 = 8.8 \cdot 10^2, a_3 = 4.209$$

Standard deviation S=1.34, and the correlation coefficient r=0.998.

7b
$$a_0 = 1.014 \cdot 10^{-2}, a_1 = -9.985 \cdot 10^{-2}, a_2 = 3.902$$

Standard deviation =0.058, and the correlation coefficient r=0.999.

To find out the actual opening of the concrete at a point, the value of the initial opening will be added to the value resulting from the 2 models. db_i (Table 4.16)

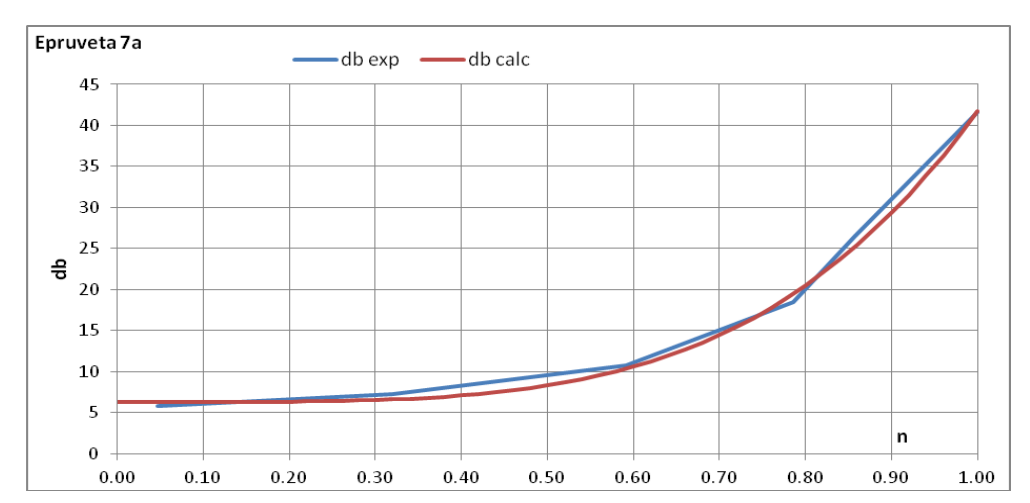


Figure 4.34 The variation of the concrete opening db depending on n, specimen 7a

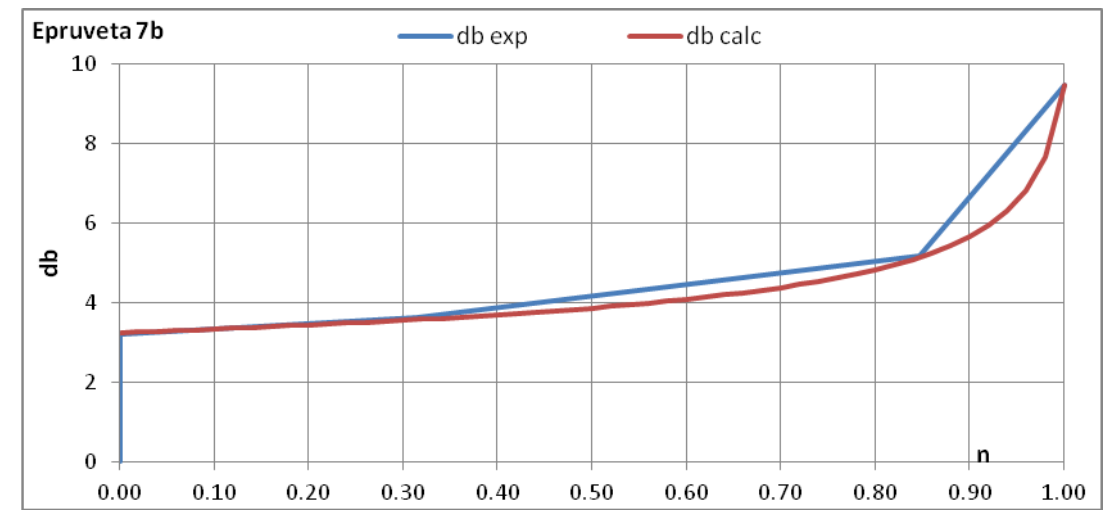


Figure 4.35 The variation of the concrete opening db depending on n, specimen 7b

Table 4.17 Experimental results, specimen 7a

Specimen	nc	n	d	f	db
	0		-	-	1.2487
	3222				1.4513
	4662				1.9438
	5142				2.0136
	5622				2.2556
	6102				2.5963
	6582				3.2163
	7062				3.7925
	7302				4.2869
7.0	7496	0.00	0	0	
7a	7510	0.05	0.879	1.157	7.0409
	7590	0.32	1.279	8.842	8.5028
	7643	0.50	2.627	19.601	
	7670	0.59	4.279	23.535	12.0697
	7685	0.64	5.384	26.045	
	7706	0.71	6.39	30.451	
	7727	0.79	7.239	35.359	19.7132
	7748	0.86	9.525	38.948	27.7478
	7769	0.93	11.367	42.748	
	7790	1.00	14.614	50	42.8647

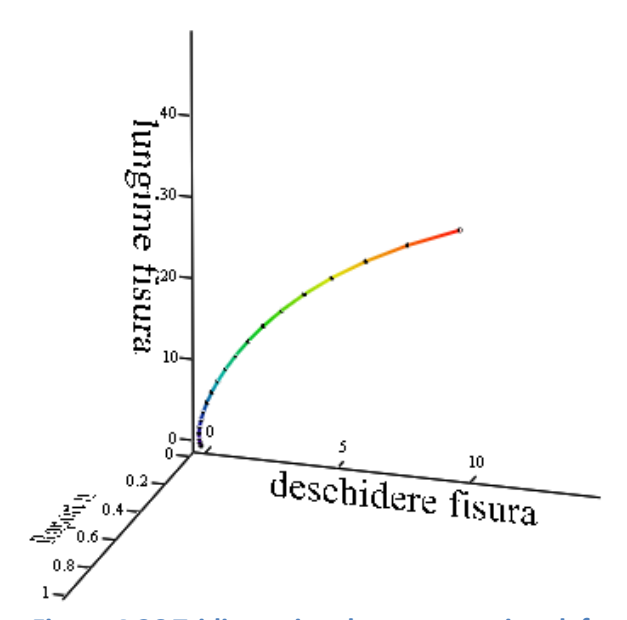
Table 4.18 Experimental results, specimen 7b

Specimen	nc	n	d	f	db
	0				1.7652
	371				1.7652
	851				2.3986
	1331				2.5386
	1811				2.6482
	2291				2.9124
7b	2771				3.2208
	3251				3.3679
	3731				3.8362
	4178	0.00	0.0000	0	4.9710
	4211	0.31	0.4978	8.3318	5.3698
	4267	0.85	1.3805	34.091	6.9224
	4283	1.00	3.3450	50	11.2365

Considering the regression models found between these 4 parameters (2 by 2), we can observe their evolution in a representation:

- tridimensional
 - o opening **d**, length **f** and number of cycles **n** (Figure 4.36 and Figure 4.37),

o opening **d** and crack length in the asphalt **f** and concrete opening **db** (Figure 4.38 and Figure 4.39)

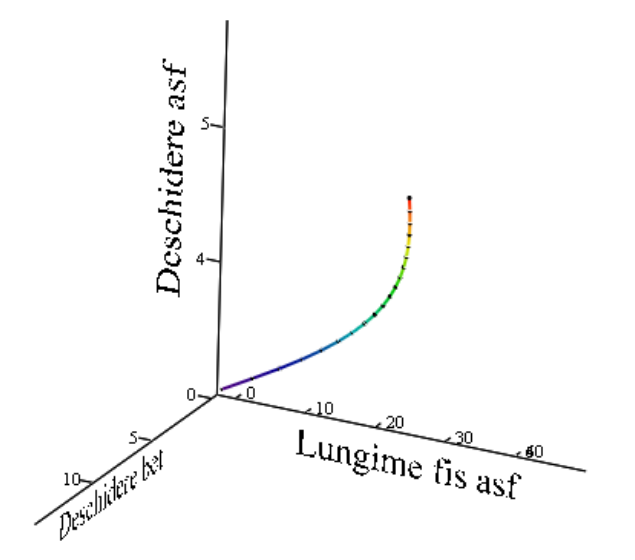


lungrinc fisura

o deschidere fisura

Figure 4.36 Tridimensional representation d, f, n, specimen 7a.

Figure 4.37 Tridimensional representation d, f, n, specimen 7b.



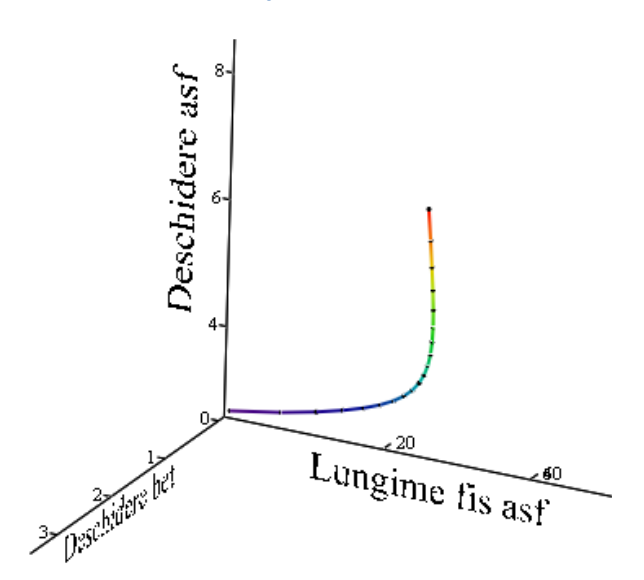
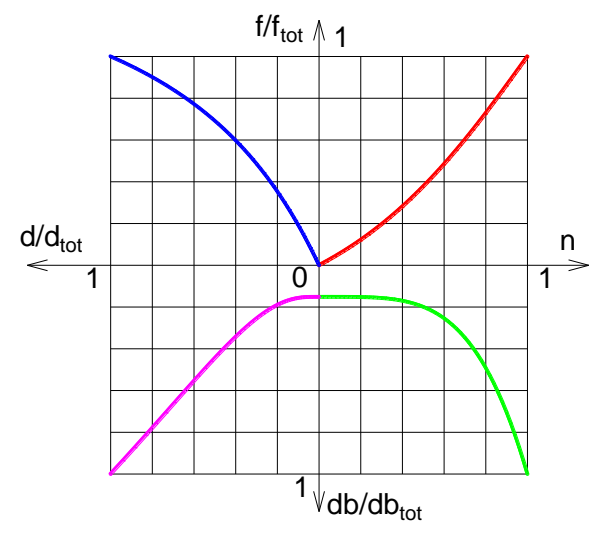


Figure 4.38 Tridimensional representation d, f, db, specimen 7a.

Figure 4.39 Tridimensional representation d, f, db, specimen 7b.

• in the same plan for all the 4 parameters (Figure 4.40 and Figure 4.41).



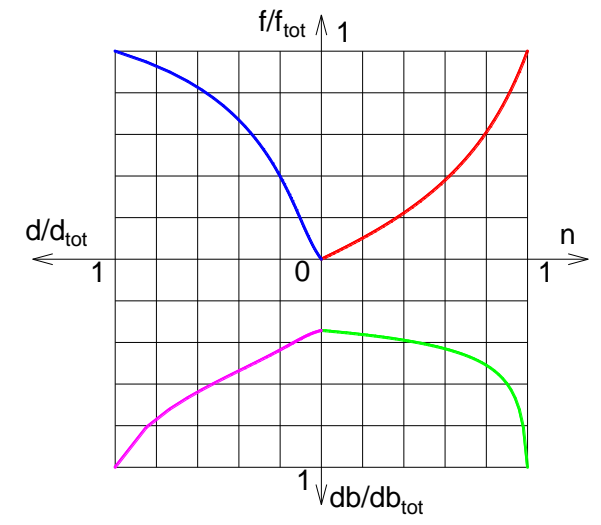
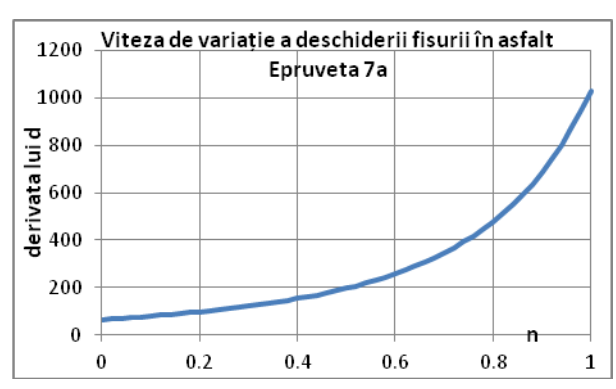


Figure 4.40 The 4 parameters graph, specimen 7a.

Figure 4.41 The 4 parameters graph, specimen 7b.

• Variation rates of crack opening (Figure 4.42, Figure 4.43), crack propagation (length) (Figure 4.44, Figure 4.45) through asphalt, and concrete opening (Figure 4.46, Figure 4.47).



400 Viteza de variație a deschiderii fisurii în asfalt

Epruveta 7b

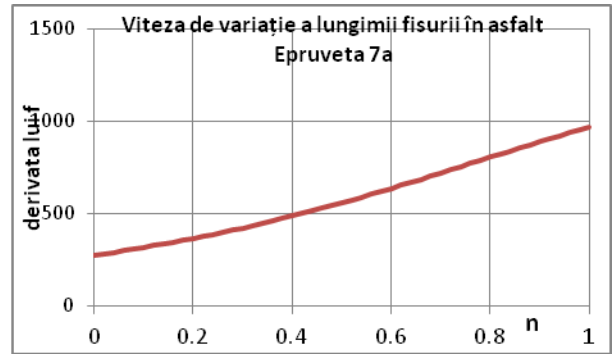
300

100

0 0.2 0.4 0.6 0.8 1

Figure 4.42 Variation speed of crack opening d, specimen 7a

Figure 4.43 Variation speed of crack opening d, specimen 7b



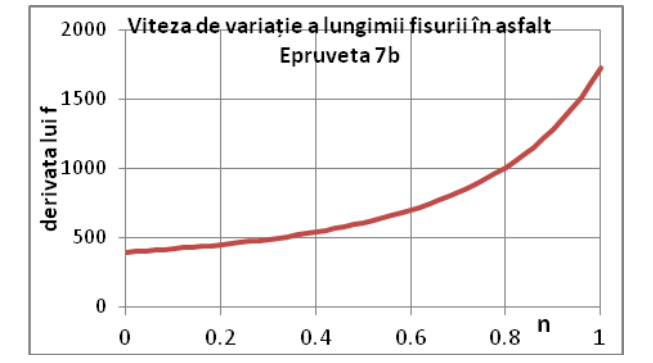
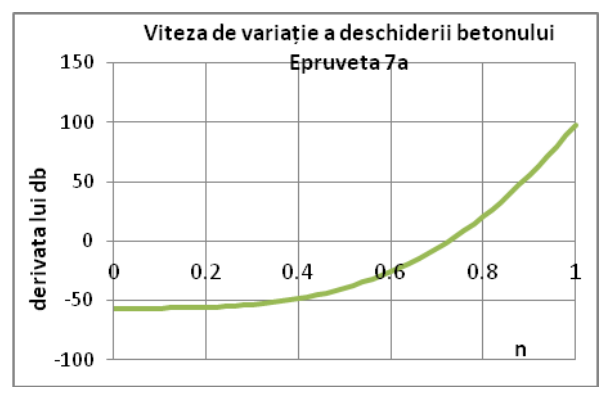
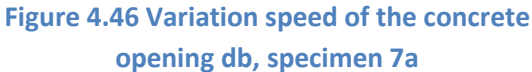


Figure 4.44 Variation speed of the crack length f, specimen 7a

Figure 4.45 Variation speed of the crack length f, specimen 7b

Research Report no. 3. Identification of the parameters of influence of crack propagation through protective asphalt layers for degraded pavements





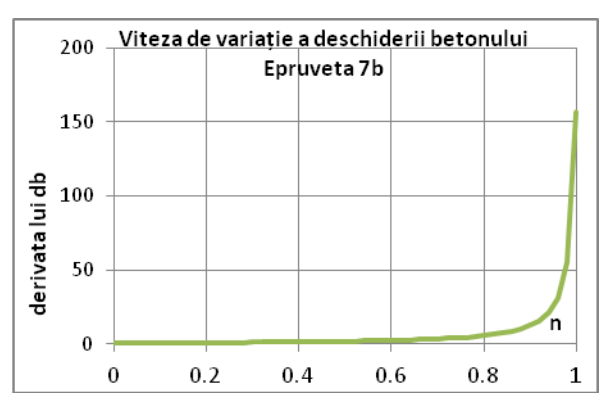


Figure 4.47 Variation speed of the concrete opening db, specimen 7b

4.5 8a şi 8b specimens

The force at which the crack of the precast concrete was transmitted in the protection layer and the specimen yielding occurred is 400daN for 8a and 440daN for 8b, the number of cycles at which the cracking occurred is n_{ci8a} =10.982 compared with n_{ci8b} =11.550, respectively the fracture n_{cR8a} =11338 compared with n_{cR8b} =12081 (Table 4.19). The total test time is 2835 seconds for 8a, respectively 3119 seconds for 8b.

From the point of view of the evolution of the vertical deformation according to the number of cycles (Figure 4.48), until the moment of the appearance of the crack in the asphalt mixture, it is found that sample **8a** has a faster growth compared to **8b**. The crack occurs at a comparable number of cycles, at a difference of 568 (142 seconds), and the fracture at 743 cycles (186 seconds) at **8a** versus **8b**.

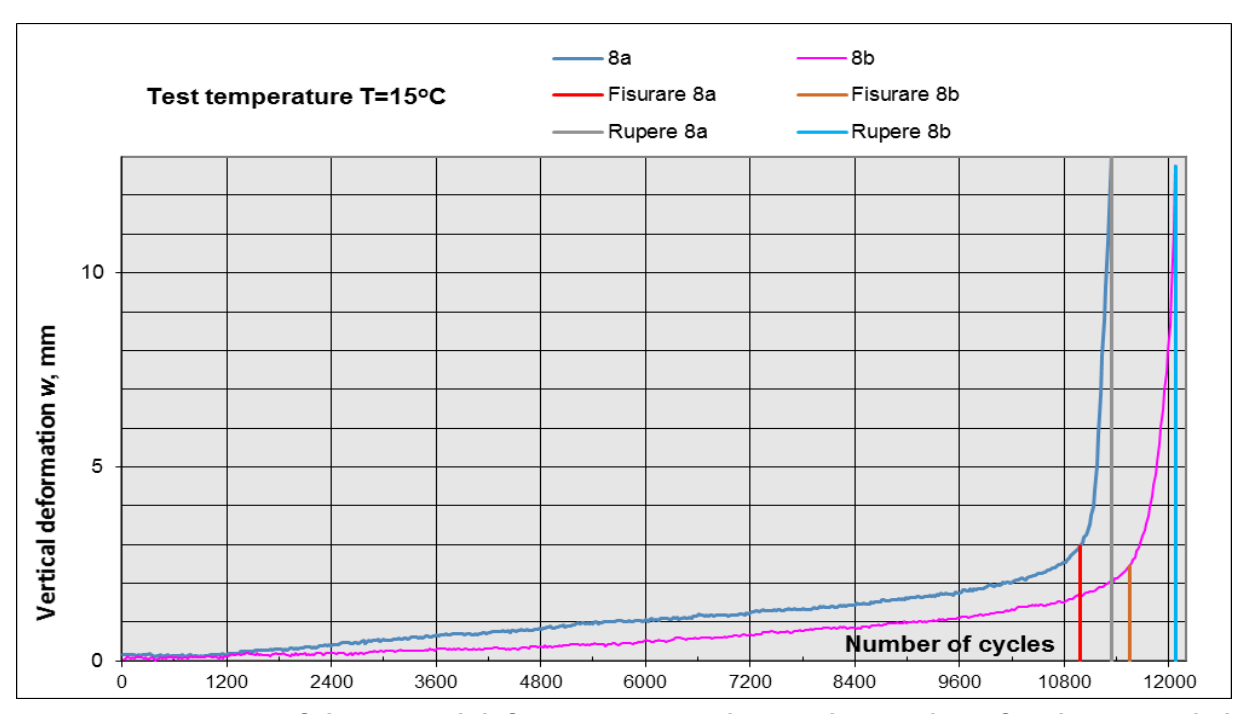


Figure 4.48 Increase of the vertical deformation according to the number of cycles, 8a and 8b

Table 4.19 The number of cycles and the vertical deformation at cracking/fracture failure, 8a and 8b

Cracking	8a	Cracking	8b
Number of cycles, n ci	Vertical deformation,	Number of cycles n.	Vertical deformation,
Number of cycles, Ild	\mathbf{w} Number of cycles, \mathbf{n}_{ci}		w
10982	2.9567	11550	2.4507
Fracture	8a	Fracture	8b
Number of cycles, n _{cR}	Vertical deformation,	Number of cycles, n cR	Vertical deformation,
Nulliber of Cycles, HcR	w	indifficer of cycles, fice	w
11338	13.0771	12081	12.7619

A simple calculation indicates that approximately 95-97% of the life of the mixture is consumed until the crack appears and 3-5% of the time is represented by the propagation of the crack through the asphalt plate. (Table 4.20.).

Table 4.20. Mixture crack index, 8a and 8b

Specimen	Reflective cracking index, $I_f = \frac{n_{ci}}{n_{cR}}$ (%)	Number of cycles
8a	96.86%	356
8b	95.60%	531

The initial crack opening of the dbi cement concrete and the initial detachment \mathbf{e}_i of the asphalt layer from the concrete slab are approximately equal. (Table 4.21). Hence the relatively small difference between the 2 samples.

Table 4.21 Initial opening values db_i and the initial detachment (bitumen bonding) e_i and the eccentricity of the crack in the asphalt e_f, 8a and 8b

Specimen	Upper view db = the initial concrete opening (mm)	Side view e= the initial detachment of the asphalt from the concrete (mm)	Side view e _f = the eccentricity of the crack of the asphalt slab compared to the crack of the concrete (<i>mm</i>)
8 a	13547		30 3118
	dbi=1.3547	ei=3.7808	e _f =30.3118



The measurements and processing of the cracking parameters (Table 4.22, Table 4.23), the length and opening of the crack in the asphalt, the opening of the concrete, for specimens 8a and 8b indicate:

• The variation of the crack opening **d**, but also of the length **f** in relation to **n**, is nonlinear (Figure 4.49, Figure 4.50). The regression model is the same as in specimen 4b:

$$y = \frac{a_0 \cdot n}{1 + a_1 \cdot n + a_2 \cdot n^2}$$

when
$$y = d$$

8a
$$a_0 = 0.588, a_1 = -1.423, a_2 = 0.564,$$

Standard deviation S=0.0616, and the correlation coefficient r=0.996.

8b
$$a_0 = 0.996, a_1 = -0.956, a_2 = 0.0536,$$

Standard deviation S=1116, and the correlation coefficient r=0.993.

when
$$y = f$$

8a
$$a_0 = 21.34, a_1 = -1.315, a_2 = 0.746,$$

Standard deviation S=1.4606, and the correlation coefficient r=0.9986.

8b
$$a_0 = 32.11, a_1 = -0.7691, a_2 = 0.3971,$$

Standard deviation S=1.5353, and the correlation coefficient r=0.995.

We can thus determine the number of cycles the crack propagation reaches half the thickness of the protective asphalt plate (h=50mm):

- 8a $-n_{cf} = 11186$ cycles (n = 0.57, or we can say that the length of the crack reached h / 2, at 57% of the total duration of its propagation).
- 8b $-n_{cf} = 11620$ cycles (n = 0.54, or we can say that the length of the crack reached h / 2, at 54% of the total duration of its propagation).

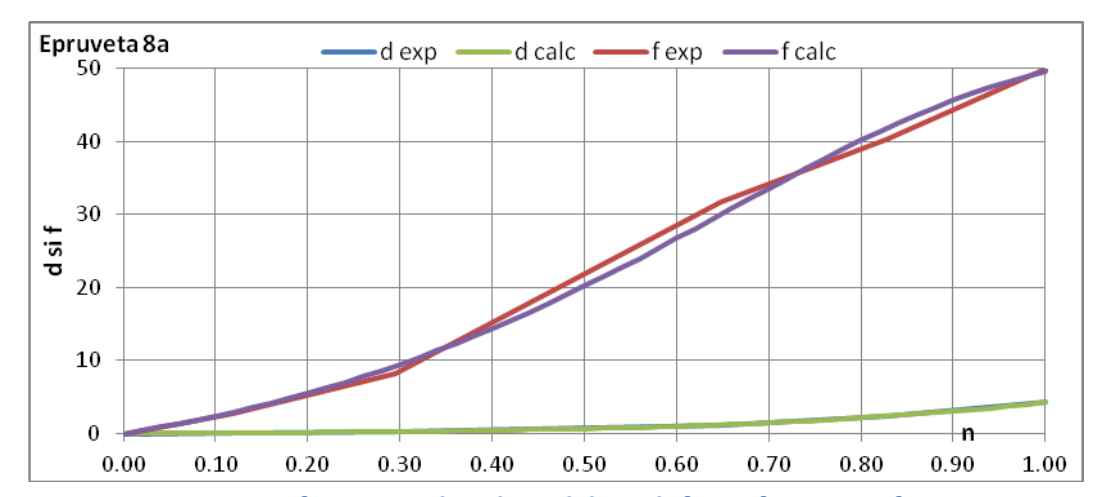


Figure 4.49 Variation of opening d and crack length f as a function of n, specimen 8a.

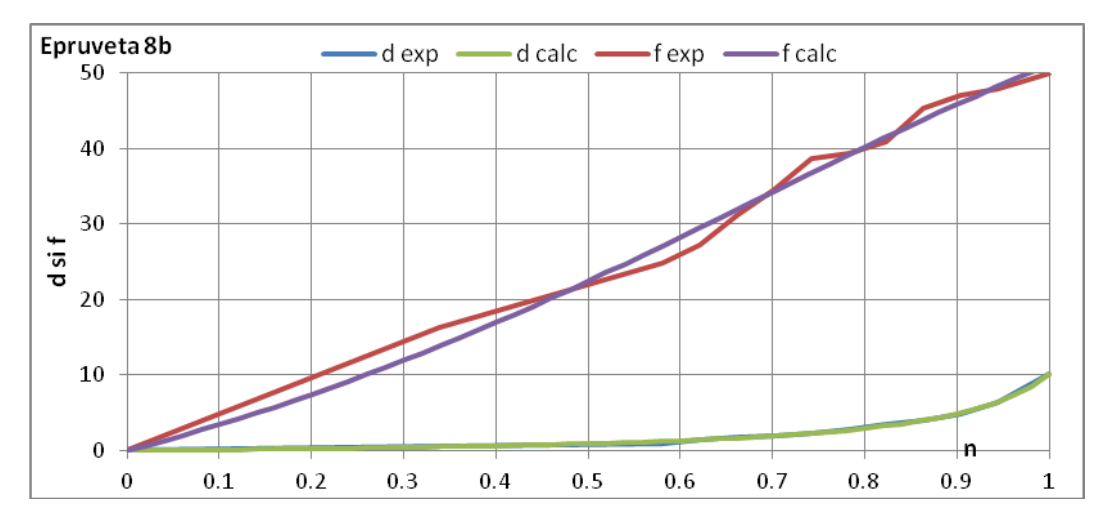


Figure 4.50 Variation of opening d and crack length f as a function of n, specimen 8b.

• The regression model found for the evolution of the concrete opening db in relation to n is the MMF for 8a and Bleasdale for 8b, Figure 4.51 and Figure 4.52:

$$8a - db = \frac{a_0 \cdot a_1 + a_2 \cdot n^{a_3}}{a_1 + n^{a_3}}$$

$$8b - db = (a_0 + a_1 \cdot n)^{-\frac{1}{a_2}}$$

8a
$$a_0 = 1.551, a_1 = 3.875, a_2 = 4.69 \cdot 10, a_3 = 5.023$$

Standard deviation S=0.127, and the correlation coefficient r=0.9998.

8b
$$a_0 = 2.488 \cdot 10^{-2}, a_1 = -2.446 \cdot 10^{-2}, a_2 = 3.515$$

Standard deviation S=0.062, and the correlation coefficient r=0.999.

To find out the actual opening of the concrete at a point, the value of the initial opening will be added to the value resulting from the 2 models db_i (Table 4.21)

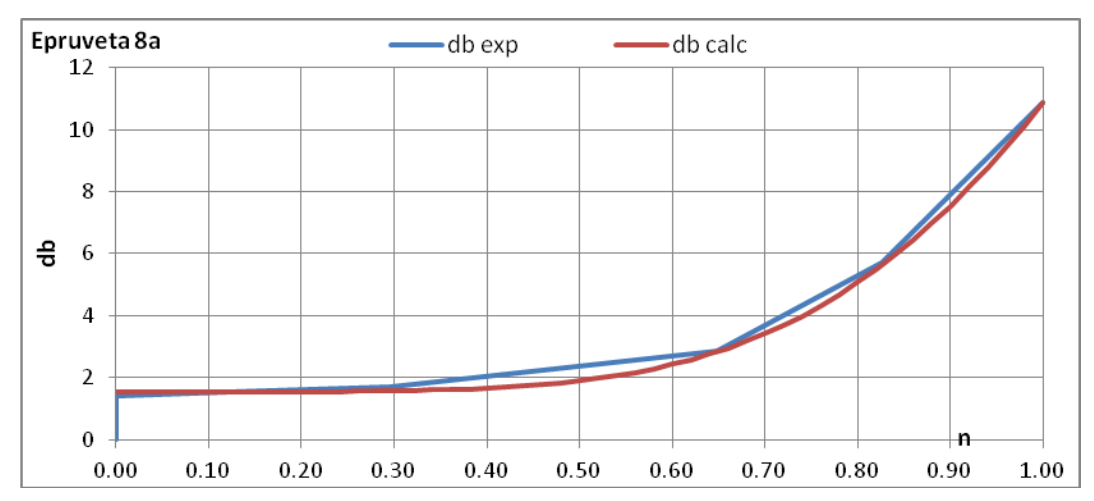


Figure 4.51 The variation of the concrete opening db depending on n, specimen 8a

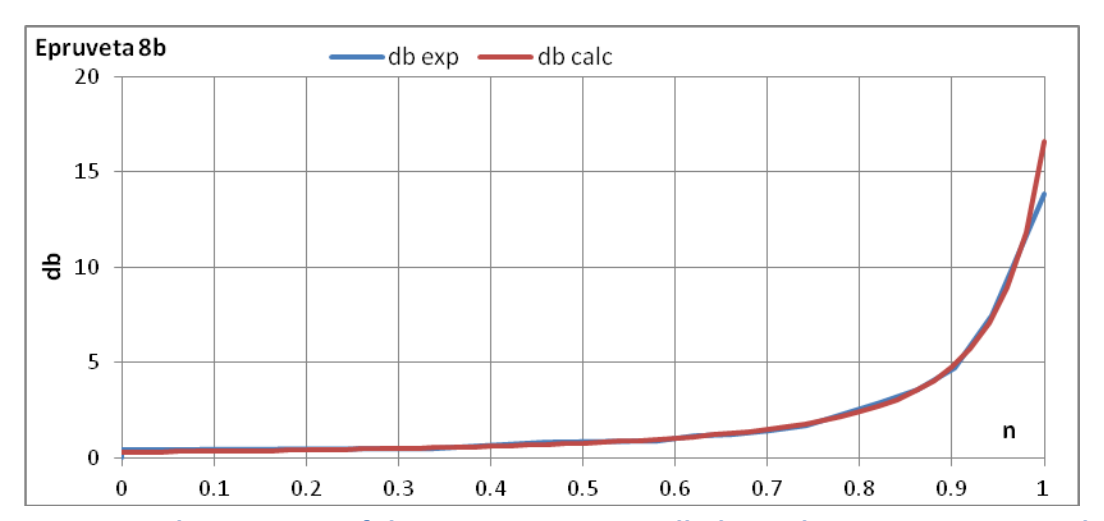


Figure 4.52 The variation of the concrete opening db depending on n, specimen 8b

Table 4.22 Experimental results, specimen 8a

Specimen	nc	n	d	f	db
	0				1.3547
	2386				1.5404
	8386				1.7762
	9586				2.1488
	10738				2.4022
0.0	10858				2.4674
8a	10982	0.00	0.00	0	2.7843
	11024	0.12	0.14	2.68	2.9045
	11087	0.29	0.34	8.13	3.0611
	11213	0.65	1.17	31.67	4.1977
	11276	0.83	2.39	40.23	7.0812
	11338	1.00	4.31	50.00	12.2109

Specimen	nc	n	d	f	db
	0				1.48
	3089				1.48
	6689				1.61
	9089				1.69
	10289				1.71
	10689				1.82
	11089	0	0.00	0.000	1.93
	11425	0.33871	0.50	16.347	1.93
	11545	0.459677	0.81	20.596	2.31
O.L.	11665	0.580645	0.97	24.916	2.36
8b	11705	0.620968	1.46	27.313	2.61
	11745	0.66129	1.81	31.132	2.69
	11785	0.701613	2.03	34.598	2.91
	11825	0.741935	2.29	38.785	3.18
	11865	0.782258	2.75	39.450	3.77
	11905	0.822581	3.41	40.994	4.40
	11945	0.862903	4.03	45.384	5.04
	11985	0.903226	4.85	47.025	6.19
	12025	0.943548	6.43	47.875	8.91
	12081	1	10.20	50.000	15.33

Table 4.23 Experimental results, specimen 8b

Considering the regression models found between these 4 parameters (2 by 2), we can observe their evolution in a representation:

tridimensional

- o opening **d**, length **f** and number of cycles **n** (Figure 4.53 and Figure 4.54),
- o opening **d** and crack length in the asphalt **f** and concrete opening **db** (Figure 4.55 and Figure 4.56)

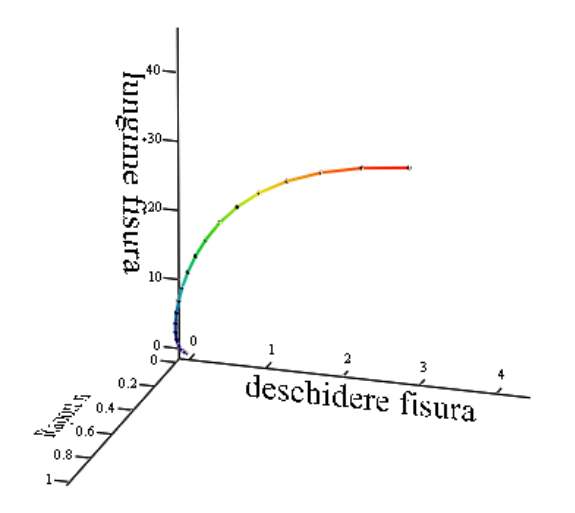


Figure 4.53 Tridimensional representation d, f, n, specimen 8a.

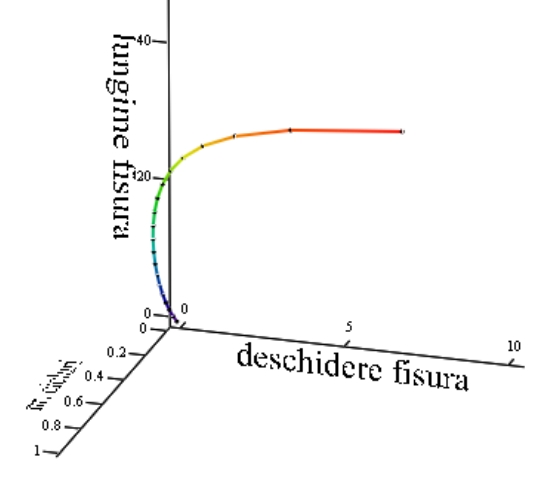
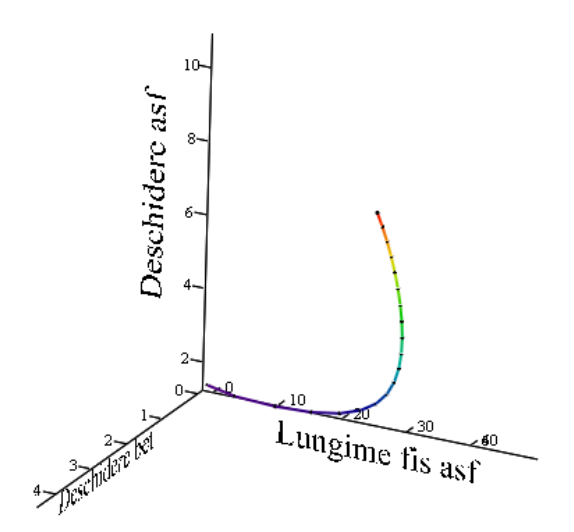


Figure 4.54 Tridimensional representation d, f, n, specimen 8b.



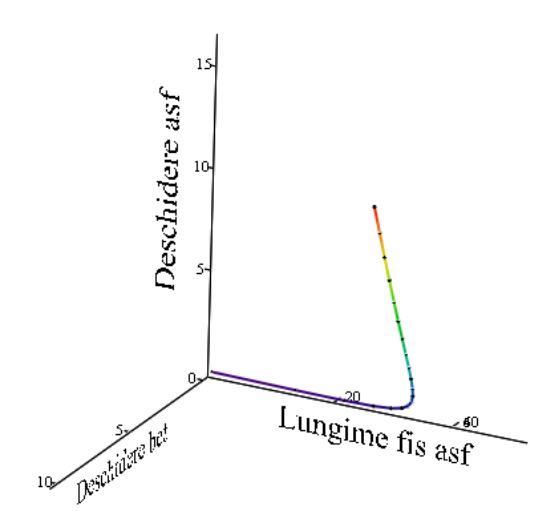


Figure 4.55 Tridimensional representation d, f, db, specimen 8a.

Figure 4.56 Tridimensional representation d, f, db, specimen 8b.

• in the same plan for all the 4 parameters (Figure 4.57 and Figure 4.58).

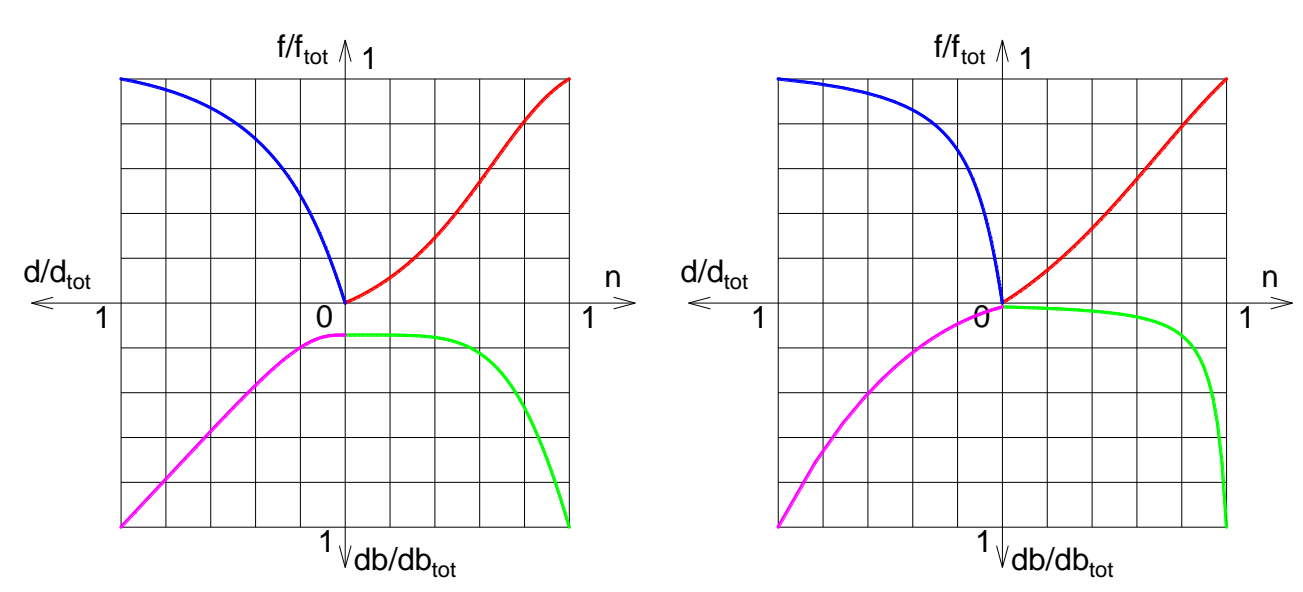
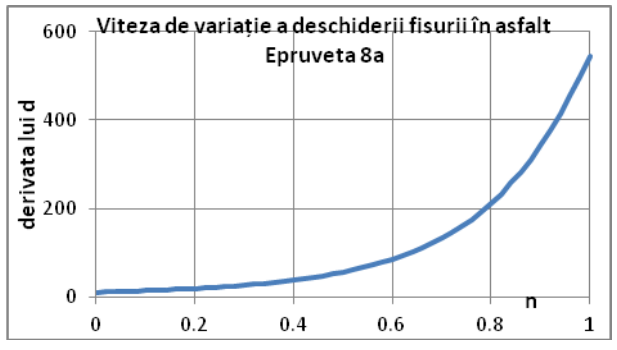


Figure 4.57 The 4 parameters graph, specimen, 8a.

Figure 4.58 The 4 parameters graph, specimen 8b.

• Variation rates of crack opening (Figure 4.28 and Figure 4.60), crack propagation (length) (Figure 4.61, Figure 4.62) through asphalt, and concrete opening (Figure 4.63, Figure 4.64).



2500 Viteza de variație a deschiderii fisurii în asfalt
Epruveta 8b

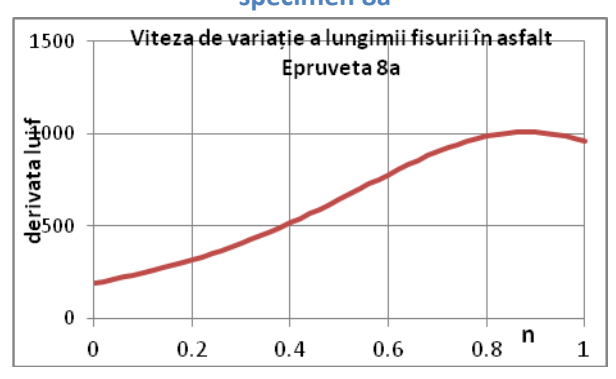
1500

500

0 0.2 0.4 0.6 0.8 1

Figure 4.59 Variation speed of crack opening d, specimen 8a

Figure 4.60 Variation speed of crack opening d, specimen 8b



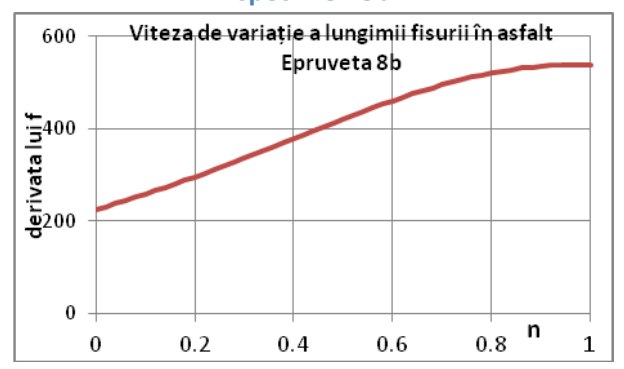
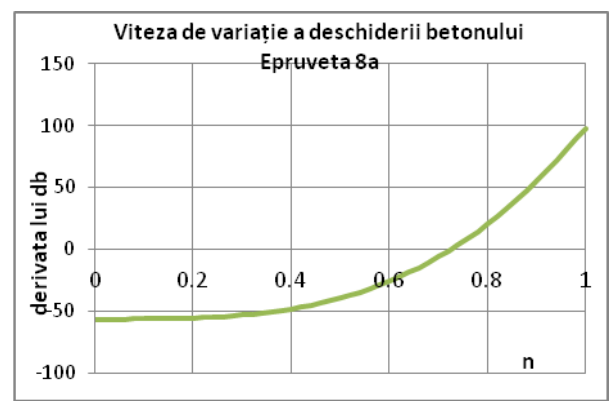


Figure 4.61 Variation speed of the crack length f, specimen 8a

Figure 4.62 Variation speed of the crack length f, specimen 8b



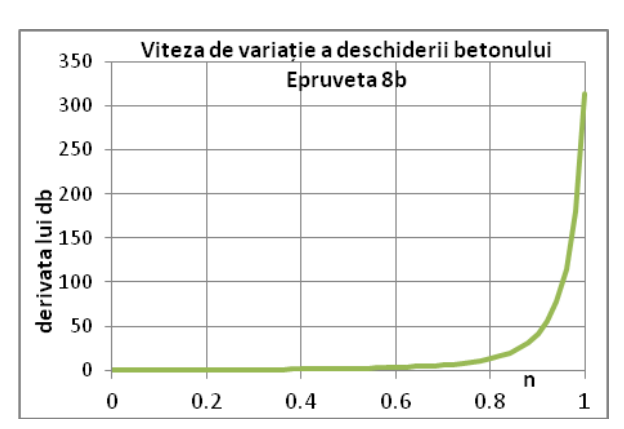


Figure 4.63 Variation speed of the concrete opening db, specimen 8a

Figure 4.64 Variation speed of the concrete opening db, specimen 8b

4.6 9a şi 9b specimens

The force at which the crack of the precast concrete was transmitted in the protection layer and the specimen yielding occurred is 400-440daN for 9a and 400-480daN for 9b, the number of cycles at which the cracking occurred is n_{ci9a} =11.972 compared with n_{ci9b} =11.612, respectively the fracture n_{cR9a} =12.536 compared with n_{cR9b} =14.552 (Table 4.24). The total test time is 3134 seconds for 9a, respectively 3638 seconds for 9b.

From the point of view of the evolution of the vertical deformation according to the number of cycles (Figure 4.65), until the moment of the appearance of the crack in the asphalt

mixture, it is found that specimens **9a** and **9b** have a similar growth. The crack occurs at a comparable number of cycles, at a difference of 360 (90 seconds) 9a > 9b, and the fracture at 2016 cycles (504 seconds) 9a < 9b.

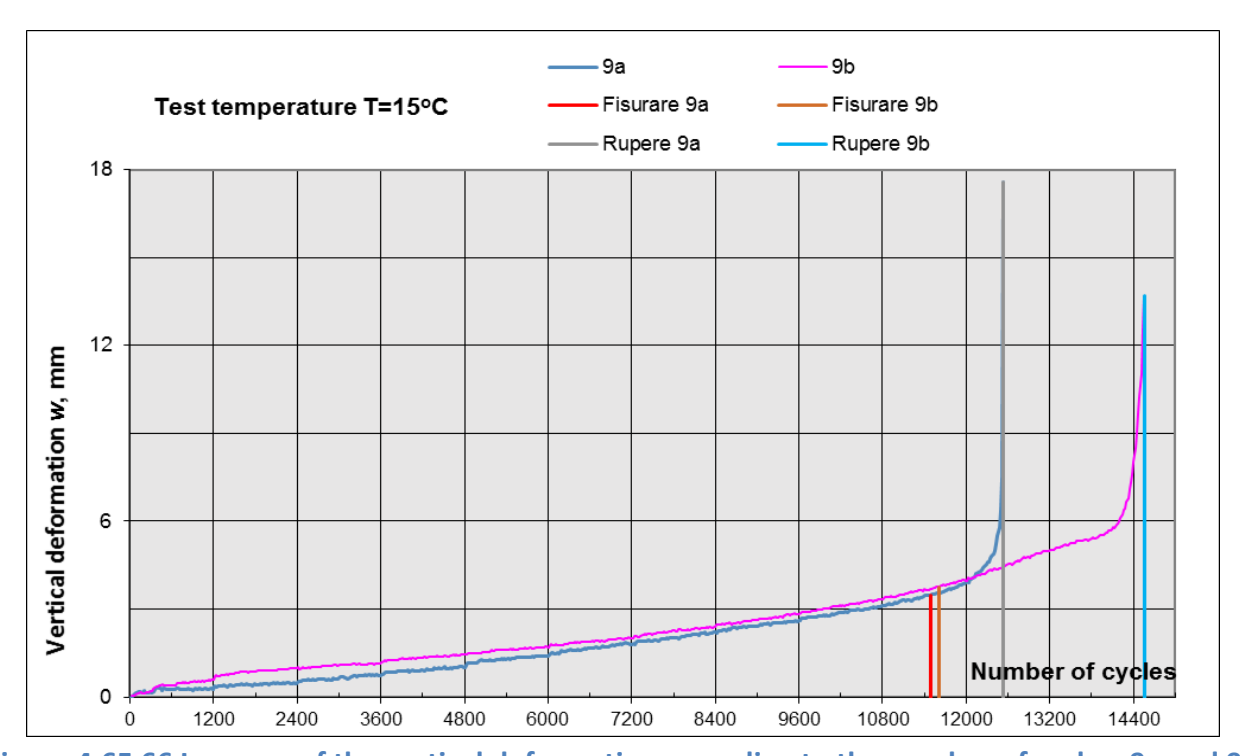


Figure 4.65 66 Increase of the vertical deformation according to the number of cycles, 9a and 9b

Table 4.24 The number of cycles and the vertical deformation at cracking/fracture failure, 9a and 9b

Cracking	9a	Cracking	9b				
Number of cycles, n ci	Vertical deformation,	Number of cycles, n ci	Vertical deformation,				
Number of cycles, fici	w	Number of cycles, IId	w				
11972	3.8478	11612	3.7641				
Fracture	9a	Fracture	9b				
Number of cycles .	Vertical deformation,	Number of cycles .	Vertical deformation,				
Number of cycles, n _{cR}	w	Number of cycles, n _{cR}	w				
12536	17.5802	14552	13.6902				

The percentage calculation shows that 95.5% (9a), respectively 80% (9b) of the life cycle of the mixture is consumed until the crack appears and 4.5% (9a), respectively 20% (9b) of the time is the propagation of the crack through the plate of asphalt ((Table 4.25). There is a considerable increase in the behavior of the protective layer after the appearance of the crack in it in specimen 9b.

Table 4.25 Mixture crack index, 9a and 9b

Specimen	Reflective cracking index, $I_f = \frac{n_{ci}}{n_{cR}}$ (%)	Number of cycles
9a	95.50%	564
9b	79.80%	2940

If for 9a and 5a, 5b, 7a, 7b, 8a, 8b, the crack index If is at least 95%, in the case of specimen 9b there is a significant increase in the number of cycles from cracking to fracture (20 % of total test duration). This is due to a change in the preparation of the specimen.

When the 2 parts of the pre-cracked concrete joined, the same bitumen was poured between them, on an area of approximately 3cm by 5cm, with which the gluing was made to bond the concrete with the mixture (Figure 4.67). This situation also occurs in the case of a crack in the concrete (crack with the initial opening larger than 5 mm), when the liquid bitumen enters this crack as well, practically modifying the transfer effect.

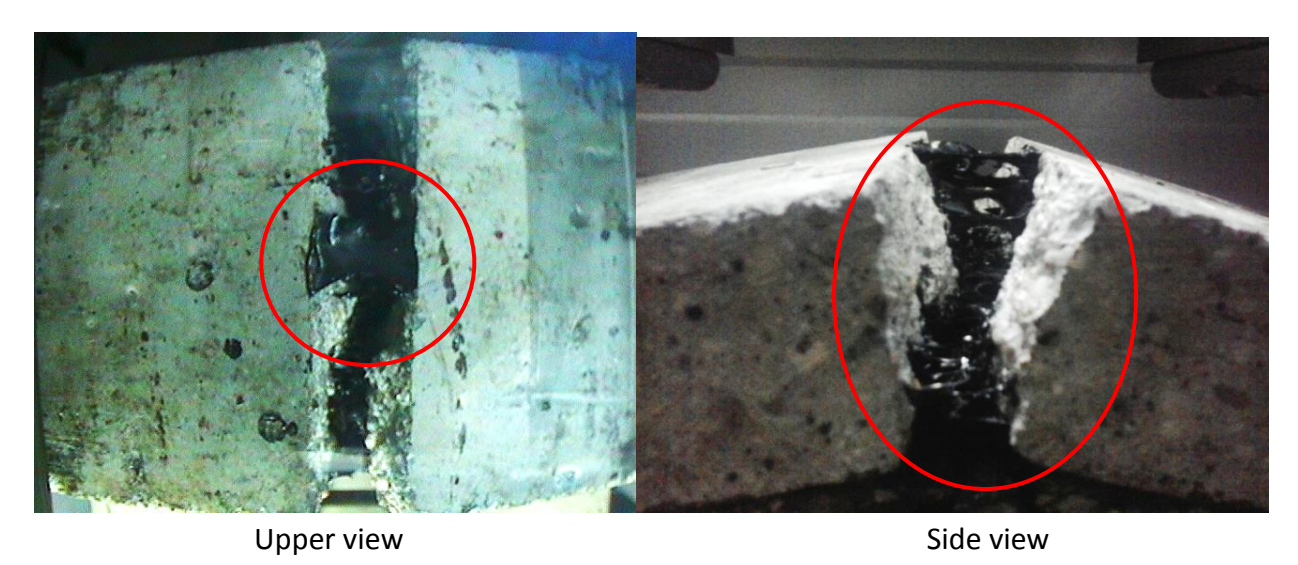
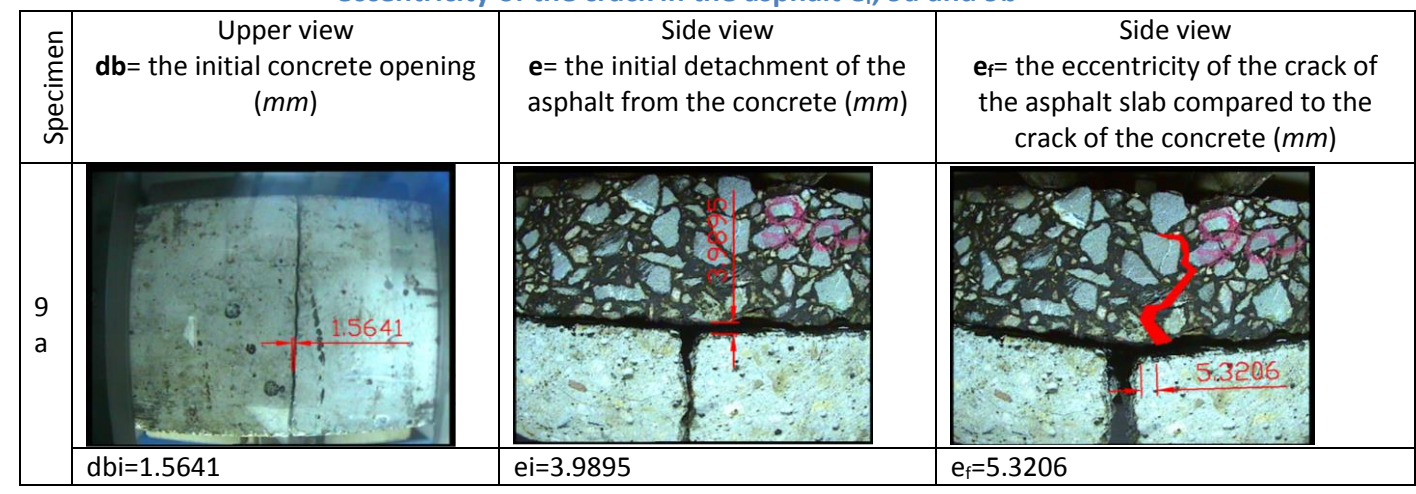
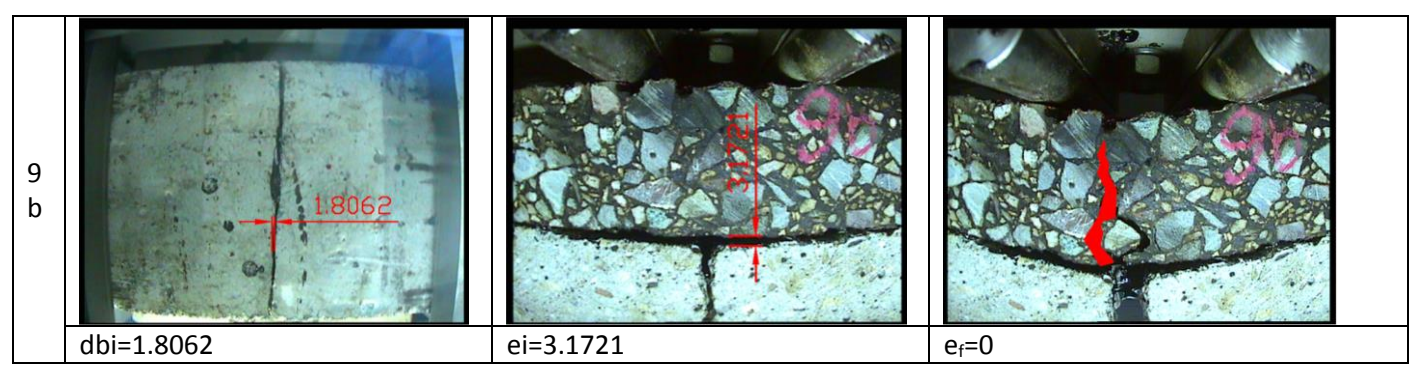


Figure 4.67 Bitumen poured between concrete slabs, specimen 9b.

The initial crack opening of the cement concrete db_i is smaller for 9a, and the initial detachment of the asphalt layer from its concrete slab is smaller at 9b (Table 4.26). In this case, the db_i parameter is a good indicator of the higher number of cycles for 9a, until the crack propagates through the mixture.

Table 4.26 Initial opening values db_i and the initial detachment (bitumen bonding) e_i and the eccentricity of the crack in the asphalt e_f, 9a and 9b





The measurements and processing of the cracking parameters (Table 4.27), the length and opening of the crack in the asphalt, the opening of the concrete, for specimen 9a indicate:

• The variation of the crack opening **d**, but also of the length **f** in relation to **n**, is nonlinear (Figure 4.68). The regression model is the same as in specimen 4b:

$$y = \frac{a_0 \cdot n}{1 + a_1 \cdot n + a_2 \cdot n^2}$$

when
$$y = d$$

$$a_0 = 2.544, a_1 = 6.294, a_2 = -6.89,$$

Standard deviation S=0.277, and the correlation coefficient r=0.9885.

when
$$y = f$$

$$a_0 = 54.28, a_1 = 2.79, a_2 = -2.677,$$

Standard deviation S=1.098, and the correlation coefficient r=0.9976.

We can thus determine the number of cycles the crack propagation reaches half the thickness of the protective asphalt plate (h=50mm): $n_{cf} = 12260$ cycles (n = 0.74, or we can say that the length of the crack reached h / 2, at 74% of the total duration of its propagation).

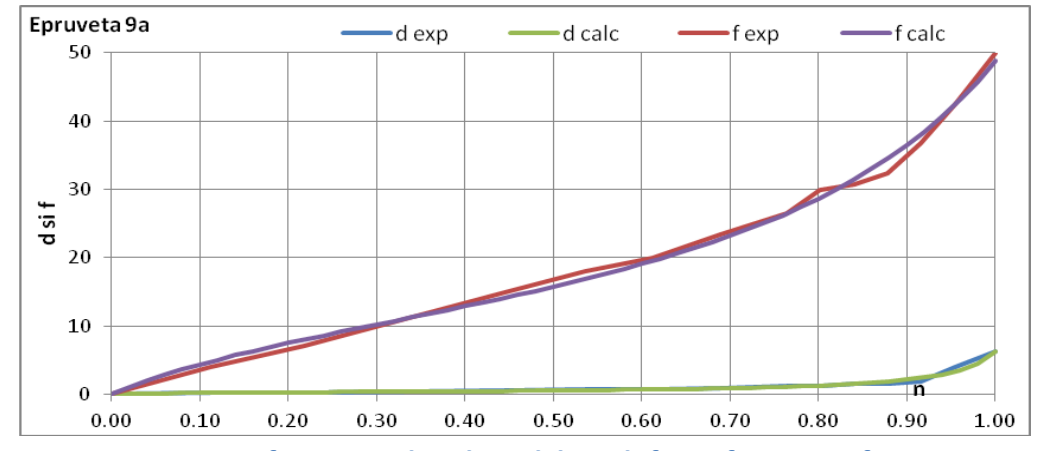


Figure 4.68 Variation of opening d and crack length f as a function of n, specimen 9a.

• The regression model found for the evolution of the concrete opening db in relation to n is the Bleasdale model, Figure 4.69:

$$db = (a_0 + a_1 \cdot n)^{-\frac{1}{a_2}}$$

$$a_0 = 3.42 \cdot 10^{-1}, a_1 = -3.322 \cdot 10^{-1}, a_2 = 1.58$$

Standard deviation S=0.876, and the correlation coefficient r=0.984.

To find out the actual opening of the concrete at a point, the value of the initial opening will be added to the value resulting from the Bleasdale model, db_i (Table 4.26)

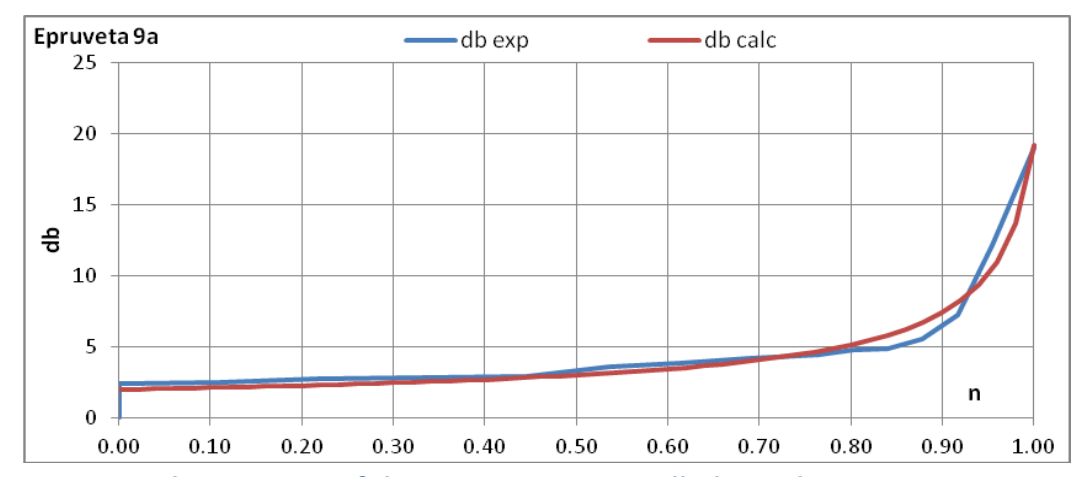


Figure 4.69 The variation of the concrete opening db depending on n, specimen 9a

Table 4.27 Experimental results, specimen 9a

Specimen	nc	n	d	f	db
	0				1.5641
	2011				1.6671
	4411				1.8963
	6811				2.0757
	8867				2.4163
	9107				2.7275
	9867				3.1849
	10347				3.4245
	10827				3.6831
	11235				3.7647
	11486	0.00	0.0000	0	3.9272
00	11603	0.11	0.1435	3.9033	4.0345
9a	11715	0.22	0.2758	7.0546	4.2811
	11955	0.45	0.4660	14.8568	4.5004
	12051	0.54	0.6720	17.971	5.1369
	12131	0.61	0.7161	19.9293	5.3992
	12211	0.69	0.8645	23.4324	5.7360
	12291	0.76	1.1917	26.5155	5.9985
	12331	0.80	1.2641	29.9217	6.3616
	12371	0.84	1.5583	30.7796	6.4132
	12411	0.88	1.5873	32.3692	7.1251
	12451	0.92	1.7793	36.7255	8.8406
	12491	0.95	3.9477	42.5254	13.7419
	12539	1.00	6.2260	50	20.5973

Considering the regression models found between these 4 parameters (2 by 2), we can observe their evolution in a representation:

- tridimensional
 - o opening **d**, length **f** and number of cycles **n** (Figure 4.70),
 - o opening **d** and crack length in the asphalt **f** and concrete opening **db** (Figure 4.71)

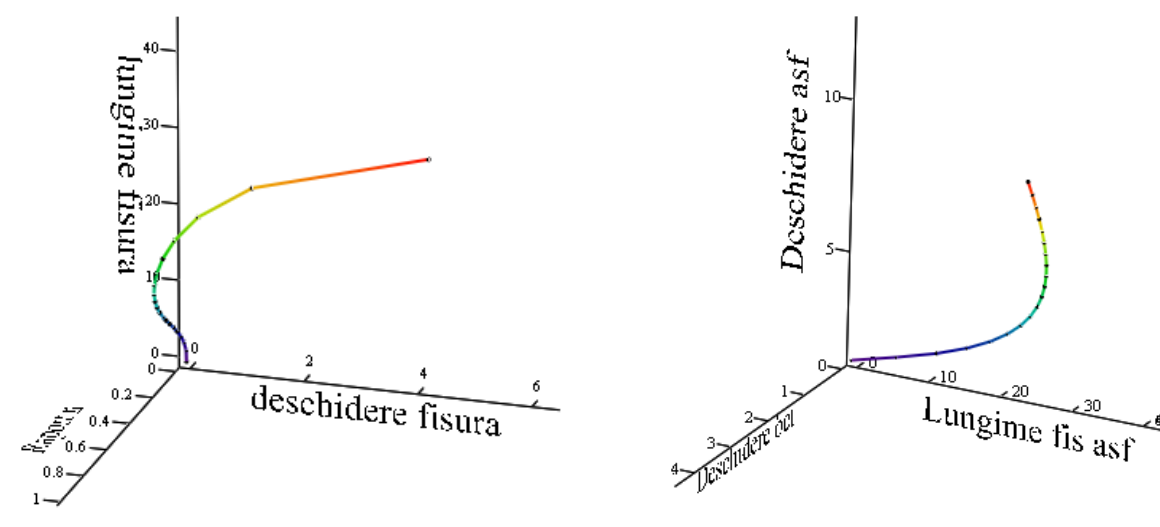


Figure 4.70 Tridimensional representation d, f, n, specimen 9a.

Figure 4.71 Tridimensional representation d, f, n, specimen 9a.

• in the same plan for all the 4 parameters (Figure 4.72).

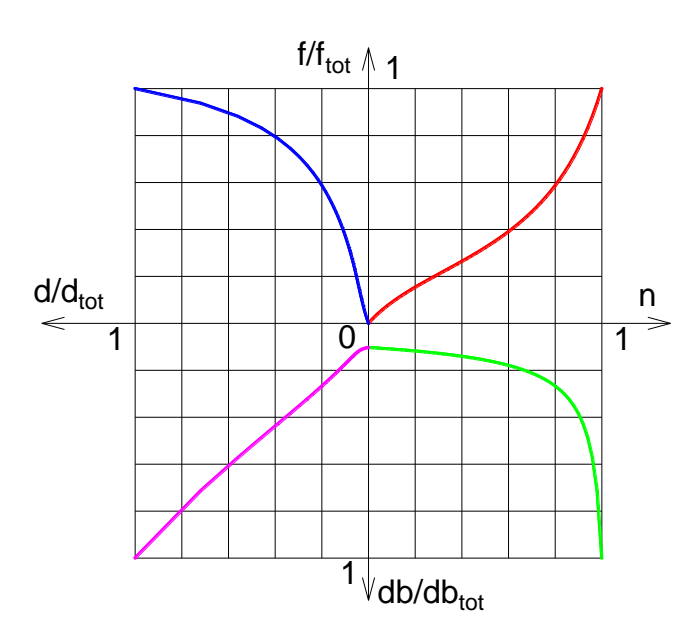
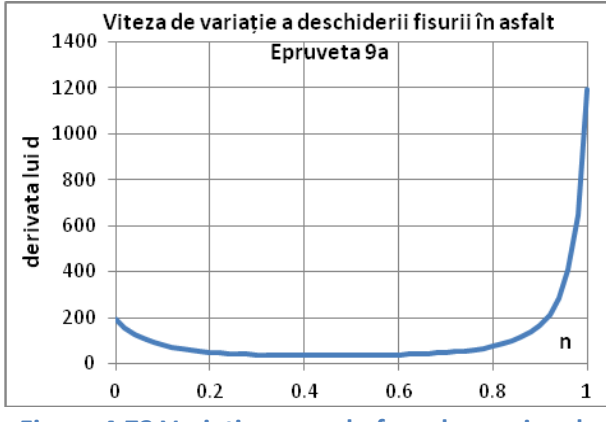


Figure 4.72 The 4 parameters graph, specimen 9a.

Variation rates of crack opening (Figure 4.73), crack propagation (length) (Figure 4.74)
 through asphalt, and concrete opening (Figure 4.75).

Research Report no. 3. Identification of the parameters of influence of crack propagation through protective asphalt layers for degraded pavements



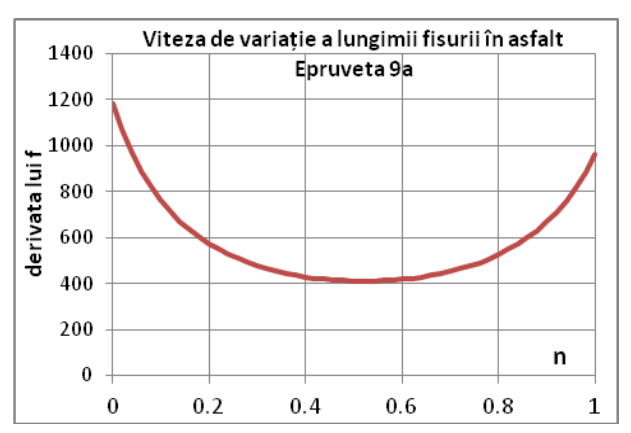


Figure 4.73 Variation speed of crack opening d, specimen 9a

Figure 4.74 Variation speed of the crack length f, specimen 9a

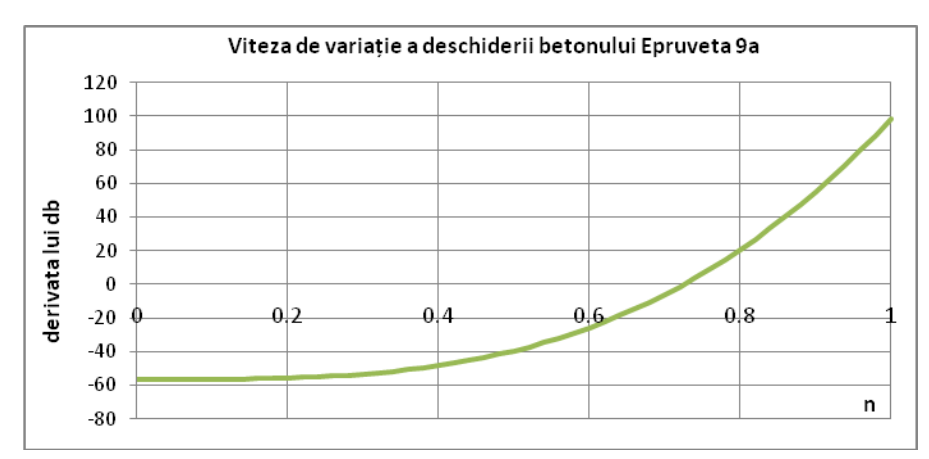


Figure 4.75 Variation speed of the concrete opening db, specimen 9a

5 CRACKING PARAMETERS

In this research report we identified and interpreted through the tests performed on the Cracking Device with Temperature Control, the following parameters of reflective cracking through the asphalt protection mat of a rigid road pavement degraded by cracking:

Analysis parameters:

- Accelerated cracking life cycle (T_f)
- Crack opening in asphalt layer (d)
- Detachment of asphalt from concrete in the crack area (e)
- Number of cycles at the initiation and propagation of the crack n_{ci}, at the opening and propagation of the crack on the thickness of the asphalt layer n_{cf} and at the yield by fracture n_{cR}=n_{ctot}.
- Vertical deformation (deflection) at the initiation and propagation of the crack w_i, at the opening and propagation of the crack on the thickness of the asphalt layer w_f, at the yield by fracture w_{fR} and at the appearance of the crack in the asphalt layer w_R.

- Crack opening in the concrete support layer (db)
- The eccentricity of the crack position in the asphalt compared to the crack position in the base layer e_f .

Specimen 4b is the test calibration test, since the imaging also showed that all the analysis parameters (nc, db, d, f) evolved through interdependence, and their variation is proportional (Figure 4.4 şi Figure 4.5).

6 MULTICRITERIAL INTERPRETATION OF THE REFLECTIVE CRACKING PROCESS

The multicriteria interpretation is defined by a series of criteria of influence for the phenomenon of reflective cracking of the asphalt layer, which has the role of protection of a layer of precast concrete (an old degraded road pavement).

Being a composite road structure (in which each layer has a different behavior when taking over traffic loads during the operation of the road), the reflective propagation of the crack from the concrete layer in the protective asphalt, depends on the parameters stated in in this research report, which must be analyzed by overlapping effects.

The main parameters that influence reflective cracking are:

- Dynamic stresses that simulate the effect of road traffic, materialized in the laboratory study by the intensity of the force (F) and its frequency of application, constant frequency in the case of Cracking Device with Temperature Control;
- The effect of the transfer to the crack, from the existing crack of the concrete layer, materialized by the analysis of the parameter **db** (opening of the crack in the concrete support layer);
- The asphalt-concrete cooperation, by evaluating the acrosage by bonding the interface between the two layers with different physical-mechanical characteristics, materialized by analyzing its parameters, e_i, e_f,, respectively detaching the asphalt from the concrete support in relation to increasing the vertical deformation (w) of the experimental model;
- The initiation of the crack and its propagation through the asphalt layer, through the opening (d) and the length (f) of the crack, which depend on the physical-mechanical characteristics of the bituminous mixtures from which the asphalt layer is made.

Consequently, the multicriteria interpretation of the process of reflective cracking in rigid road structures rehabilitated by laying a protective asphalt, involves a combined analysis between the influencing factors of the process of transmission and propagation of the crack from the cracked concrete pavement to the asphalt layer.

These influencing factors are described in the form of parametric indices:

- the index of the cyclic stress parameter Inc (Table 6.1 the index of the cyclic stress parameter IncTable 6.1),
- the index of the variation parameter of the opening in time of the existing crack in the concrete support Idb (Table 6.2),
- the index of opening of the reflective crack in the asphalt layer Id,
- the crack propagation index through the asphalt layer If.

 db_i Specimen \mathbf{n}_{cR} \mathbf{n}_{ci} n_{cR} - n_{ci} 9974 1.1480 6a 10520 546 7790 7496 1.2487 7a 294 1.3547 8a 11338 11100 238 1.4843 8b 12081 11550 531 1.5641 9a 12536 11972 564 12429 12116 1.7432 5b 313 1.7652 7b* 4283 4183 100 9b*** 1.8062 14552 11612 2940 2.1008 12556 12200 356 5a 4b** 3.0088 1259 1000 259

Table 6.1 the index of the cyclic stress parameter Inc

where: n_c – the number of cycles for which the calculation of I_{nc} is desired ($n_c \ge n_{ci}$).

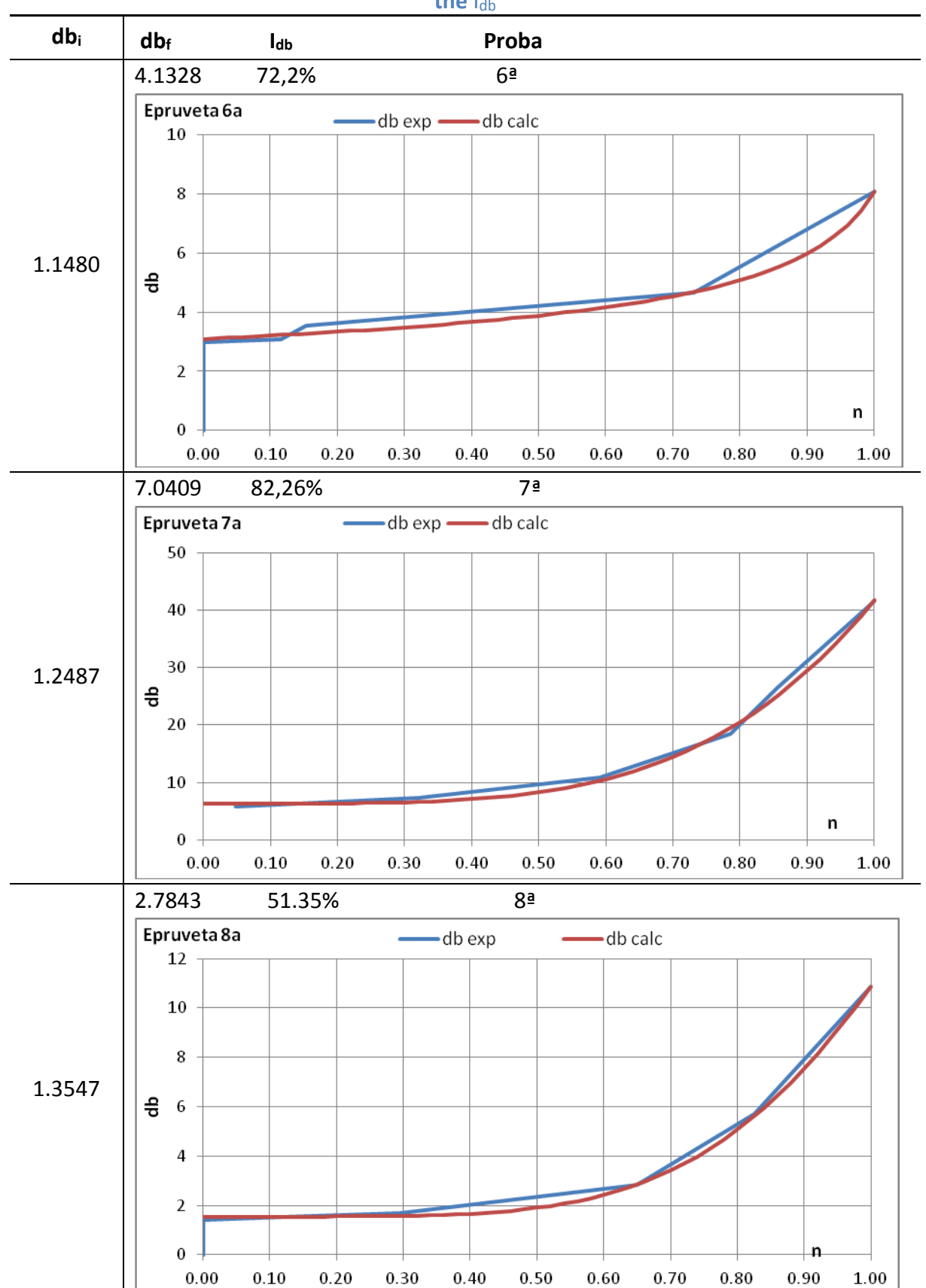
The Inc index is in fact the ratio n used to process the experimental results (graphs of variation of the opening, the length of the crack in the asphalt, respectively the crack opening in the concrete).

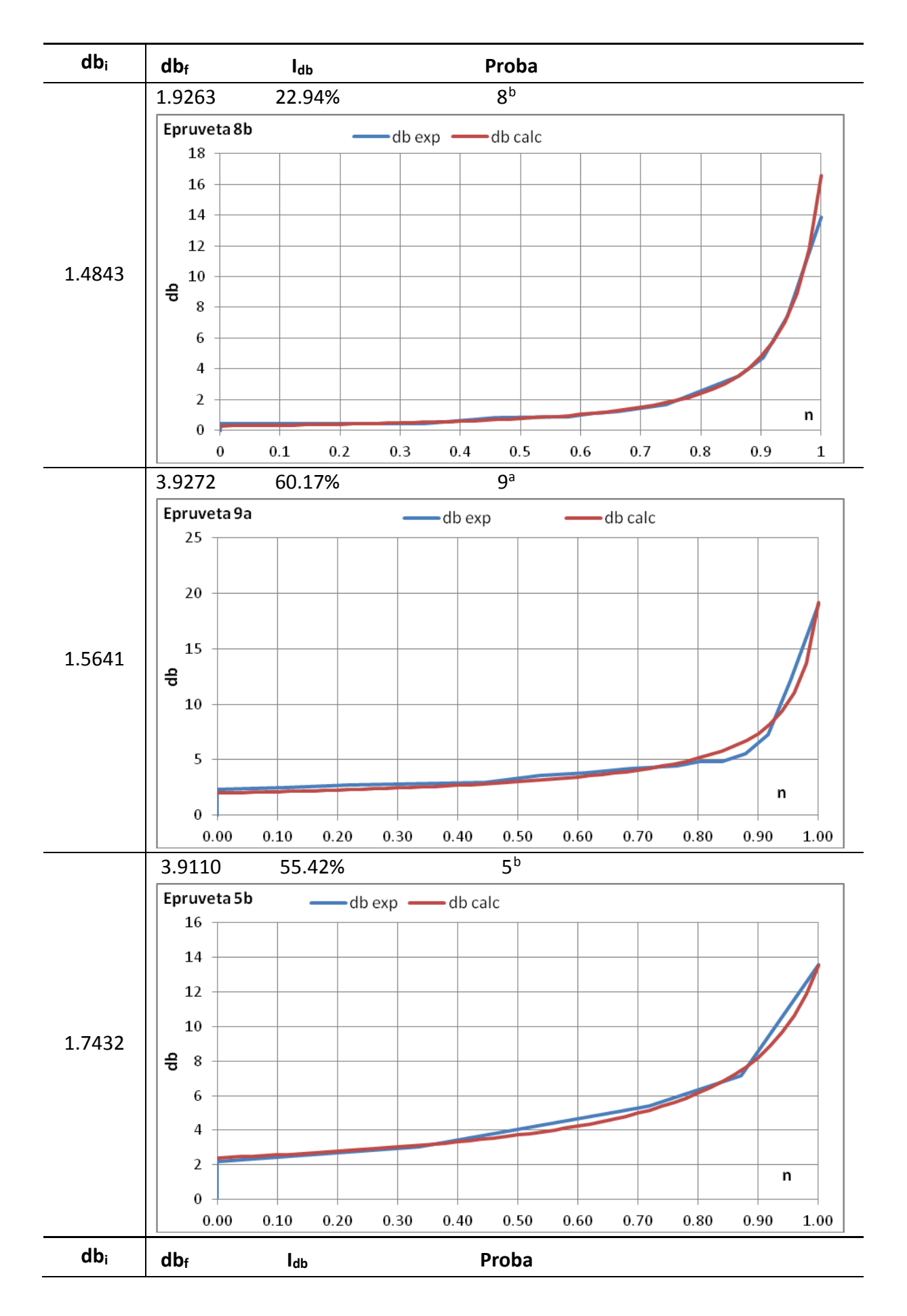
The values between 238 and 564 are retained from Table 6.1. The other specimens are excluded as having values outside the range, respectively sample 7b, in which the number of cycles is reduced until the appearance of the reflective crack, being a recipe problem of the asphalt mixture (see also sample 7a), specimen 9b, in which the crack transfer from the precracked concrete slab was modified by the presence of bitumen used for bonding.

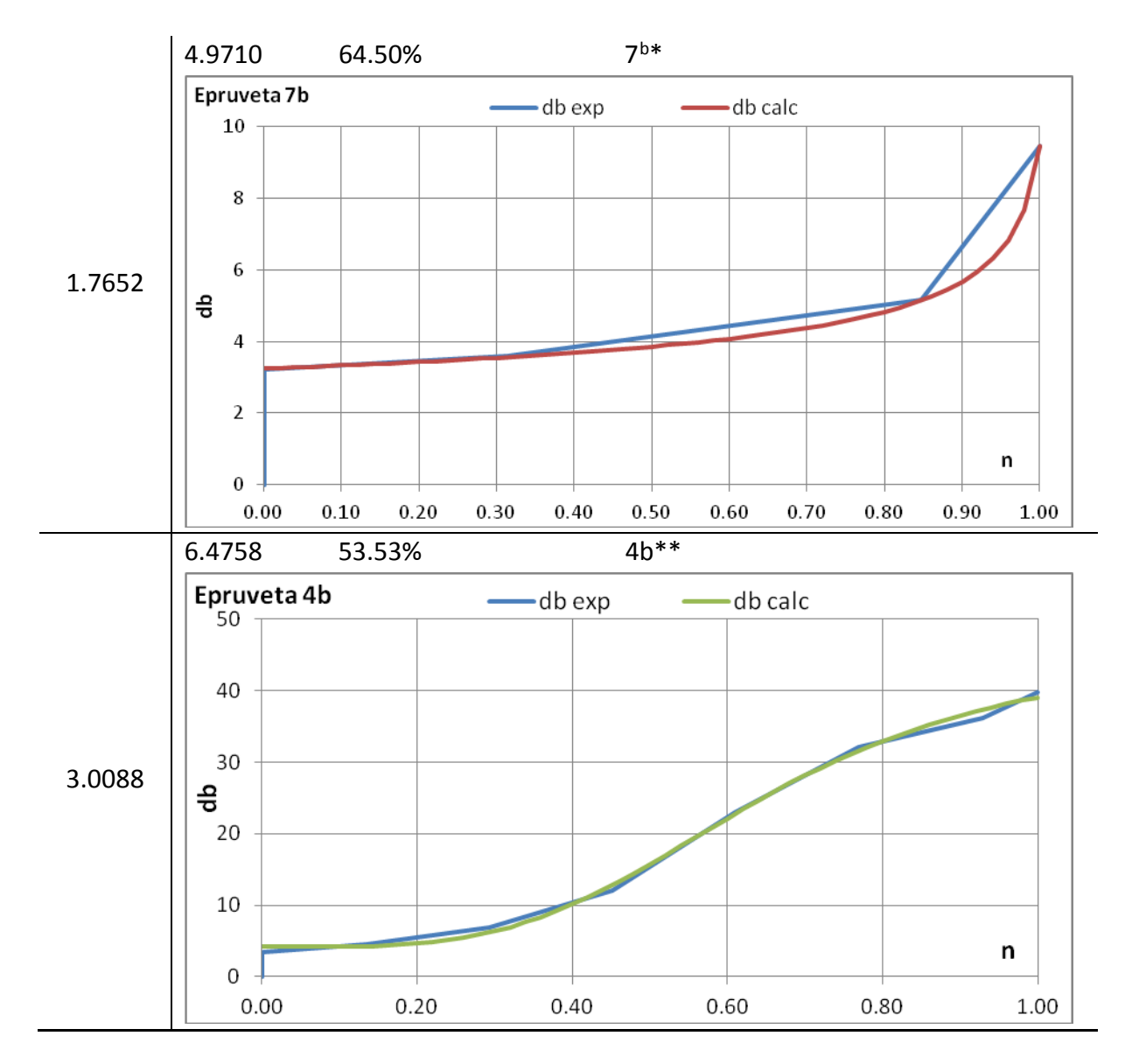
The number of cycles (n_c) at which the specimens (protective layer of MASF16, glued to the same concrete slab) break is between 10500 and 12500. The corresponding force (FR) is between 360 and 440daN.

The index of the parameter of variation of the opening in time of the existing crack in the ldb concrete support highlights the wear of the crack walls as the number of loads increases in successive tests of asphalt specimens that used practically the same prefabricated concrete support.

Table 6.2 The index of the parameter of variation of the opening in time of the existing crack in the I_{db}







The initial crack opening in the cement concrete (db_i) has values between 1.2 and 2.0 mm, except for the specimen 4b (3mm) whose evolution differs from the other samples precisely because of this (Table 6.1).

The time in which the crack is transmitted from the concrete to the mixture represents 95-98% of the total life (at fracture) of the specimen, and is between 100-564 cycles, except for specimens 4b and 9b (Table 6.3).

The time in which the crack propagates over the entire thickness of the asphalt mixture is 2-5% (Table 6.3), from the moment the crack starts.

Reflective cracking indices. Specimen $I_f = \frac{n_{ci}}{n_{cR}} \ (\%)$ Ratio $(n_{cR}-n_{ci})/n_{cR}$ 94.81% 5.19% 6a 7a 96.23% 3.77% 97.90% 2.10% 8a 8b 95.60% 4.40% 9a 95.50% 4.50% 97.48% 5b 2.52% 7b 97.67% 2.33% 9b 79.80% 20.20% 97.16% 2.84% 5a

Table 6.3 Reflective cracking indices.

If in the bonding process, the bitumen is liquid enough to penetrate the cracks in the old concrete layer, then the transfer to the crack is modified by "gluing the crack walls". This is the case for specimen 9b, where the time during which the crack propagates through the mixture increases to 20% (compared to 5% for the other specimens) of the total duration of the test.

CONCLUSIONS

Reflective cracking parameters

The main parameters that influence reflective cracking are:

- Dynamic stresses that simulate the effect of road traffic, materialized in the laboratory study by the intensity of the force (F) and its frequency of application, constant frequency in the case of Cracking Device with Temperature Control;
- The effect of the transfer to the crack, from the existing crack of the concrete layer, materialized by the analysis of the parameter db (opening of the crack in the concrete support layer);
- The asphalt-concrete cooperation, by evaluating the acrosage by bonding the interface between the two layers with different physical-mechanical characteristics, materialized by analyzing its parameters, e_i , e_f , respectively detaching the asphalt from the concrete support in relation to increasing the vertical deformation (w) of the experimental model;
- The initiation of the crack and its propagation through the asphalt layer, through the opening (d) and the length (f) of the crack, which depend on the physical-

mechanical characteristics of the bituminous mixtures from which the asphalt layer is made.

Mathematical processing of experimental data indicates:

• The variation of the crack opening **d**, but also of the length **f**, in relation to **n** is described for all specimens by a rational function of the form:

$$y = \frac{a_0 \cdot n}{1 + a_1 \cdot n + a_2 \cdot n^2}$$

• The variation of the crack opening in concrete **db**, in relation to **n** is described by the MMF or Bleasdale models:

MMF
$$db=\frac{a_0\cdot a_1+a_2\cdot n^{u3}}{a_1+n^{a_3}}$$
 Bleasdale
$$db=\left(a_0+a_1\cdot n\right)^{-\frac{1}{a_2}}$$

7.2 Asphalt mixture

Regarding the asphalt mixture used in these experiments, it can be concluded that:

- Reflective cracking (transmission of the crack from the concrete to the protective layer) occurs at 95% of the test duration. If, following the field investigations, the approximate moment at which the crack is transmitted in the asphalt layer is determined, knowing how much time has passed since its laying, it can be appreciated when it is necessary to intervene on the asphalt layer with the lowest costs.
- If in the bonding process, the bitumen is liquid enough to penetrate the cracks in the old cement concrete layer, then the transfer to the crack is modified by "gluing the crack walls". This increased the time in which the crack propagated through the protective layer from 5% to 20% in the case of sample 9b.

7.3 Cracking Device with Temperature Control

The Cracking Device with Temperature Control is an important tool for determining in the laboratory the behavior of the various asphalt mixture recipes used over a pre-cracked concrete.

However, some changes need to be made regarding both the specimen preparation methodology and the working methodology with the device.

- Better control over how the surface is bonded (by controlling the amount and distribution of the bitumen used on the surface of the concrete slab)
- Better control over how the test piece is placed so that the distance between its edges and the supports of the appliance is equal. This reduces the eccentricity with which the crack is transmitted from the concrete to the asphalt layer.

• The way in which the cracking parameters are measured (opening, crack length in asphalt, concrete crack opening) by an imaging processing after the end of the experiment. The processing must be done on the images recorded during the experiment, so that we have as many values as possible (a shorter time at which the photos are saved in the computer).

8 BIBLIOGRAPHY

- [1] S. Jercan, Mechanism of cooperation and prevention of cracking of asphalt pavements on concrete foundation, *IX National Conference of Roads and Bridges, Volume 1 Roads,* Constanţa, 1994.
- [2] M. Dicu, Concerns in the field of analysis of the cracking process in road pavement, Bucharest: Conspress, 2012.
- [3] University of Minesota, Department of Civil Engineering, «Load testing of instrumented pavement sections,» Minesota, 1999.
- [4] M. Dicu, Road pavements. Investigations and interpretations, Conspress, 2000.
- [5] V. Goanță, Fracture Mechanics, Iași: Performantica, 2006.
- [6] T. Anderson, Fracture Mechanics. Fundamentals and Applications. Second Edition, CRC Press, 1995.
- [7] D. Laveissiere, «Modelisation de la Remontee de Fissure en Fatigue dans le Structures Routieres par Endommagement et Macro-Fissuration,» Ecole Doctorale STS, L'universite de Limoges, Faculte des Sciences, Limoges, 2002.
- [8] J. R. Rice, «A path independent integral and the approximate analisys of strain concentration bz notches and Cracks,» *Journal of Applied Mechanics*, vol. 35, pp. 379-386, 1968.
- [9] J. A. Begley y J. D. Landes, «The J-Integral as a fracture criterion,» ASTM, Philadelphia, 1972.
- [10] «PD177-2001, Norm for sizing flexible and semi-rigid road systems (Analytical method), 2001.
- [11] M. M. Elseifi y I. L. Al-Qad, «A Simplified Overlay Design Model against Reflective Cracking Utilizing Service Life Prediction,» de *Transportation Research Board, 82nd Annual Meeting,* Washington, D.C., 2003.
- [12] C. Romanescu y C. Răcănel, Rheology of bituminous binders and asphalt mixtures, Bucharest:

Matrix Rom, 2003.

- [13] J. C. Pais y P. A. Pereira, «Prediction of existing reflective cracking potential of flexible pavements,» de *Fourth International RILEM Conference on Reflective Cracking in Pavements Research in Practice*, 2000.
- [14] F. Zhou y L. Sun, «Lab asphalt testing evaluation of reflective cracking,» de *Accelerated Pavement Testing International Conference*, Reno, Nevada, 1999.
- [15] P. F. Jimenez, M. R, M. A, B. R y V. G, «New procedures and criteria for asphalt mixes and pavements design regarding fatigue failure and thermal stresses,» de *24th World Road Congress Proceedings: Roads for a Better Life: Mobility, Sustainability and Development*, Mexico, 2011.
- [16] M. L. Nguyen, C. Sauzeat, H. Di Benedetto y L. Wendling, «Investigation of cracking in bituminous mixtures with a 4PBT,» de 6th RILEM International Conference. Cracking in Pavements, Chicago, 2008.
- [17] H. L. Von Quintus, J. Mallela, W. Weiss, S. Shen y R. L. Lytton, «Techniques for Mitigation of Reflective Cracks,» Auburn University, Alabama, 2009.